NASA/CR-97- 112555

NAG-5-2310

Incorporation of Boreal Forest Ecosystem Description into Climate Modeling Framework

Final Report to the
National Aeronautics and Space Administration

Project Number NAG-5-2310

Robert E. Dickinson, Principal Investigator
Institute of Atmospheric Physics
The University of Arizona
Tucson, Arizona 85721

October 24, 1997

INCORPORATION OF BOREAL FOREST ECOSYSTEM DESCRIPTION INTO CLIMATE MODELING FRAMEWORK

Final Report

to the

National Aeronautics and Space Administration

Project Number NAG-5-2310

Prepared by R. E. Dickinson, K. J. Schaudt, J. C. Morrill and M. Jin

Robert E. Dickinson, P. I.

Institute of Atmospheric Physics

The University of Arizona, Tucson, Arizona 85721

October 24, 1997

TABLE OF CONTENTS

1. Introduction 1

1.1 Project Overview 2

1.2 Progress Timeline 2

2. Non-canopy Vegetation: Representing Moss and Lichen in BATS (K. J. Schaudt and J. C. Morrill) 4

2.1 Introduction 4

2.2 Boreal lichen and moss ecology 6

2.3 Previous modeling of boreal forests and ecosystems. 9

2.4 The BOREAS Sites 11

2.5 Moss and lichen in the BATS Model 12

2.6 Atmospheric forcing data 13

2.7 Standard BATS soil in the boreal forest 13

2.8 Description of the 3-layer soil model 14

2.9 Results from the 3-layer model 18

2.10 Conclusions for the 3-layer model 19

2.11 Description of the current 10-layer soil model (BATS/LAMA model) 28

2.12 Preliminary results from the 10-layer model 32

2.13 Conclusions for the 10-layer model 34

3. A skin temperature diurnal cycle algorithm using satellite data, CCM3/BATS and surface observations (M. Jin) 45

3.1 Introduction 45

3.2 Data 45

3.3 Methodology 45

3.4 Results 47

3.5 Conclusions 48

4. Plant Chemistry Algorithm (K. J. Schaudt) 56

5. Other BOREAS Studies with Off-line BATS (J. C. Morrill) 57

5.1 Introduction 57

5.2 The sensitivity of BATS to changes in the diurnal distribution of downward longwave radiation. 57

5.3 The downward longwave radiation data 58

5.4 BATS sensitivity simulations 59

5.5 Results 60

5.6 Conclusions 62

6. Current Research 69

7. References 70

8. Appendix A 74

LIST OF FIGURES

Figure 2.1: Sensitivity of soil latent heat to model parameter c_1, for OBS sites, for the 3-layer soil model with the moss-parameterization. 20

Figure 2.2: Sensitivity of soil latent heat to model parameter c_2, for OBS sites, for the 3-layer soil model with the moss-parameterization. 20

Figure 2.3: Sensitivity of soil latent heat to model parameter c_3, for OBS sites, for the 3-layer soil model with the moss-parameterization. 21

Figure 2.4: Sensitivity of soil latent heat to model parameter W_f, for OBS sites, for the 3-layer soil model with the moss parameterization. 21

Figure 2.5: Soil latent heat for the Old Black Spruce sites in the Northern and Southern Study Areas, using the 3-layer soil model. 22

Figure 2.6: Soil latent heat for the Old Jack Pine and Old Aspen sites in the Northern and Southern Study Areas, using the 3-layer soil model. 23

Figure 2.7: July soil moisture profile for the Old Black Spruce sites, using the 3-layer soil model. 24

Figure 2.8: July soil moisture profile for the Old Jack Pine and Old Aspen sites, using the 3-layer soil model. 25

Figure 2.9: Total runoff for Old Black Spruce sites in the Northern and Southern Study Areas, using the 3-layer soil model..... 26

Figure 2.10: Total runoff for the Old Jack Pine and Old Aspen sites in the Northern and Southern Study Areas, using the 3-layer soil model..... 27

Figure 2.11: Soil latent heat for Old Black Spruce sites in the Northern and Southern Study Areas, using the 10-layer soil model. 35

Figure 2.12: Soil latent heat for the Old Jack Pine and Old Aspen sites in the Northern and Southern Study Areas, using the 10-layer soil model. 36

Figure 2.13: July soil moisture profile for the Old Black Spruce sites in the Northern and Southern Study Areas, using the 10-layer soil model..... 37

Figure 2.14: July soil moisture profile Old Jack Pine and Old Aspen sites in the Northern and Southern Study Areas, using the 10-layer soil model..... 38

Figure 2.15: Total runoff for the Old Black Spruce sites in the Northern and Southern Study Areas, using the 10-layer soil model. 39

Figure 2.16: Total runoff for the Old Jack Pine and Old Aspen sites in the Northern and Southern Study Areas, using the 10-layer soil model..... 40

Figure 2.17: July soil temperature profile for the Old Black Spruce sites in the Northern and Southern Study Areas, using the 10-layer soil model. 41

Figure 2.18: January soil temperature profile for the Old Black Spruce sites in the Northern and Southern Study Areas, using the 10-layer soil model..... 42

Figure 2.19: July soil temperature profile for Old Jack Pine and Old Aspen sites in the Northern and Southern Study Areas, using the 10-layer soil model..... 43

Figure 2.20: January soil temperature profile for the Old Jack Pine and Old Aspen sites in the Northern and Southern Study Areas, using the 10-layer soil model.... 44

Figure 3.1: July grid-averaged skin temperature diurnal cycle over 40-45°N..... 49

Figure 3.2: Comparison of the typical patterns and FIFE monthly observations. FIFE data is site-averaged. Vegetation type over FIFE is crop/mixed farming..... 50

Figure 3.3: Same as Fig.3.2, except for BOREAS. Vegetation type over BOREAS is evergreen needleleaf tree. (a) January; (b) July; (c) August; (d) September. 51

Figure 3.4: Comparison of the algorithm-produced diurnal cycle with FIFE observations for January 1987. 52

Figure 3.5: Comparison of the algorithm-produced diurnal cycle with FIFE observations for July 1987. 53

Figure 3.6: Comparison of the algorithm-produced diurnal cycle with FIFE observations for September 1987..... 54

Figure 3.7: Comparison of the algorithm-produced diurnal cycle with BOREAS observations for July 1996. 55

Figure 5.1: July 1987 diurnal cycles of surface air temperature, downwards longwave radiation and net longwave radiation, at 53.5°N, 105.5°W. 64

Figure 5.2: July 1987 diurnal cycles of upwards longwave radiation and latent heat flux, at 53.5°N, 105.5°W 65

Figure 5.3: July 1987 diurnal cycles of sensible heat and soil heat fluxes, at 53.5°N, 105.5°W. 66

Figure 5.4: April 1987 diurnal cycles of precipitation, snowmelt and total runoff, at 53.5°N, 105.5°W. 67

Figure 5.5: April 1987 diurnal cycles of precipitation, snowmelt and total runoff, at 55.5°N, 98.5°W. 68

LIST OF TABLES

Table 2.1: Dominant vegetation species of the BOREAS study area 12

Table 2.2: Vegetation parameters that vary with site 16

Table 2.3: Constant vegetation parameters 16

Table 2.4: Constants for all soils in the 3-layer soil BATS model 17

Table 2.5: Soil parameters that vary with soil type and surface cover. 17

Table 2.6: Layer thickness, depth and root fraction 30

Table 2.7: Soil type with depth for each of the six simulations 30

Table 2.8: Porosity 31

Table 2.9: Saturated soil water potential (mm) 31

Table 2.10: Saturated hydraulic conductivity (mm/s) 31

Table 2.11: Clapp and Hornberger "*b*" parameter 32

Table 2.12: Saturated soil thermal conductivity 32

Table 5.1: Maximum and average changes of net longwave radiation during January diurnal cycles. 61

Table 5.2: Maximum and average changes of net longwave radiation during July diurnal cycles. 61

TABLE OF ACRONYMS

AVHRR	Advanced Very High Resolution Radiometer
BATS	Biosphere Atmosphere Transfer Scheme
BOREAS	BOReal Ecosystem Atmosphere Study
CCM3	Community Climate Model-version 3
ECMWF	European Centre for Medium-range Weather Forecasting
EOS	Earth Observing System
GEWEX	Global Energy and Water Experiment
GSWP	Global Soil Wetness Project
IFC	Intensive Field Campaign
ISCCP	International Satellite Cloud Climatology Project
ISLSCP	International Satellite Land Surface Climatology Project
LAMA	Lichen and Moss Algorithm
NASA	National Aeronautics and Space Administration
NCAR	National Center for Atmospheric Research
NSA	Northern Study Area (of BOREAS)
OA	Old Aspen site
OBS	Old Black Spruce site
OJP	Old Jack Pine site
SCCM3	Single Column version of CCM3
SSA	Southern Study Area (of BOREAS)

TABLE OF SYMBOLS

b	Clapp and Hornberger parameter "*b*"
c_1, c_2, c_3	Empirically based constants for Equation. 2.1
E_B	Standard BATS soil evaporation
E_{SOIL}	Modified soil evaporation
E_w	Moss evaporation parameter
K_s	Saturated hydraulic conductivity
W	Soil water
α_{sn}	Soil/moss/lichen saturated NIR albedo
α_{sv}	Soil/moss/lichen saturated visible albedo
ϕ	Porosity
λ	Thermal conductivity
λ_s	Thermal conductivity at saturation
ψ_w	Soil water potential wilting point (mm)
ψ_{fc}	Soil water potential at field capacity (mm)
ψ_s	Saturated soil water potential(mm)
ψ_w	Soil water potential wilting point (mm)

1. Introduction

This investigation has been focused on increasing understanding of the role and improving the modeling of the boreal forests in the climate system. Its overall intended product has been an improvement of the representation of the boreal forest ecosystem in climate models.

The objectives of this BOREAS research as stated in the original proposal have been to:

1) Relate the BOREAS study to land surface parameterization on the Biosphere Atmosphere Transfer Scheme (BATS) for application in global climate models;

2) Carry out modeling studies to establish the relative sensitivity of surface-atmospheric exchanges of energy, moisture and carbon to various parameters and processes for boreal forests; and

3) Use the results of BOREAS to improve the representation of boreal forests in the BATS code through better specification of parameters and improved process descriptions.

1.1 Project Overview

The initial formulation of this investigation was toward the use of BOREAS data to improve land aspects of climate models. This objective has been closely coordinated with a wider EOS investigation with the same objectives for the use of EOS data. In working toward this objective, in the context of the BOREAS field observations, we realized that the role of moss and lichen was among the most poorly treated aspect of the boreal forests in current climate models. Hence, over the last two years of the investigation, we have narrowed the focus of the research to the incorporation of the hydraulic, thermal and reflective properties of moss and lichen into BATS. The observations in the BOREAS experiment have shown the presence of moss or lichen change the surface/atmosphere interactions considerably. This narrowed focus has allowed us to makes significant progress toward the full incorporation of moss and lichen into BATS.

EOS related research into refining a diurnal skin temperature algorithm where observed skin temperatures are available twice daily (roughly 12 hours apart) was linked to the BOREAS data under this grant. The diurnal cycle of skin temperature is of interest to the climate community. However, most satellites cannot produce the daily cycle due to the nature of their orbits. Knowledge gained in this research for the BOREAS sites, as well as similar research with other field studies, will be used to apply the diurnal skin temperature algorithm on a global basis using observations from AVHRR and EOS satellites.

Other research performed under this grant includes producing cloud climatology for the BOREAS area on a limited time scale, some preliminary work on a remotely sensed plant chemistry algorithm and some off-line BATS sensitivity studies.

1.2 Progress Timeline

Carried out the modeling intercomparison as agreed upon at the 1994 meeting in Montana and sent the data to Dr. J. Coughlan. (1994)

ISCCP B3 data was obtained and processed for years prior to 1994 and was used to produce climatological background cloud distributions over the BOREAS area among others. Data for later years was obtained, but as no interest was expressed in the use of this data, no cloud distributions were calculated. (1994)

Off-line BATS studies began with the ISLSCP Initiative 1 data. Preliminary results were presented at the summer IUGG meeting in Boulder, CO. (1995)

Dr. Schaudt attended the BOREAS fall meeting in Maryland and communicated with Dr. E. Middleton concerning plant chemistry. Through attendance at this meeting and discussion with Dr. F. Hall, arrangements were made to perform the planned, but delayed, chemical analysis on the frozen leaf samples from the 94 summer IFC's. (1995)

Began incorporation of a moss layer into the upper soil layer of the off-line version of BATS, with the 3-layer soil model. (1996)

Used monthly BOREAS skin temperatures to validate CCM3/BATS simulations (1996)

Schaudt attended BOREAS meeting in MD, presented research results of Schaudt, Morrill, and Jin. (1997)

More work on the incorporation of a moss-layer into the 3-layer soil model of BATS; began working on including both moss and lichen more realistically into the new BATS 10-layer soil model, added vertical heterogeneity of soil hydrologic properties to 10-layer soil model. (1997)

2. Non-canopy Vegetation: Representing Moss and Lichen in BATS

(K. J. Schaudt and J. C. Morrill)

2.1 Introduction

The effort to include moss and lichen into climate models has required an extensive review of the current understanding as summarized here. The boreal forest is an important biome, covering over 11% of the earth's land surface area (almost 15 million km^2) (Bonan and Shugart, 1992). As a mixture of coniferous and deciduous trees, it circles the northern polar region in North America, northern Europe and northern Asia. Since the boreal forest environment may have significant influence on the dynamics of energy and carbon in the global atmosphere, understanding and being able to model the large-scale boreal forest interactions is important. There is much more to the boreal forest than just trees. The presence of permafrost, forests bogs and an unusual forest floor organic layer, combined with cold temperatures and a short growing season, make this ecosystem unique.

The last twenty years have seen an increasing amount of interest and research into the boreal forest. Recently research has begun to focus on the importance of the ecosystem as a whole, and also begun to establish the importance of the surface organic layer, the mosses and lichens, which carpet much of the forest floor. In many areas the mosses and lichens may contribute more to the total aboveground biomass than the surrounding trees. (Bonan and Shugart, 1992) Moss and lichen were recognized as being important to the carbon balance (Skre and Oechel, 1979; Longton, 1992; Sveinbjörnsson and Oechel, 1992). Their role in the succession of plants that grow as the land recovers from fire has also been well-documented (Dryness and Norum, 1983; Bonan, 1989b; Bonan and Kortzukhin, 1989; Payette, 1992; Bonan, 1992b). The thick moss layer in much of the mature coniferous boreal forests is responsible for encouraging the creation and maintaining of much of the permafrost (Larsen, 1980). It also serves as an important sink for carbon dioxide in the high latitudes.

With the establishment of the Boreal Ecosystem-Atmosphere Study (the BOREAS research program) in 1993, intense research began at two study areas in the Candian boreal forest (Sellers et al., 1995a). Observations taken during the 1994 BOREAS summer Intensive Field Campaigns (IFCs) revealed that the presence of moss or lichen, which covers most exposed soil surfaces in the conifer sites, has a profound effect on the surface energy balance. This, in turn, has profound effects on some of the biological processes (such as transpiration rate) in the boreal forest. The 1994 summer BOREAS IFCs led to the following observations of the effects of moss and lichen:

1) Moss and lichen greatly reduce the surface evaporation. This results in lower latent heats and higher sensible heats (i.e. the presence of moss or lichen makes it drier and hotter). This leads to the following consequences.

   a) The soil and peat beneath the moss or lichen has a considerably higher moisture content than bare soil would, subject to the same conditions.

   b) The near-surface relative humidity is greatly reduced. This reduction in relative humidity coupled with the increase in sensible heat creates very high vapor pressure deficits especially during clear, mid-summer afternoons. This high vapor pressure deficit in turn causes the trees to greatly reduce their transpiration even though the soil moisture is well above the wilting point.

2) Moss acts as a thermal barrier to the transfer of heat between the atmosphere and the soil. This results in cooler summer soil temperatures and slightly warmer winter soil temperatures than those of bare soil subject to identical atmospheric conditions. This insulating effect may lead to an increase in the amount of permafrost present.

3) Moss and lichen change the "soil" (background) albedo, especially the near infrared albedo. This effects the combined soil-canopy albedo, which effects the surface energy balance.

4) Moss and lichen themselves transpire, which effects the carbon balance. Under some conditions the moss may be more productive (be a larger sink for carbon) than the surrounding trees.

5) In the wet conifer forests, the majority of the roots of the trees lie in the decomposing moss (the peat) layer, rather than in the deeper mineral-soil layer.

This research is concerned primarily with modeling the role moss and lichen play in the thermal and water transport within the soil as well as the changes moss and lichen produce in the surface albedo. Our goal was to alter the hydrologic and thermal components of the soil model in the Biosphere-Atmosphere Transfer Scheme (BATS) to produce results which realistically simulated field observation. We have not yet considered incorporating the effects the moss and lichen had on the carbon cycle or nutrient storage.

This section will first briefly summarize some of the important aspects of lichen and moss ecology and describe previous modeling studies of the boreal forest ecosystem. Then the specific BOREAS sites of interest will be discussed followed by descriptions, results and conclusions from two different versions of BATS.

2.2 Boreal lichen and moss ecology

Many books and articles discuss in detail the ecology of lichen and/or moss, and the important effect they have on their environment (e.g., Ahti, 1977; Pruit, 1978; Larsen, 1980, 1989; Richardson, 1981; Bonan and Shugart, 1989; Bonan, 1992a; and Bates and Farmer, 1992; the last volume contains During, 1992; Longton, 1992; and Sveinbjörnsson and Oechel, 1992).

Boreal forest lichen and mosses have many similarities including a high water capacity (650-1700 per cent of dry weight) and relatively low osmotic potentials (1-10 MPa) (During, 1992). When the water potential drops below a certain threshold value, both bryophytes and lichens tend to desiccate rapidly. They are both poikilohydric, meaning the plants dry almost as rapidly as their surrounding environment, but can resume normal metabolic activity (growth and respiration) upon rewetting (Richardson, 1981). Neither

mosses nor lichens have roots or stomata. Water (and nutrients) are absorbed over the entire surface of the plant. This tends to make them more susceptible to environmental pollution.

Lichens are not individual organisms, but rather leafless plants that result from a symbiotic association between fungus and alga (Richardson, 1981). In the boreal forests, lichens often form extensive mats on the forest floors. These lichens covers tend to be found in areas where competition from higher-order plant is limited, because lichens lack the ability to compete with faster-growing species. Lichen mats are often associated with dry, sandy acidic nutrient poor soils (such as the BOREAS Old Jack Pine sites), but can also be found in wetter woodlands with acidic peat-rich soils (Bonan and Shugart, 1989).

Lichens tend to be grayish rather than green, giving them a much higher reflectivity than both the material they cover and most other plants. This high reflectivity combined with a low thermal conductivity allows a lichen mat to act as an insulator, hindering the flux of heat into the underlying soil (Bonan and Shugart, 1989). This results in lower soil temperatures than would otherwise be observed.

The lichen mat also "maintains soil moisture at or near field capacity throughout the growing season, reducing moisture stress and allowing growth on soils that otherwise would be too dry to support tree growth" (Bonan and Shugart, 1989).

Mosses have similar effects as lichens on the thermal and soil moisture regime. Like lichen, mosses have a low thermal conductivity. Although moss reflectivity is not as high as that of lichens, it is still higher than that of the soil, especially in the near-infrared range. Mosses also have a high water-absorbing capacity, able to hold water much like a sponge. In some species (including the boreal feather mosses *Pleurozium screberi* and *Hylocium splendens*) 80-90% of the water in saturated moss can be held externally (Busby and Whitfield, 1978; Larsen, 1980). These factors enable a thick moss-organic layer to lower soil temperatures and maintain high soil moisture contents (Bonan, 1992b).

Unlike lichens, which prefer open woodlands with a fair amount of sunlight, the circumboreal feather mosses prefer well-drained shady forests (Larsen, 1980). They are

commonly associated with forest of *Picea mariana* (black spruce) or *Picea glauca* (white spruce). According to Bonan and Shugart (1989),

> "Mosses thrive and form a continuous cover where conditions are both moist and shady. In cold, wet *Picea marina* stands, up to 80-90% of the aboveground biomass may be contained in the moss layer and annual moss production may be twice that of annual foliage production and almost the same as total aboveground tree production. Moss establishment and productivity are apparently promoted by the low temperature, high water content, and poor nutrient status of *Picea marina* soils."

The spruce forests are often found in association with permafrost. Larsen (1980) wrote "Only the annual spring and summer thawing of a shallow surface active layer makes possible the growth of vegetation in region where permafrost is found. ... The shallow root systems of *Picea mariana* and *Picea glauca* permit growth of these species on sites with an active layer so shallow that it excludes species possessing tap roots, such as *Pinus banksiana*, and most if not all deciduous trees". The thick moss layer, by keeping the soil moist and cool during the summer months, aids in the maintenance of the permafrost layer.

In the context of global change, understanding and being able to model the relationship between the moss-carpeted spruce forest and the permafrost is important. Sveinbjörnsson. and Oechel (1992) wrote:

> "Bryophytes are particularly important in the development and functioning of northern ecosystems which are systems likely to be affected by global change. These systems are potentially sensitive to global change for several reasons including the fact that they are also permafrost dominated, that permafrost development interacts with moss development and abundance, that the presence of permafrost affects many environmental and ecosystem variables, that with increasing CO_2 levels northern ecosystems are expected to undergo the largest increase in temperature of all the terrestrial regions, and that the anticipated temperature rise is sufficient to cause the deepening or eventual loss of permafrost over large areas."

In our BATS/LAMA model, we introduce the high reflectivity, low thermal conductivity, and changes in the hydraulic properties in an attempt to simulate the lower soil temperatures and increased soil moisture during the growing season.

2.3 Previous modeling of boreal forests and ecosystems.

There have been previous modeling efforts of the boreal forests, but the majority of this modeling has been to study forest dynamics, forest biomass, and the carbon balance, rather than to primarily focus on the exchange of energy and water fluxes between the biosphere and the atmosphere.

Gordon Bonan performed many of these modeling studies, in addition to his other boreal research. Bonan and Krozukin (1989) examined the relationship among trees, the moss layer on the ground, and the conditions of the site (i.e. light exposure, soil chemistry, and nutrient availability). Using a model of forest dynamics, they studied the interactions between the trees, the moss layer, and their environment, and discussed how these interactions affect forest succession. Bonan (1989a) used a model to study "the interactions among solar radiation, soil moisture, soil freezing and thawing, the forest floor organic layer, and forest fires." The model was capable of reproducing local patterns of solar radiation, soil moisture and freeze/thaw depths for various boreal forest sites in Alaska. Using an individual tree model of forest dynamics, Bonan (1989b) described how forest vegetation patterns in several forest types (conifer, hardwood and mixed) were affected by various environmental factors. Bonan et al. (1990) used a gap model to study the effects the presence/absence of permafrost had on the sensitivity of various sites to changes in air temperature and precipitation. The effects that global climate changes might have on permafrost are of considerable interest to many in the global change/climate modeling community.

Others researchers have been involved with boreal forest modeling as well. Korzukhin and Antonovskii (1992) described different aspects of population-level models of forest dynamics that can be applied the boreal forest and other areas. This includes a description on the modeling of moss dynamics, in terms of biomass and the carbon balance. Antonovskii et al. (1992) modeled forest-fire dynamics and the post-fire succession stages of vegetation cover. Leemans (1992) considers some of the ways that the biological components of boreal forest dynamics differ from that of other models with traditional gap-phase dynamics. Duniker et al. (1992) discusses the use of stand

simulation models to examine forest response to environmental in the context of forest management.

Coughlan and Running (1994) oversaw the comparison of a number of different types of models (land-atmosphere models, canopy carbon balance models, forest dynamics or forest ecosystems models) using data collected at the BOREAS sites. Bonan and Davis (1996) compared standard LSM fluxes with tower fluxes measured at BOREAS old jack pine and old aspen sites. The primary focus was on diurnal cycles of sensible heat, latent heat, net radiation and CO_2 fluxes. Vegetation, thermal and hydraulic parameters were based on generic, not site-specific, parameters.

Research that attempts to incorporate the observed thermal and hydrological properties of moss and lichen into a land-surface/atmosphere model is at its beginning stages.

2.4 The BOREAS Sites

The boreal forest in the BOREAS Study Areas of several different subsystems, among them:

1) Wet coniferous forests – the old black spruce (OBS) sites. These have a vegetation canopy cover consisting largely of black spruce (*Picea mariana*) and a ground cover of feather mosses (*Pleurozium screberi* and *Hylocium splendens).* Above the mineral soil there is usually a thick (up to 4 m) organic-rich layer of peat from decomposing feather and/or sphagnum mosses.

2) Dry coniferous forests – the old jack pine (OJP) sites. Here the vegetation canopy consists primarily of jack pine (*Pinus banksiana)* with an underlying sandy, acidic, nutrient-poor soil. The sand is covered with a relatively thin layer of lichen (*Cladonia (Cladinia) mitis, C. Stellaris).*

3) Deciduous forests – the old aspen (OA) sites. In the BOREAS study area, the deciduous forest has a two-layer canopy, the overstory consists of almost exclusively of trembling aspen (*Populus tremuloides*) and the understory consisting largely of hazelnut (*Corylus americana*). The clay-rich soil in this area is not covered by significant amounts of moss or lichen.

4) Fens and bogs. These are very complex systems with slowly running water covering much of the fens and with stagnate or intermittent water present in the bogs. Both contain thick layers of sphagnum mosses (*Sphagnum fuscum, S. capillifolium)* and other small shrubs.

These vegetation classes and their dominant vegetation types are summarized in **Table-2.1**. As fens and bogs usually have standing water and no trees, the evaporation mechanisms differ from forested land. The research presented here is limited by BATS to canopy-covered land surfaces, and does not address the effects of moss on the fens and bogs, although we hope to study this issue in a future version of the model.

Table 2.1: Dominant vegetation species of the BOREAS study area

Site	*Location*	*Common Name*	*Scientific Name*
OBS	canopy	black spruce	*Picea mariana*
OJP	canopy	jack pine	*Pinus banksiana*
OBS	on ground	feather mosses	*Pleurozium screberi, Hylocium splendens*
OJP	on ground	lichens	*Cladonia (Cladinia) mitis, C. Stellaris*
OA	main canopy	trembling aspen	*Populus tremuloides*
OA	understory	hazelnut	*Corylus americana*
FEN	on ground	peat moss	*Sphagnum fuscum, S. capillifolium*

2.5 Moss and lichen in the BATS Model

The research performed here incorporates a moss and lichen layer into BATS. The model used is a modified version of the off-line Biosphere Atmosphere Transfer Scheme (BATS) with standard 3-layer and the new 10-layer soil models. The use of the off-line version of BATS does not allow for all the observed effects of moss and lichen to be modeled. In particular, it cannot simulate the reduction in the near-surface relative humidity and the subsequent reduction in the transpiration rate, because relative humidity is a function of certain forcing variables in the off-line version. However, off-line BATS can and does simulate the increase in the sub-surface soil moisture. The 10-layer model also simulates the insulating effects of the moss and lichen. Both models can simulate the effects of a more realistic surface albedo. BATS does not currently have a carbon model adequate for capturing the influence of moss and lichen on the carbon balance.

The simulation of the effects the moss or lichen are performed in fundamentally different manner in the 3-layer soil model and in the 10-layer soil model. The structure of the three-layer soil model does not allow for the hydraulic and thermal properties to be separately specified for each of the three layers. Therefore the reduction in the surface

layer (soil) moisture must be prescribed artificially. The thermal effects of the moss and lichen were not modeled in the three-layer model.

In both the 3 and 10-layer models, the soil surface albedo was replaced by moss and lichen albedo when appropriate. BATS then used these modified values of albedo in its calculations of (total) surface albedo, which in turn effects the (total) surface energy balance.

2.6 Atmospheric forcing data

The near-surface atmospheric data used to force BATS comes from two sources.

1) The 1989 hourly forcing data provided to Coughlan and Running (1994) by Alan Betts and John Ball.

2) The 1987-1988 ISLSCP 1 forcing data (Meeson et al., 1995; Sellers et. al, 1995b) for the two points closest to the NSA and the SSA. This data was provided in 6-hour time-block and interpolated to hourly intervals by the same methods described by the International GEWEX Project Office (1995) for use in the ISLSCP/GEWEX Global Soil Wetness Project.

Both sets of data included: precipitation, downward shortwave radiation, downward longwave radiation, near-surface wind speed, near-surface air temperature, dew point temperature and surface pressure.

2.7 Standard BATS soil in the boreal forest

The BATS 3-layer (mineral) soil model calculates the soil evaporation (E_B) as the minimum of the soil supply term and the atmospheric demand term. It is anticipated that the soil evaporation and therefore the soil latent heat will be high in comparison to BOREAS observations. This is due to the fact that dry moss reduces the upward transport of water compared to what mineral soil would do, for the same underlying soil moisture. The amount of the reduction is quite significant.

2.8 Description of the 3-layer soil model

In the standard BATS 3-layer soil model, all soil layers must share the same hydraulic and thermal properties. Due to this structure, the reduction in soil evaporation was accomplished by multiplying standard BATS soil evaporation, E_B, by a factor E_w parameterized as

$$E_w = c_2 * \exp(-t_m / c_3) + c_1 \qquad \textbf{Eq. 2.1}$$

where c_1, c_2 and c_3 are empirically based constants and t_m is the time elapsed since the last precipitation event. E_w is always less than or equal to $c_2 + c_1$. Equation 2.1 allows the inclusion of a time scale for reducing the soil evaporation at an increasing rate as time elapses from the last precipitation event. The time scale for this decrease , given by c_3 is on the order of a few days, is based on conversations with members of the OBS-SSA summer 1994 IFC-2. The standard BATS determines soil evaporation (E_B) and is multiplied by the factor E_w, which falls below 1.0 when soil transport limits the supply. The soil water for the current time step (W) depends on the soil water in the previous time step (W_{old}) and on the amount of water evaporated from the soil in the current time step, as shown in Eq. 2.2. The soil evaporation in the presence of moss (E_{soil}) depends on both E_B and E_w. E_B depends on soil moisture (W), which will be changed by E_w as shown below:

$$W \propto W_{old} - E_{soil} \qquad \textbf{Eq. 2.2}$$

$$E_{soil} = E_B(W) * E_w \qquad \textbf{Eq. 2.3}$$

So as the evaporation from the soil (E_{soil}) is reduced, W increases which in turn changes $E_B(W)$ from what it would have been under the standard BATS run. As a result the effects are accumulative and the soil evaporation can vary by less than the single factor of E_w. The default values of c_1, c_2 and c_3 are 0.05, 1.00 and 3 days respectively. The sensitivity of the soil latent heat to each of these three fitting parameters was tested.

The 3-layer model also was used to investigate the effects of reducing the upward motion of water from the sub-surface soil layer to the surface soil layer by reducing it to a

fraction (W_f) of its normal value. As with the effects of E_w, the effects of W_f can be accumulative and the values after spin-up can be greater than a single factor of W_f. The default W_f is 0.15. A sensitivity test of model output to this parameter was also performed. Further work with this parameterization would involve removal of the c_1 in Eq. 2.1, as in theory the maximum value of E_w should be 1.0. It might also be more realistic to allow c_3 to depend on vapor pressure deficit or net radiation.

A spin-up period of 25 years was used for all runs. All results shown for the three-layer model are from runs forced with the 1989 data.

The majority of the values for soil (loam, peat, sand and clay) and vegetation parameters for the two sites and various vegetation classes come from Coughlan and Running (1994). Observations from Bubier et al. (1997) are used to obtain values for the moss and lichen albedos. Many of the remaining parameters are standard BATS parameters, as other sources of observations could not be found. **Table 2.2** gives some of the important vegetation characteristics used in BATS. **Table 2.3** gives additional vegetation parameters that do not vary depending on latitude. **Table 2.4** lists a number of soil parameters that are constant for the 3-layer model regardless of soil type. **Table 2.5** lists soil parameters that depend on soil type. Note that under the moss and lichen, only the albedo has been listed. This is because it is the only soil parameter changed in the 3-layer model and effectively there is no moss or lichen layer within the soil itself.

Table 2.2: Vegetation parameters that vary with site

Site	Canopy Height (m)	Maximum LAI	Minimum LAI
NSA-OBS	10	2.5	2.0
SSA-OBS	12	5.0	4.5
NSA-OJP	10	1.25	1.0
SSA-OJP	13	2.5	2.0
NSA-OA	15	2.25	0.5
SSA-OA	20	4.5	3.0

Source: Coughlan and Running (1994)

Table 2.3: Constant vegetation parameters

	OBS, OJP	OA
Maximum fractional vegetation cover	0.8	0.8
Minimum fractional vegetation cover	0.7	0.5
Aerodynamic roughness length (m)	1.0	0.8
Stem area index	2.0	2.0
Vegetation albedo VIS	0.07	0.11
Vegetation albedo NIR	0.11	0.61

Sources: Coughlan and Running (1994) and Dickinson et al. (1993)

Table 2.4: Constants for all soils in the 3-layer soil BATS model

Parameter	Value
Surface soil (or moss) layer depth:	91 mm, 9.1 cm
Rootzone soil layer depth:	230 cm, 2.3 m
Total soil layer depth	286 cm, 2.86 m
Fraction of total roots in surface layer	0.166
Fraction of total roots in sub-surface layer	0.834
Soil water potential at wilting point (mm)	1.53e5
Soil water potential at field capacity (mm)	3300

Sources: Coughlan and Running (1994) and Dickinson et al. (1993)

Note: These soil depths may seem odd, but they were picked to correspond with depths of certain layer interfaces from the 10-layer model.

Table 2.5: Soil parameters that vary with soil type and surface cover.

Soil Type	ϕ	ψ (mm)	K_s (mm/s)	b	λ_s (mm/s)	α_{sv}	α_{sn}
Loam	0.40	85	0.0063	7	8.20e-5	0.08	0.16
Peat	0.80	120	0.02	4	4.61e-5	0.05	0.10
Sand	0.40	120	0.02	4	1.52e-4	0.11	0.22
Clay	0.40	150	0.00217	10	1.05e-4	0.05	0.10
Moss surface	-	-	-	-	-	0.11	0.31
Lichen surface	-	-	-	-	-	0.30	0.55

Sources: Coughlan and Running (1994), Dickinson et al. (1993) and Bubier (1997).

2.9 Results from the 3-layer model

The sensitivity studies of the soil latent heat to c_1, c_2 and c_3 and W_f are shown in **Figures 2.1 through 2.4** for the OBS sites in both the NSA and the SSA. The sensitivity of the soil latent heat to the four variables in order of decreasing sensitivity is: c_2, c_1, c_3 and W_f. Changes in the W_f parameter alone do not result in significant reductions in the soil latent heat. Comparison of results obtained here and those obtained in the BOREAS summer IFC's in 1994 can only be qualitative in nature as the data used for forcing BATS is for years other than 1994. No adequate observations (a full year of site or near site meteorological observations) for 1994 were taken nor have adequate observations been assimilated at present. As 1994 was an extremely hot, dry year, the observations obtained may well be anomalous in magnitude. It is therefore hard to find any reasonable observations to fit the four fitting parameters c_1, c_2, c_3 and W_f to.

The following discussion uses the default values for c_1, c_2, c_3 and W_f and compares bare soil results to those with moss and with lichen present.

The presence of moss produces a reduction in the soil latent heat of up to 50% during spring and fall, as shown in **Figure 2.5**. However, this decrease in soil latent heat is a combination of effects from the change in soil evaporation and from the effects of "soil" albedo. **Figure 2.6** illustrates the effects of changing the soil albedo in the OJP. The latent heat for the lichen-covered sand can be up to 40% less than just sand alone, however the difference is typically considerably smaller and often is reversed.

The soil moisture profiles are shown in **Figures 2.7 and 2.8**. One may note that when moss is present the uppermost soil layer is wetter than the underlying soil layers, which is opposite to observations. While this is not consistent with observations, it is to be expected because the soil evaporation in the 3-layer model is prescribed and model does not change any of the soils hydraulic properties. The reduction is evaporation appears to cause the water to build up in the surface soil layer.

The total runoff was increased with the presence of moss and lichen as illustrated in **Figures 2.9 and 2.10**. The increase in total runoff was due in large part to the increase in subsurface runoff due to wetter soils.

The transpiration goes up with the presence of the moss in the OBS-SSA while it remain basically unchanged in the OBS-NSA. The cause of this is the fact that the SSA soil was drier overall than the NSA soil, therefore the increase in soil moisture had a larger impact in the SSA. The presence of lichen (whose only difference is the change in albedo) produced marked reductions in transpiration in both OJP sites. However, these results are not truly suitable for comparison because BATS is run off-line and humidity is a forcing variable and is often rather high for the forcing data used. This means that effects moss and lichen may have on the near-surface humidities could not be modeled. The effects moss and lichen had on the total evapotranspiration varied, that is during some months for some sites there was an increase and for other months and other sites there was a decrease in evapotranspiration. As the effects on transpiration are unrealistic the results on total evapotranspiration are also unrealistic.

2.10 Conclusions for the 3-layer model

If the appropriate meteorological observations were available, the soil latent heat could be used to tune the soil evaporation parameters c_1, c_2, and c_3 and the upper water flux parameter W_f. However, doing so will not guarantee that the soil moisture profiles will be in agreement with the observed profiles. As the 3-layer model's method used to achieve the reductions in soil latent heat is not physically realistic, rather comes about due to the nature of the 3-layer model, this model is extremely limited in its ability to mimic nature. The more sophisticated 10-layer model allows these physically unrealistic limitations to be avoided.

Reductions of up to 50% in the soil latent heat were predicted with reasonable values for c_1, c_2, c_3, and W_f.

Reducing the upward motion of the water through the soil is not adequate to produce significant reductions in soil latent heat.

Total runoff is increased in the presence of moss or lichen.

When BATS, or any other land/surface model is run in an off-line mode, changes in relative humidity and its effects on the transpiration can not be observed.

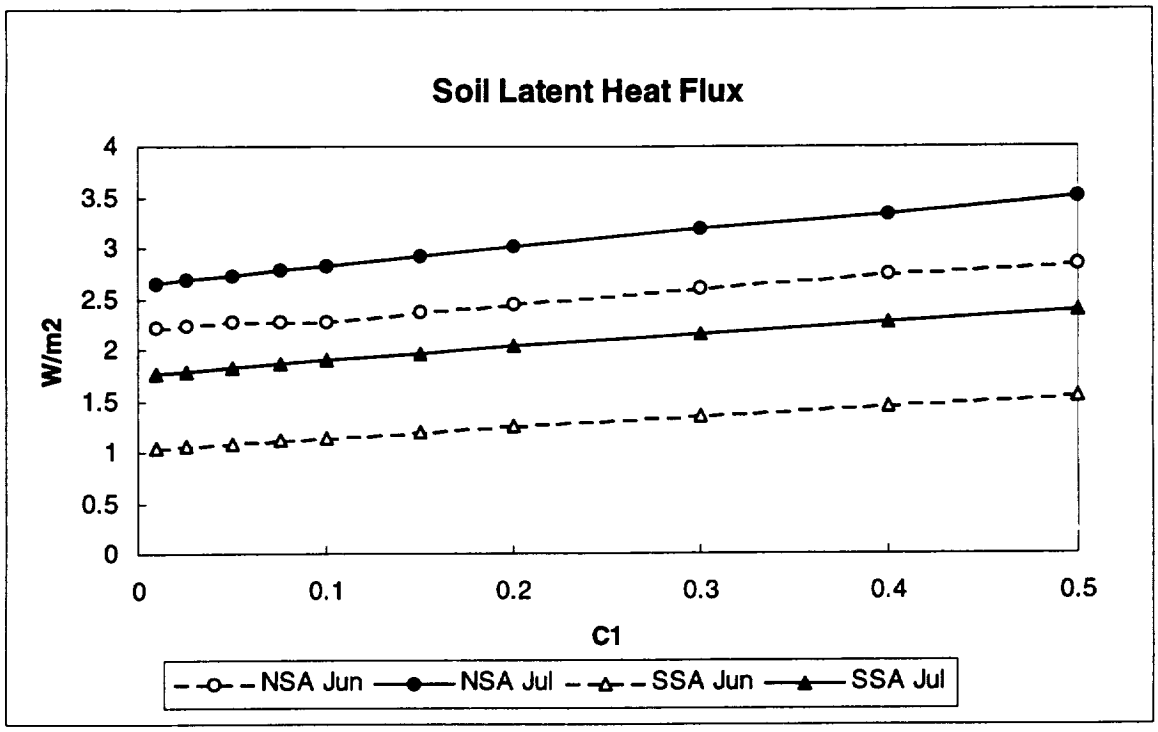

Figure 2.1: **Sensitivity of soil latent heat to model parameter c_1, for OBS sites, for the 3-layer soil model with the moss-parameterization.**

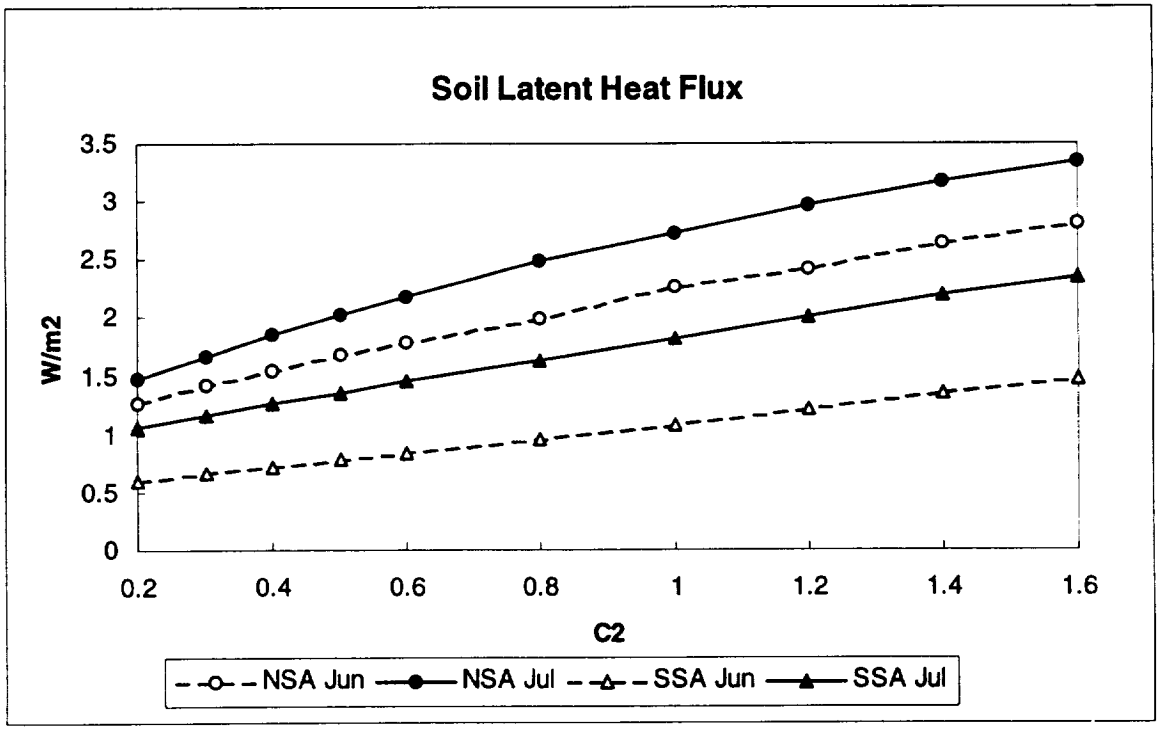

Figure 2.2: **Sensitivity of soil latent heat to model parameter c_2, for OBS sites, for the 3-layer soil model with the moss-parameterization.**

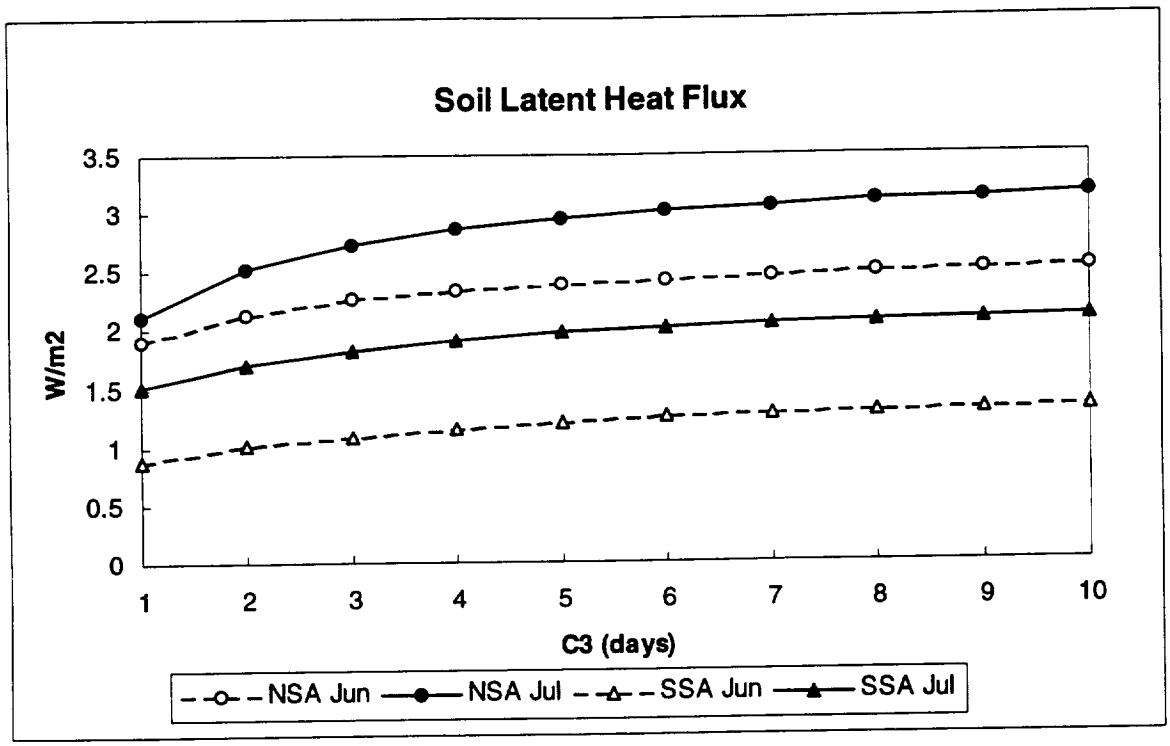

Figure 2.3: **Sensitivity of soil latent heat to model parameter c_3, for OBS sites, for the 3-layer soil model with the moss-parameterization.**

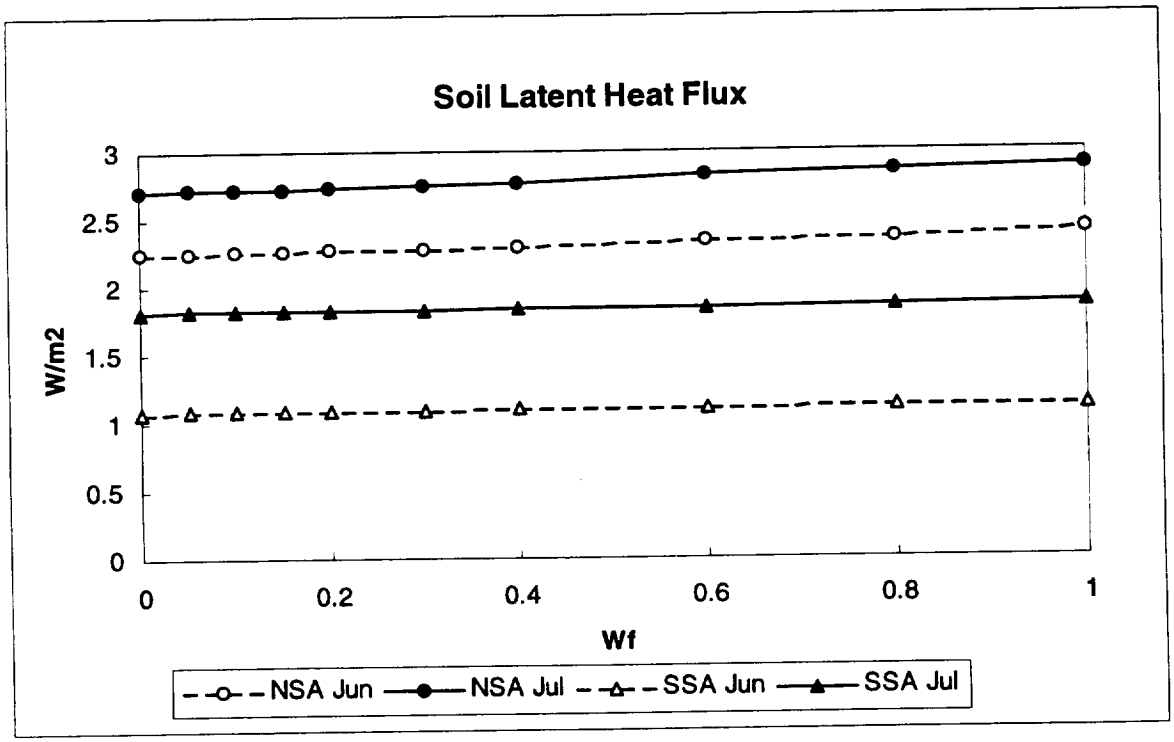

Figure 2.4: **Sensitivity of soil latent heat to model parameter W_f, for OBS sites, for the 3-layer soil model with the moss parameterization.**

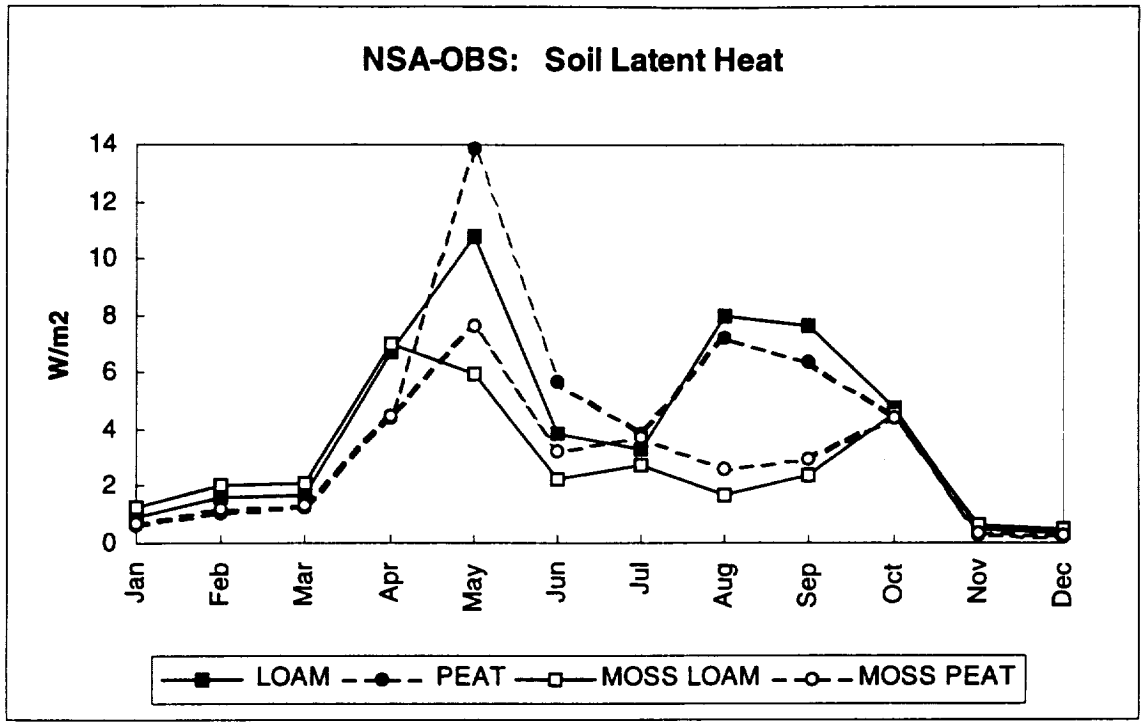

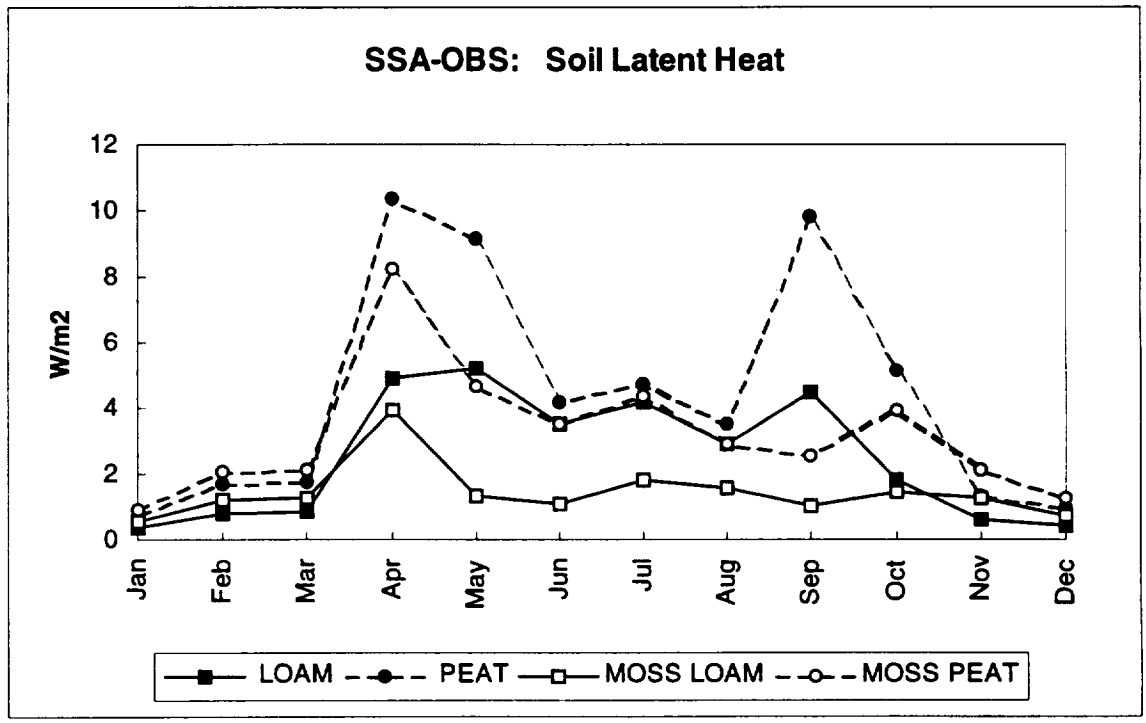

Figure 2.5: **Soil latent heat for the Old Black Spruce sites in the Northern and Southern Study Areas, using the 3-layer soil model.**

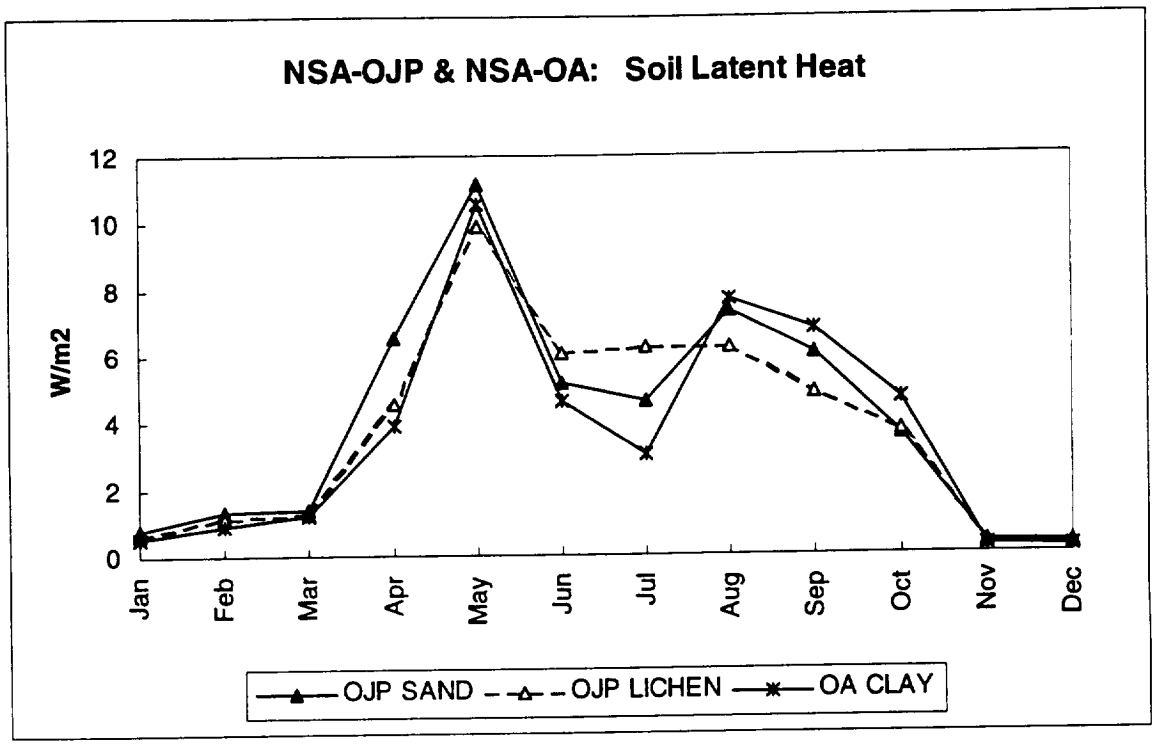

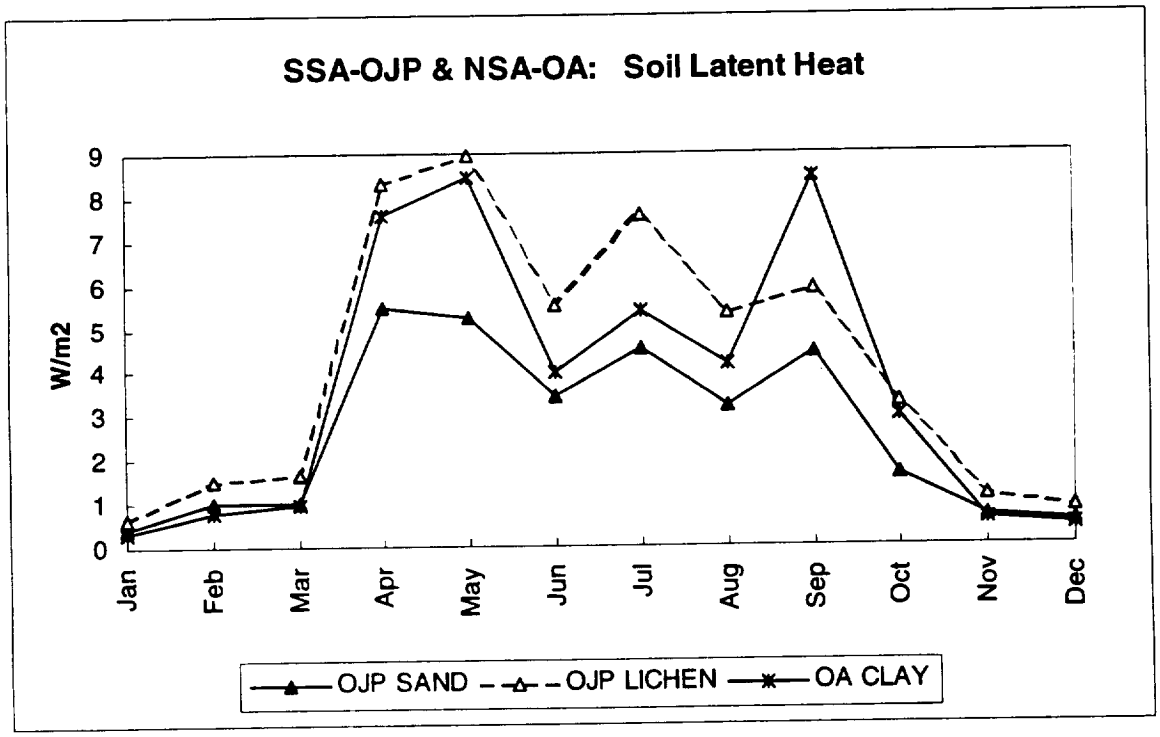

Figure 2.6: **Soil latent heat for the Old Jack Pine and Old Aspen sites in the Northern and Southern Study Areas, using the 3-layer soil model.**

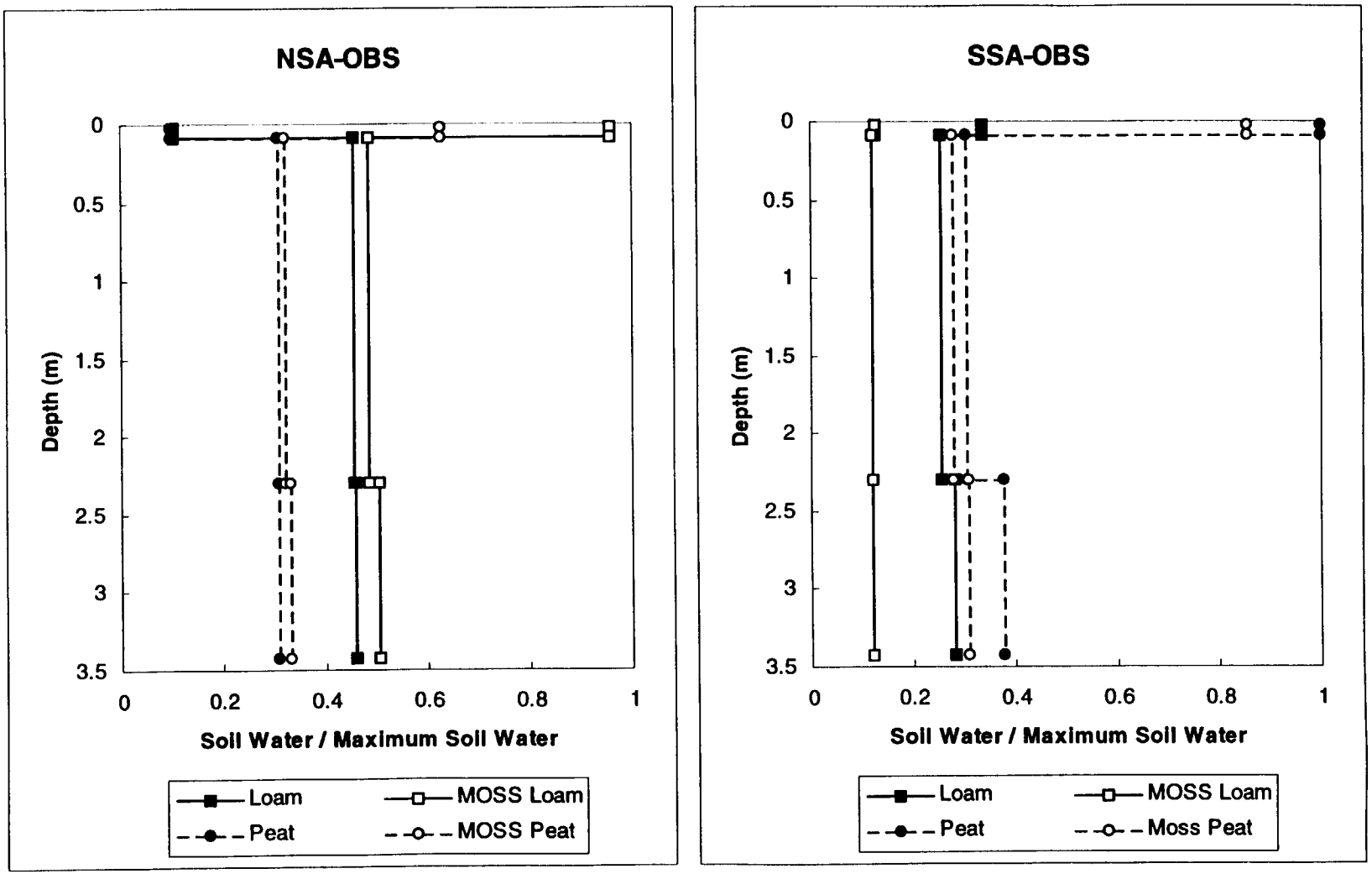

Figure 2.7 **July soil moisture profile for the Old Black Spruce sites, using the 3-layer soil model.**

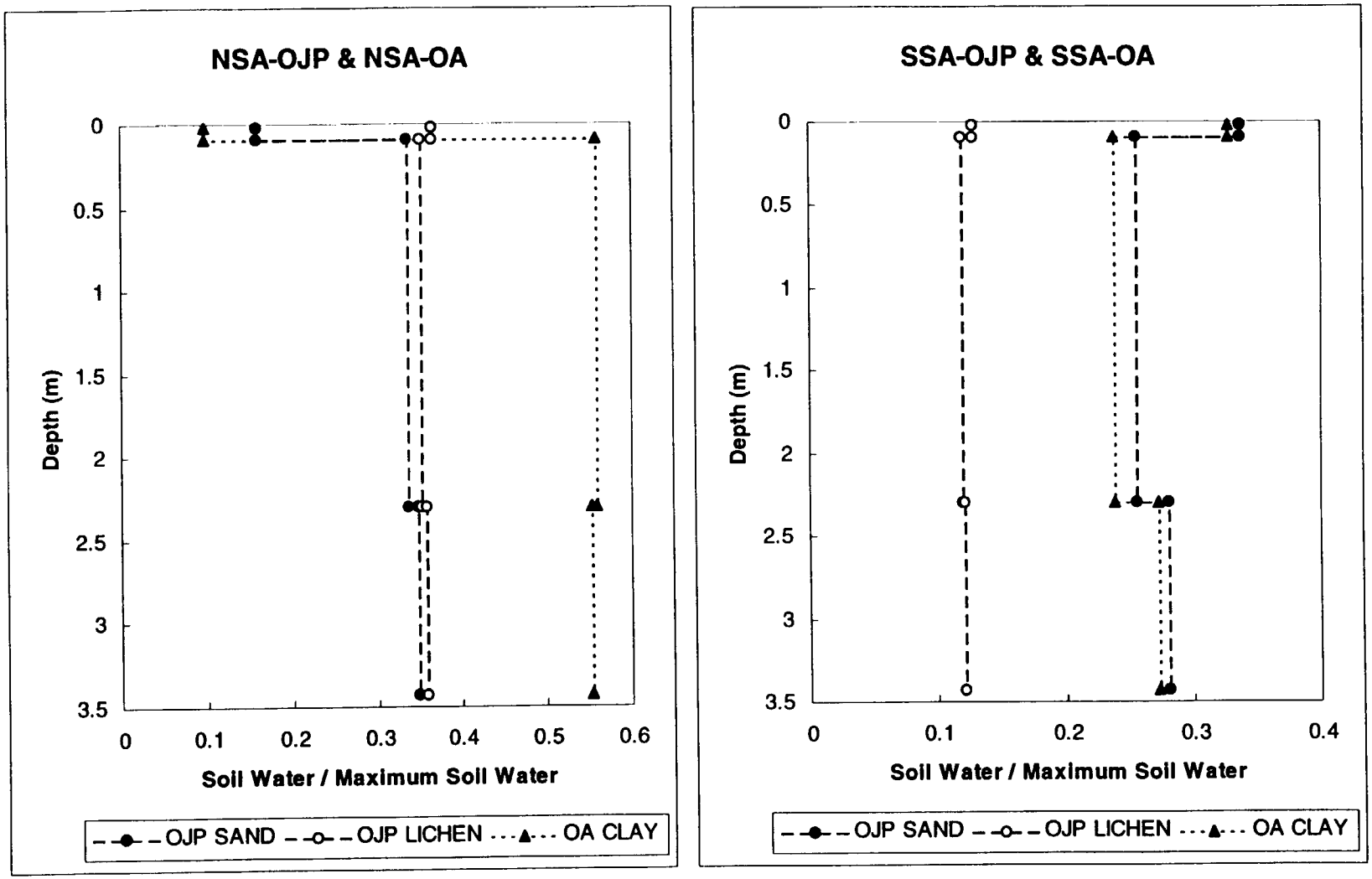

Figure 2.8 **July soil moisture profile for the Old Jack Pine and Old Aspen sites, using the 3-layer soil model.**

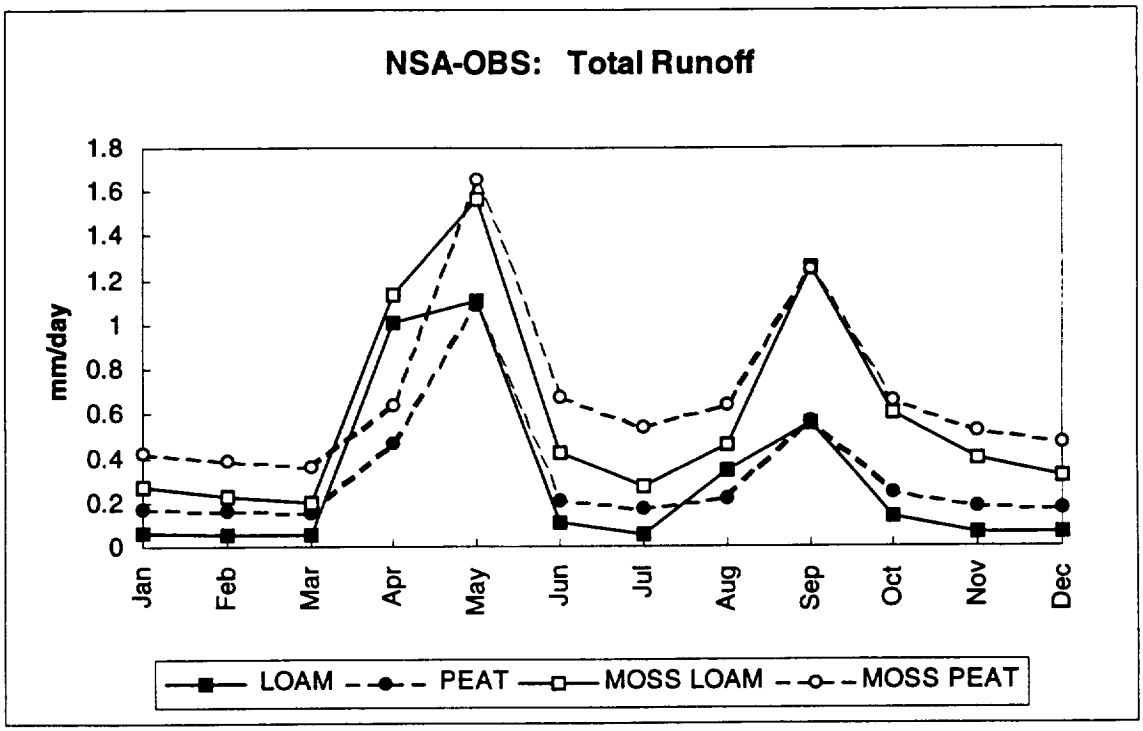

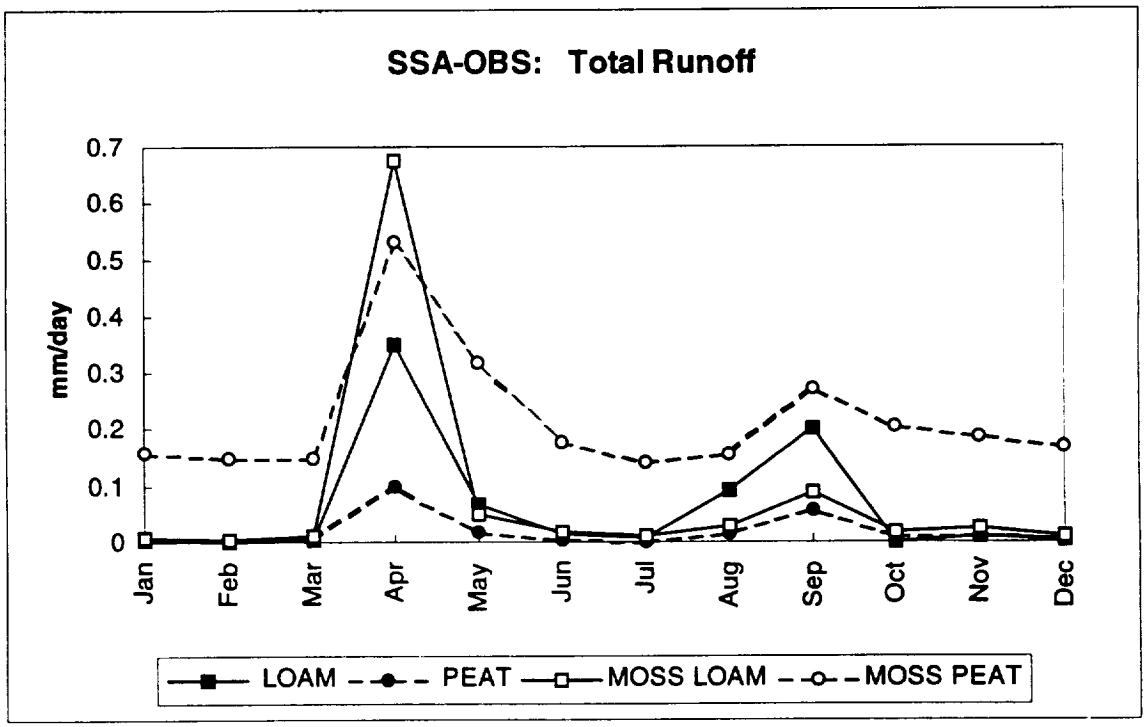

Figure 2.9: **Total runoff for Old Black Spruce sites in the Northern and Southern Study Areas, using the 3-layer soil model.**

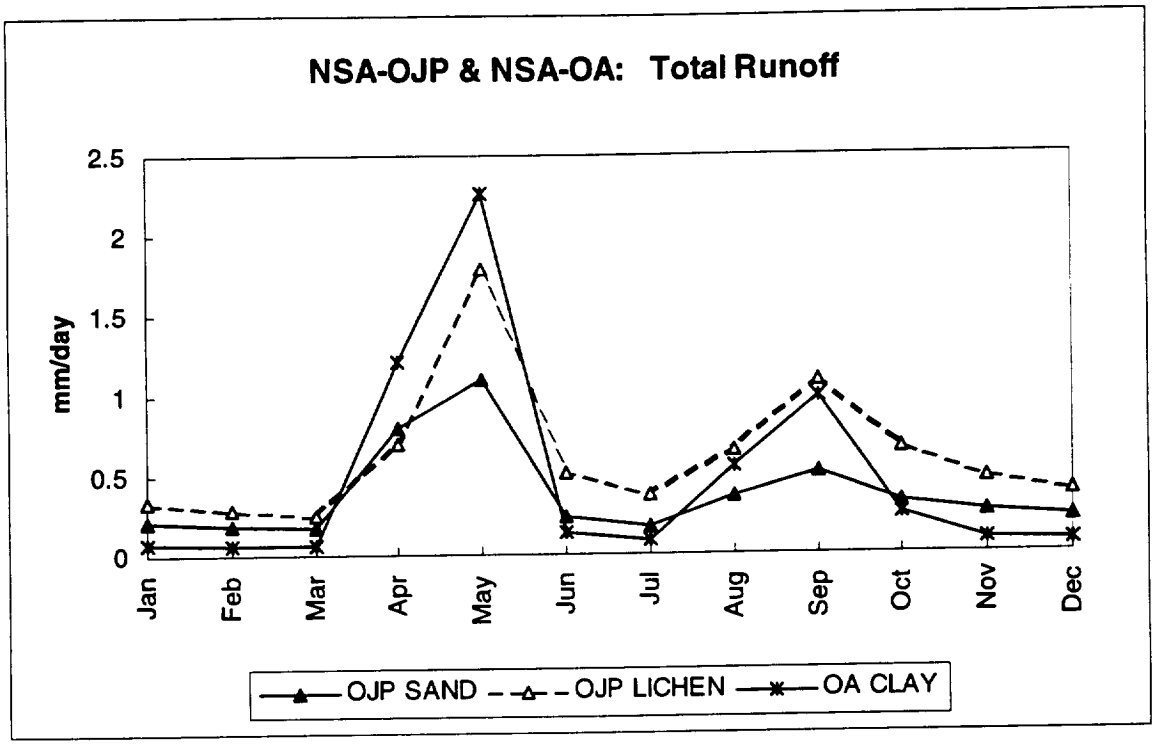

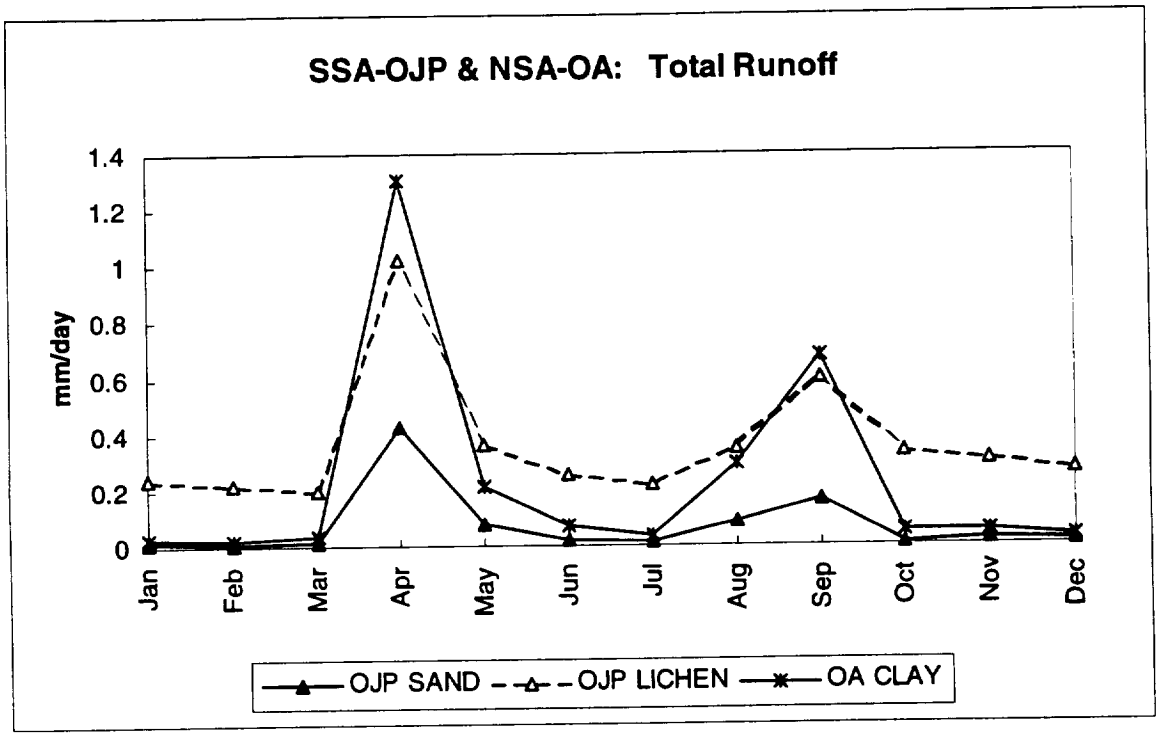

Figure 2.10: Total runoff for the Old Jack Pine and Old Aspen sites in the Northern and Southern Study Areas, using the 3-layer soil model.

2.11 Description of the current 10-layer soil model (BATS/LAMA model)

The 10-layer soil model is fundamentally different than the three layer soil model. The new (and still incomplete) 10-layer model is a physically more realistic model than the 3-layer model. The original version of the BATS 10-layer model, as an improved version of Bonan (1996), allows the thermal properties of each of the 10 soil layers to be specified independently. Morrill further modified the code structure to allow for the hydraulic properties (ψ_s, ϕ, K_s, and b) to also be separately specified for each layer. Hence, expressing the moss and lichen properties in terms of standard, well-understood physical soil properties allows for much more realistic predictions of soil thermal and hydraulic profiles, as well as soil latent heat. Some difficulties surrounding the implementation of this new 10-layer soil code are still being addressed. Energy and water balance problems are aggravated by an overestimation of soil evaporation rates at low-medium water contents. Work to correct this problem is in progress. For this reason, the results from the 10-layer model, although producing the desired qualitative behaviors, are still preliminary.

The way in which the hydraulic parameters ψ_s, ϕ, K_s and the Clapp and Hornberger "b" parameter affect the variables that control the movement of water within the soil are given by the following equations. The soil water potential, which controls how much energy is required to move water from one point to another within the soil, is given by

$$\psi = \psi_s W^{-b} \qquad \textbf{Eq. 2.4}$$

where W is the soil water content (unitless). The unsaturated hydraulic conductivity K, which determines, in part, the rate at which the water moves through the soil, is given by

$$K = K_s W^{2b+3} \qquad \textbf{Eq. 2.5}$$

Gravitational drainage is also present and changes because the hydraulic conductivity is changed in the presence of moss or lichen. The porosity, ϕ, determines the amount of water (as a fraction of total soil volume) the soil can hold at saturation. Available soil water can limit maximum potential transpiration and soil evaporation. In an area with a

soil with a small porosity or limited infiltration and high potential evapotranspiration, plants become stressed more readily.

Table 2.6 gives information on the soil depths used in the 10-layer model. These values are the default 10-layer values. **Table 2.7** shows the make-up by "soil" type of the 10-layers for the six simulations performed at both the northern and southern study areas. Note that here there are true moss and lichen layers present within the "soil". The loam, peat, and moss are all used exclusively in OBS sites. The sand and lichen are used exclusively at OJP sites and the clay used only at OA sites. **Table 2.8** gives the porosity, ϕ, for the various soil types. **Table 2.9** gives the saturated soil water potential for the various soil types. **Table 2.10** gives the saturated hydraulic conductivity, K_s, for the various soil types. **Table 2.11** gives the Clapp and Hornberger "b" parameter for the various soil types. Finally, **Table 2.12** gives the thermal conductivity at saturation.

Vegetation parameters (given in **Table 2.2** and **Table 2.3**) are the same for the 10-layer model and the 3-layer model.

Table 2.6: Layer thickness, depth and root fraction

	Layer Thickness (mm)	*Bottom of layer (m)*	*Root fraction*
1	17.5	0.0175	0.0344
2	27.6	0.0451	0.0518
3	45.5	0.0906	0.0794
4	75.0	0.166	0.116
5	124.0	0.289	0.157
6	204.0	0.493	0.188
7	336.0	0.829	0.183
8	554.0	1.38	0.128
9	913.0	2.30	0.0528
10	1140.0	3.43	0.00909

Table 2.7: Soil type with depth for each of the six simulations

		LOAM	*PEAT*	*MOSS*	*SAND*	*LICHEN*	*CLAY*
1	A	Loam	Peat	MOSS	Sand	LICHEN	Clay
2	A	Loam	Peat	MOSS	Sand	LICHEN	Clay
3	B	Loam	Peat	MOSS	Sand	Sand	Clay
4	C	Loam	Peat	Peat	Sand	Sand	Clay
5	C	Loam	Peat	Peat	Sand	Sand	Clay
6	C	Loam	Peat	Peat	Sand	Sand	Clay
7	C	Loam	Peat	Peat	Sand	Sand	Clay
8	D	Loam	Loam	Loam	Sand	Sand	Clay
9	D	Loam	Loam	Loam	Sand	Sand	Clay
10	D	Loam	Loam	Loam	Sand	Sand	Clay

Table 2.8: Porosity

		LOAM	*PEAT*	*MOSS*	*SAND*	*LICHEN*	*CLAY*
1-2	A	0.4	0.8	0.8	0.4	0.8	0.4
3	B	0.4	0.8	0.8	0.4	0.4	0.4
4-7	C	0.4	0.8	0.8	0.4	0.4	0.4
8-10	D	0.4	0.4	0.4	0.4	0.4	0.4

Sources: Coughlan and Running (1994)

Table 2.9: Saturated soil water potential (mm)

		LOAM	*PEAT*	*MOSS*	*SAND*	*LICHEN*	*CLAY*
1-2	A	85	120	120	120	120	150
3	B	85	120	120	120	120	150
4-7	C	85	120	120	120	120	150
8-10	D	85	85	85	120	120	150

Sources: Coughlan and Running (1994) and Dickinson, et al. (1993)

Table 2.10: Saturated hydraulic conductivity (mm/s)

		LOAM	*PEAT*	*MOSS*	*SAND*	*LICHEN*	*CLAY*
1-2	A	0.0063	0.02	0.05	0.02	0.05	0.0217
3	B	0.0063	0.02	0.05	0.02	0.02	0.0217
4-7	C	0.0063	0.02	0.02	0.02	0.02	0.0217
8-10	D	0.0063	0.0063	0.0063	0.02	0.02	0.0217

Sources: Coughlan and Running (1994) and Dickinson, et al. (1993)

Table 2.11: Clapp and Hornberger "*b*" parameter

		LOAM	*PEAT*	*MOSS*	*SAND*	*LICHEN*	*CLAY*
1-2	A	7	4	1	4	1	10
3	B	7	4	1	4	4	10
4-7	C	7	4	4	4	4	10
8-10	D	7	7	7	4	4	10

Sources: Coughlan and Running (1994) and Dickinson, et al. (1993)

Table 2.12: Saturated soil thermal conductivity

		LOAM	*PEAT*	*MOSS*	*SAND*	*LICHEN*	*CLAY*
1-2	A	8.20e-5	4.61e-5	3.07e-5	1.52e-4	3.07e-5	1.17e-4
3	B	8.20e-5	4.61e-5	3.07e-5	1.52e-4	1.52e-4	1.17e-4
4-7	C	8.20e-5	4.61e-5	4.61e-5	1.52e-4	1.52e-4	1.17e-4
8-10	D	8.20e-5	8.20e-5	8.20e-5	1.52e-4	1.52e-4	1.17e-4

Sources: Coughlan and Running (1994) and Dickinson, et al. (1993)

2.12 Preliminary results from the 10-layer model

As mentioned above, there remains some instability in the 10-layer model whose source has yet to be identified. Therefore, the results given should be considered preliminary. For all results below, the presence of the moss and lichen layer means the albedo, thermal properties and the hydraulic properties have all been changed to the values given in **Tables 2.8 through 2.12**, unless otherwise stated. All results are from model runs forced with either the 1987 or 1989 data.

Expressed as a percentage of total soil latent heat, the reductions in the soil latent heat in the presence of moss in the 10-layer model are not as profound as the results obtained in the 3-layer model. However, the magnitude of the reduction is roughly the same in both models. This is due to the fact the soil latent heat of bare soil in the 10-layer model is

significantly larger in magnitude than in the soil latent heat for bare soil in the 3-layer model. The soil latent heat for the OBS sites are given in **Figure 2.11** and for the OJP and OA in **Figure 2.12**. Until the problems in the 10-layer model are fixed, it is difficult to know how well the soil latent heat can be modeled adequately with only changes in soil parameters.

The effects of the presence of moss on the soil moisture profile are shown in **Figure 2.13**. The open squares, which are the moss on peat on loam, show good qualitative agreement with observations, although they may overall be a bit too moist. That is because the moss itself is quite dry and the underlying soil layers more moist than results with bare soil (compare the shaded squares (peat on loam) to the open squares for the 4-7th soil layers and the solid squares (loam only) to the open squares for the 8th layer downward (at or below 1.5 m). The effects of lichen atop the sand are shown in **Figure 2.14**. The lichen itself is also dry like the moss, but the increase in the underlying soil moisture is not as great as in the moss case. The OA values are also given in **Figure 2.14**.

The effects of moss and lichen on the total runoff are shown in **Figures 2.15 and 2.16**. Overall, there is an increase in runoff in the presence of moss or lichen. As in the case of the 3-layer model, the increase comes primarily from the increase in subsurface runoff.

The effects of moss on the soil temperature profiles are shown in **Figure 2.17** for July, and **Figure 2.18** for January. The July soil temperature profiles of the moss on peat on loam show a decrease in temperature when compared to either peat on loam or loam only. Thus, the moss acts as insulation. The January soil temperature profiles of the moss on peat on loam show near the surface the soil temperatures are higher than the bare soils for the SSA and are nearly identical in the NSA over only the peat on loam soil group. Furthermore, the deep soil temperatures show a decrease overall in January and the depth at which the permafrost in July is shallower in the case where moss is present. This insulating effect models the increase in permafrost in the presence of moss as observed by Sveinbjörnsson and Oechel (1992).

The effects of lichen atop sand on the temperature profiles again are not as marked as in the case of moss. **Figures 2.19** and **2.20** illustrate the effects of lichen on the July and January soil temperature profiles.

2.13 Conclusions for the 10-layer model

Although the results are preliminary, it appears that many of the effects of moss and lichen on the water and heat transfer within the soil can be adequately modeled using existing soil parameters. The presence of moss and, to a slightly lesser extent, the presence of lichen decrease the moisture in the uppermost soil layers and increase the moisture in the underlying peat and loam or sand, as well as increase the total runoff. A value for the Clapp and Hornberger "*b*" parameter of about 1, a saturated hydraulic conductivity of about 0.02 mm/s, a porosity of 0.8, a saturated soil water potential of 120 mm, and a moss layer 9.1 cm thick and a lichen layer 4.5 cm thick are preliminarily suggested values for the moss and lichen "soil" parameters. As observational values for these parameters, as well as for the thermal conductivity, for moss and lichen have not, to the best of our knowledge, been established by measurement, these values where chosen because they are within reasonable ranges for the parameters and produce the correct qualitative results. The primary difference between the moss and lichen is the depth of the layer with the moss layer being thicker than the lichen layer. This difference does appear to decrease the effects the lichen layer has on the water and energy balance as compared with the thicker moss layer, however the higher visible and NIR albedo of lichen tends to counteract some of the effects of the decreased thickness.

The insulating effects of moss and lichen were predicted using reasonable, slightly lower than peat, values for the thermal conductivity. In addition to the insulating effects an increase in the amount of permafrost was found.

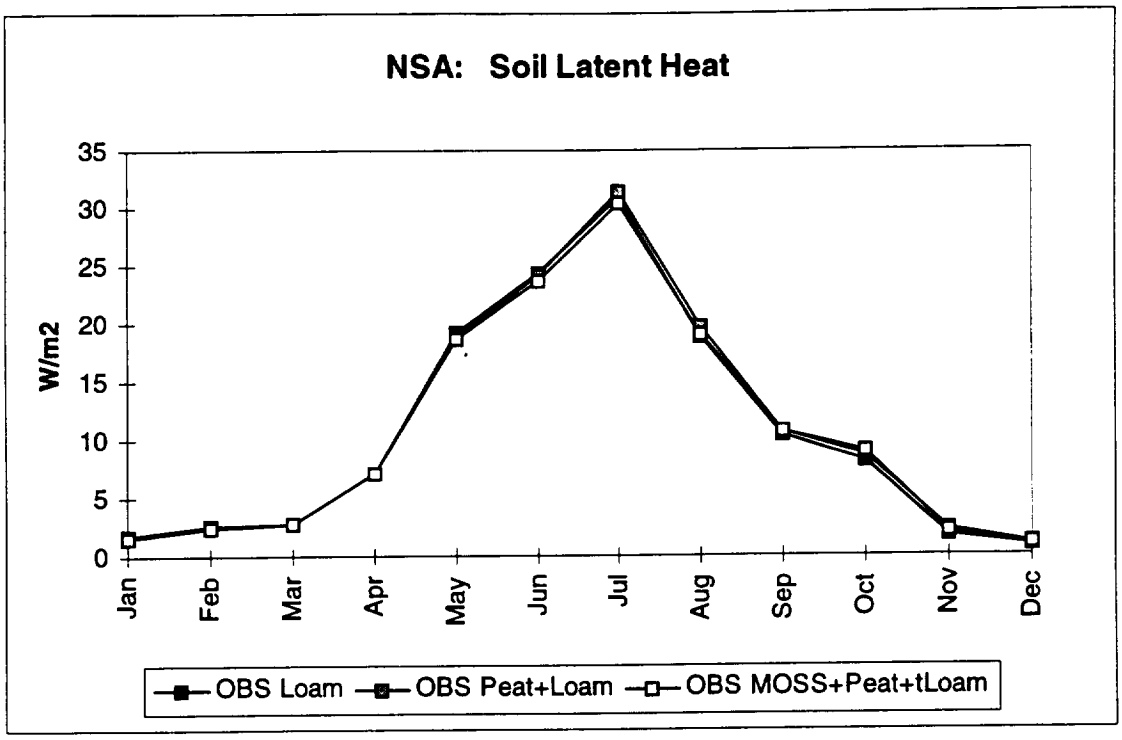

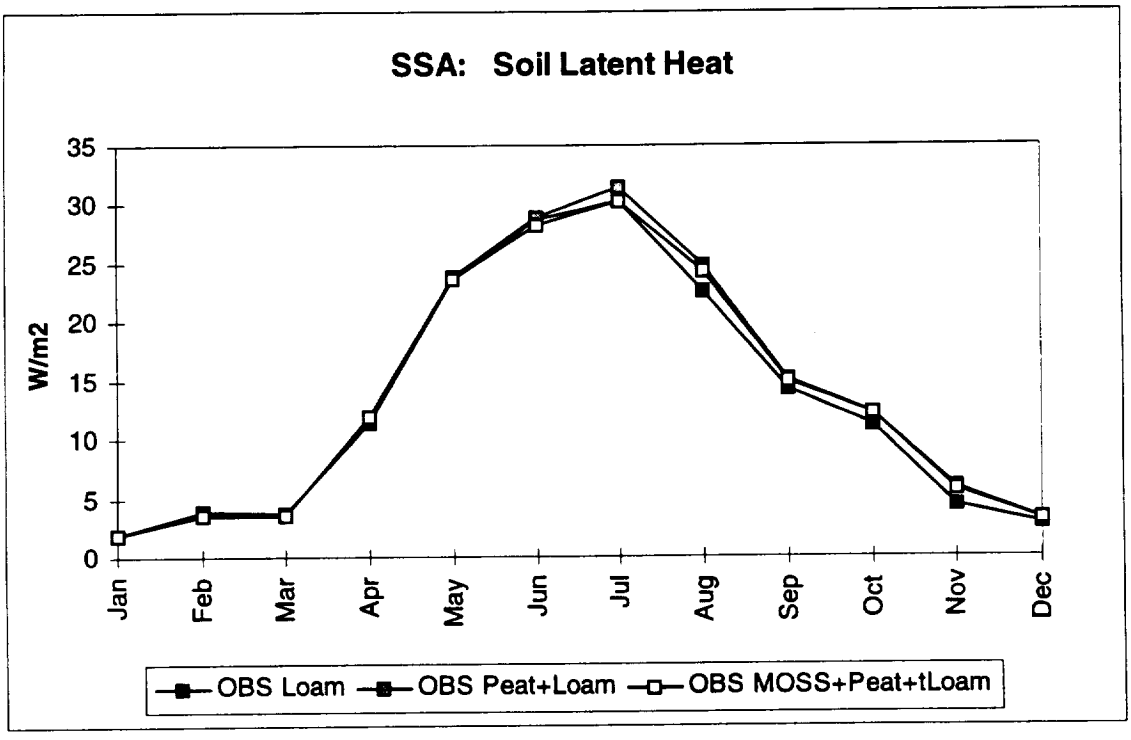

Figure 2.11: Soil latent heat for Old Black Spruce sites in the Northern and Southern Study Areas, using the 10-layer soil model.

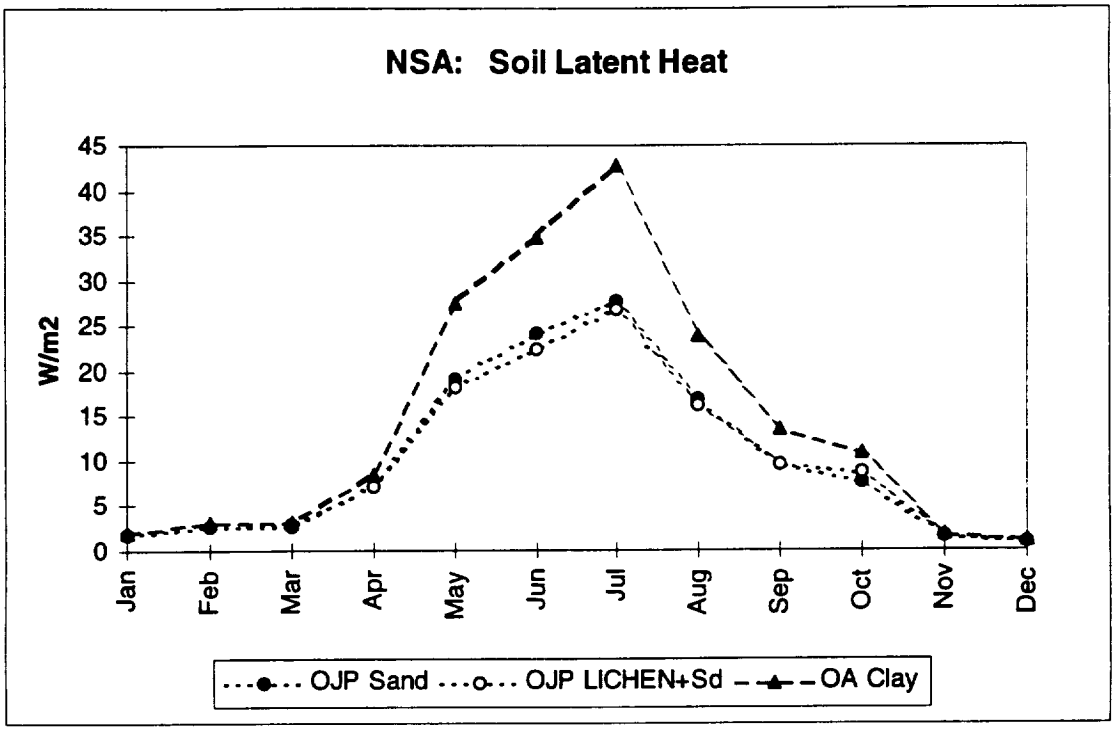

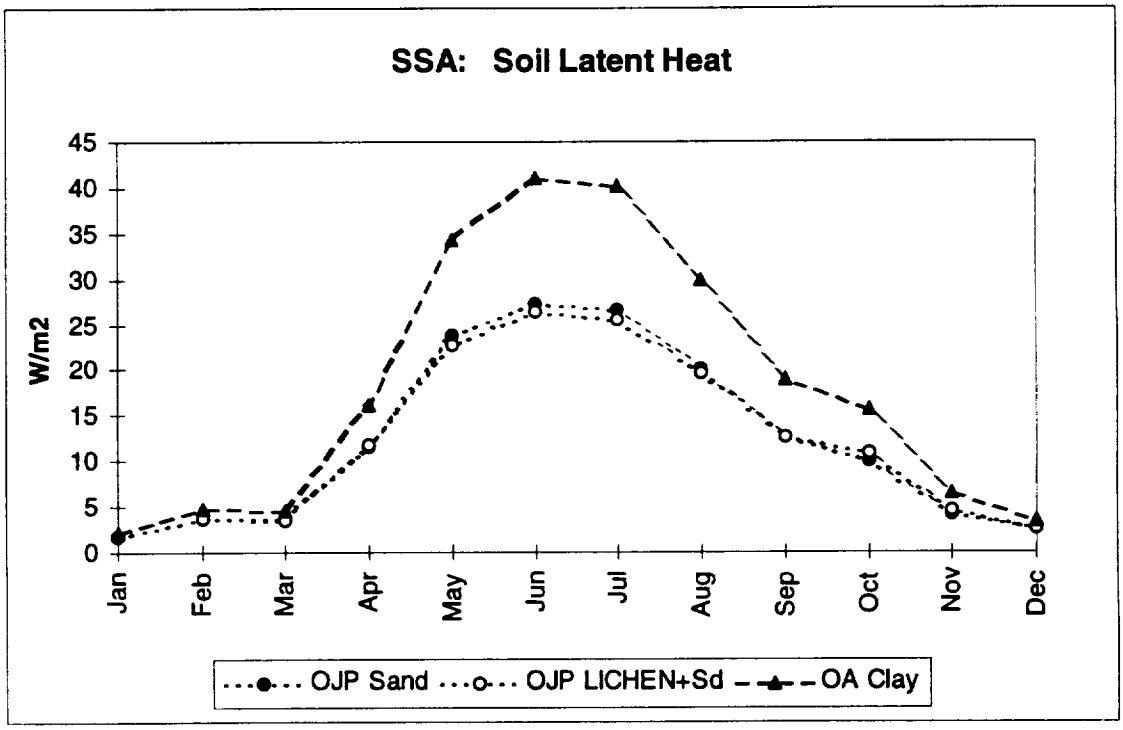

Figure 2.12: Soil latent heat for the Old Jack Pine and Old Aspen sites in the Northern and Southern Study Areas, using the 10-layer soil model.

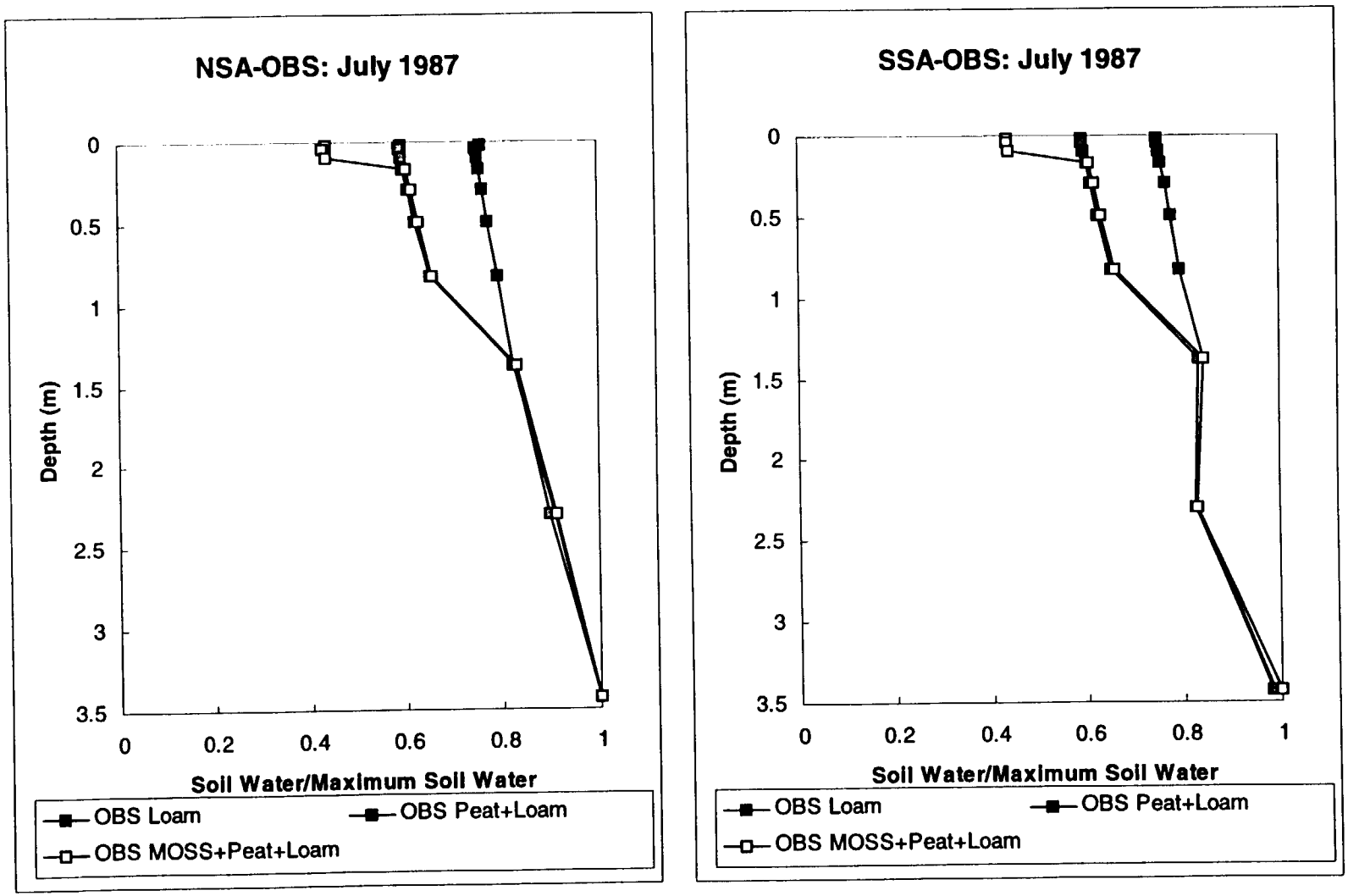

Figure 2.13 **July soil moisture profile for the Old Black Spruce sites in the Northern and Southern Study Areas, using the 10-layer soil model.**

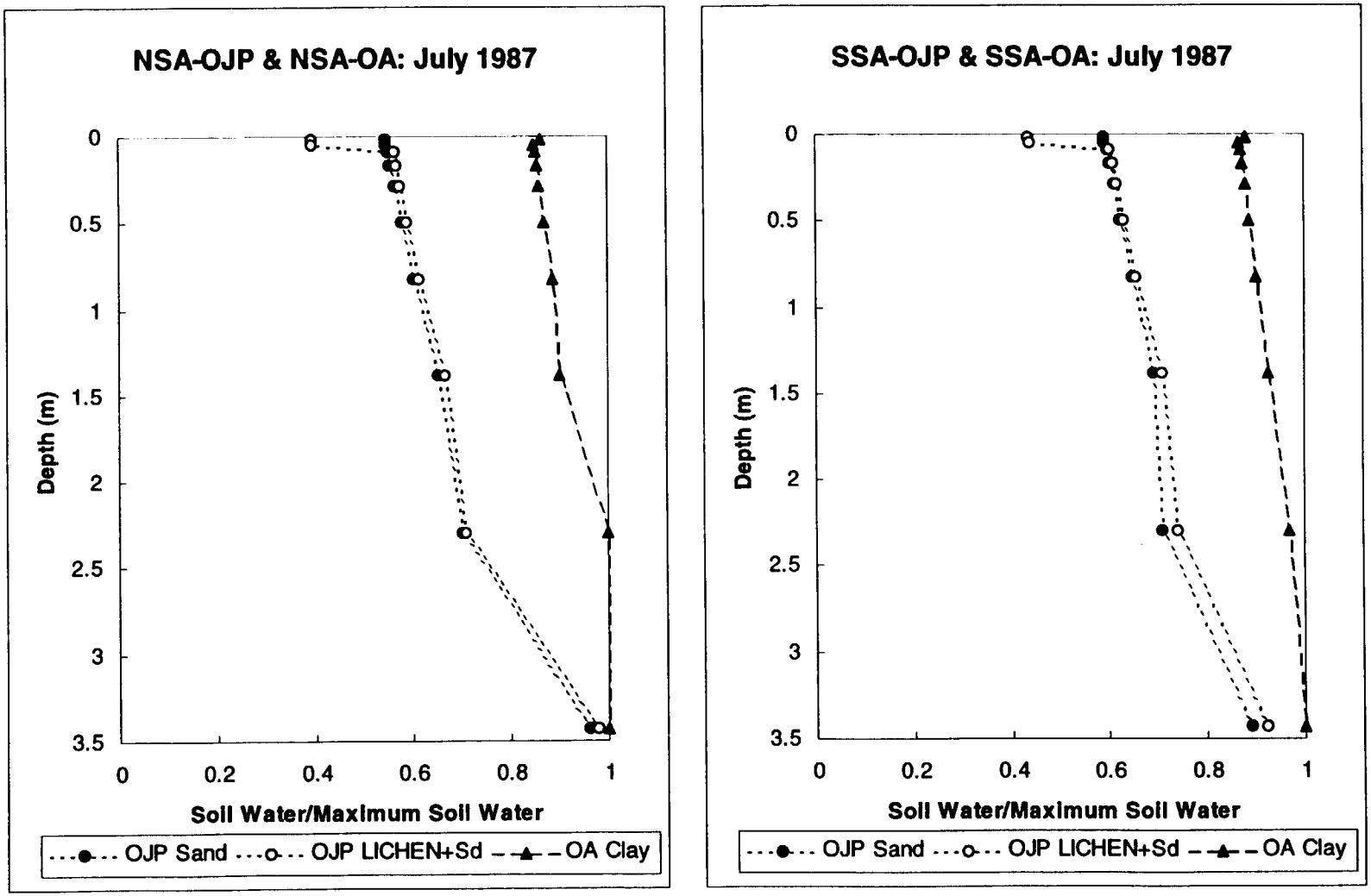

Figure 2.14 **July soil moisture profile Old Jack Pine and Old Aspen sites in the Northern and Southern Study Areas, using the 10-layer soil model.**

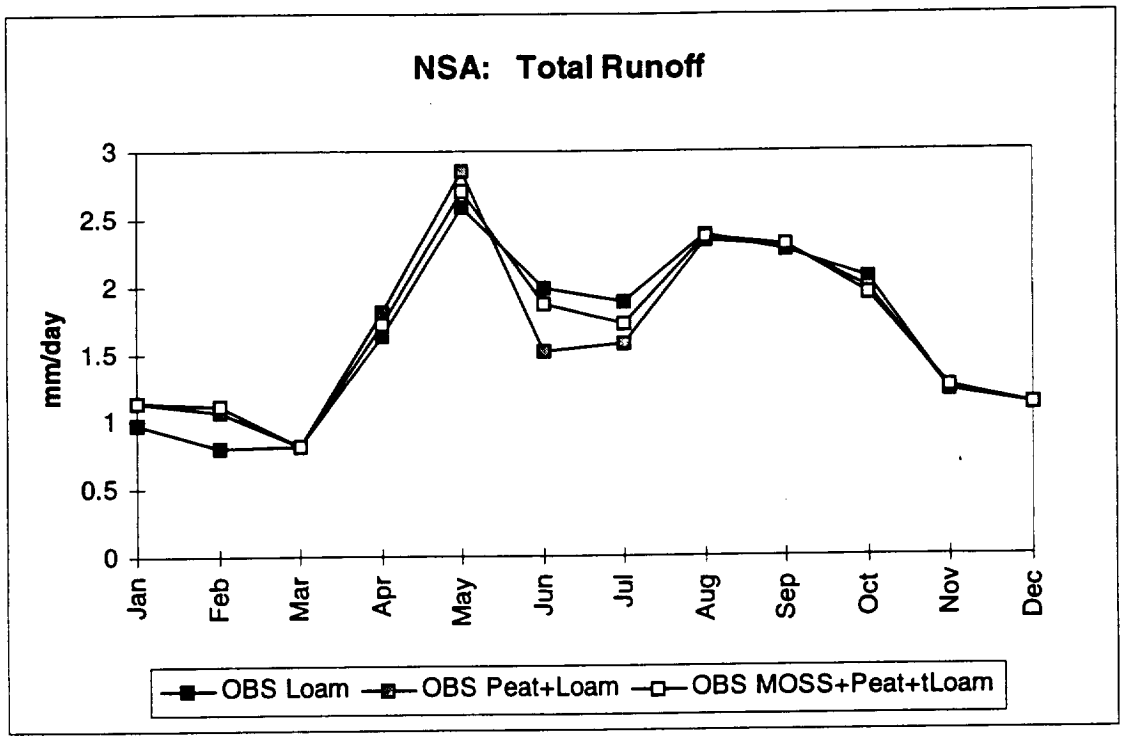

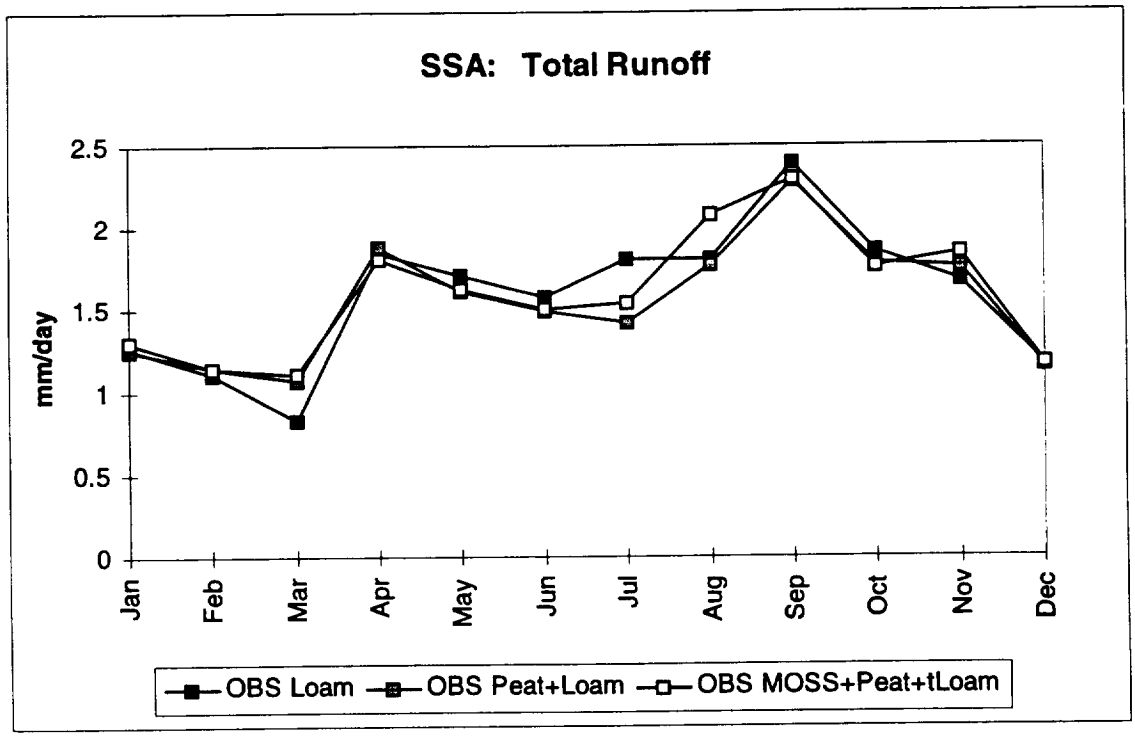

Figure 2.15: Total runoff for the Old Black Spruce sites in the Northern and Southern Study Areas, using the 10-layer soil model.

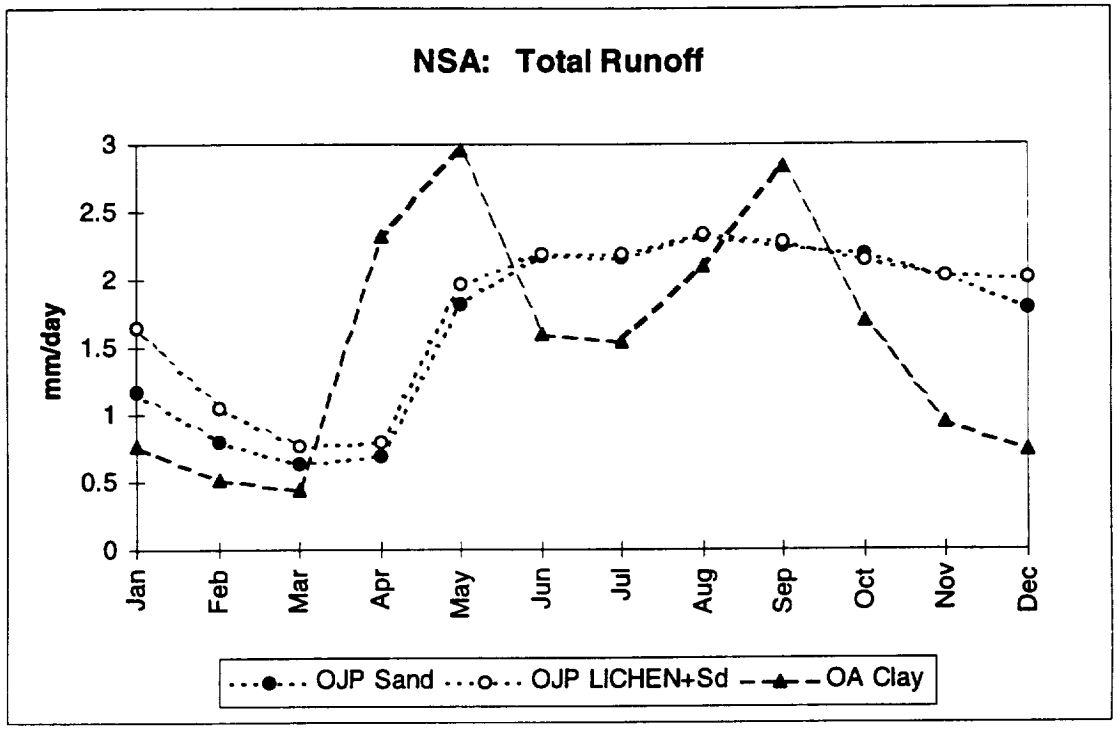

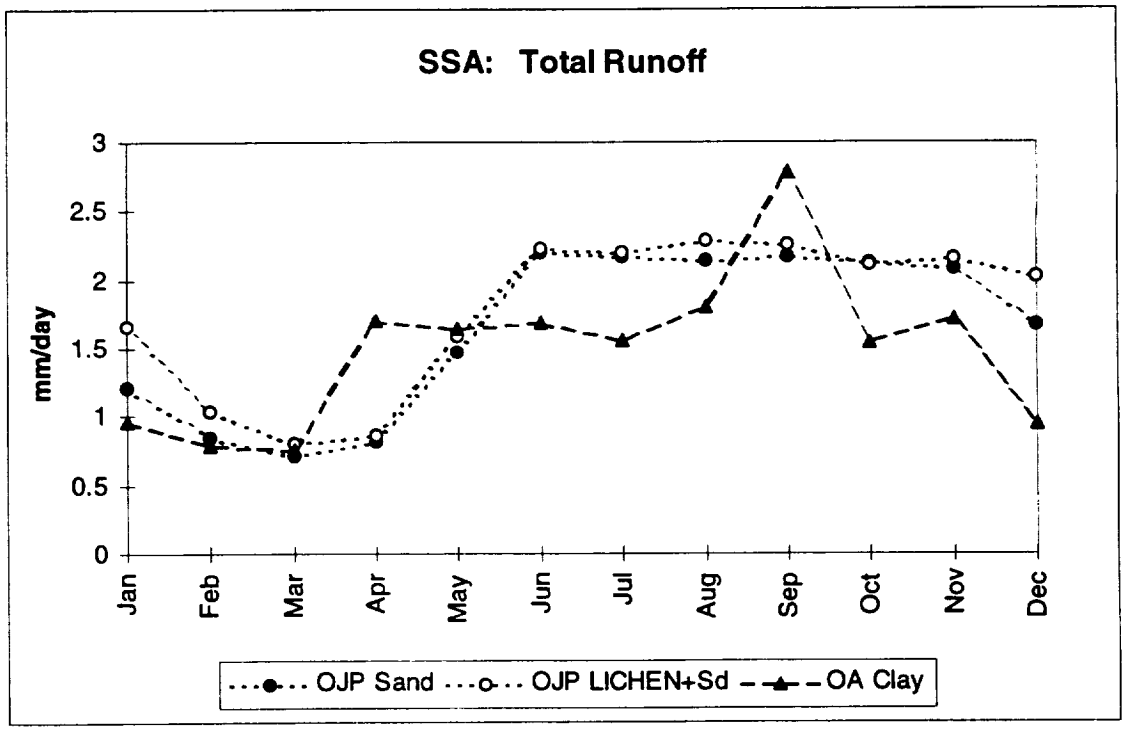

Figure 2.16: Total runoff for the Old Jack Pine and Old Aspen sites in the Northern and Southern Study Areas, using the 10-layer soil model.

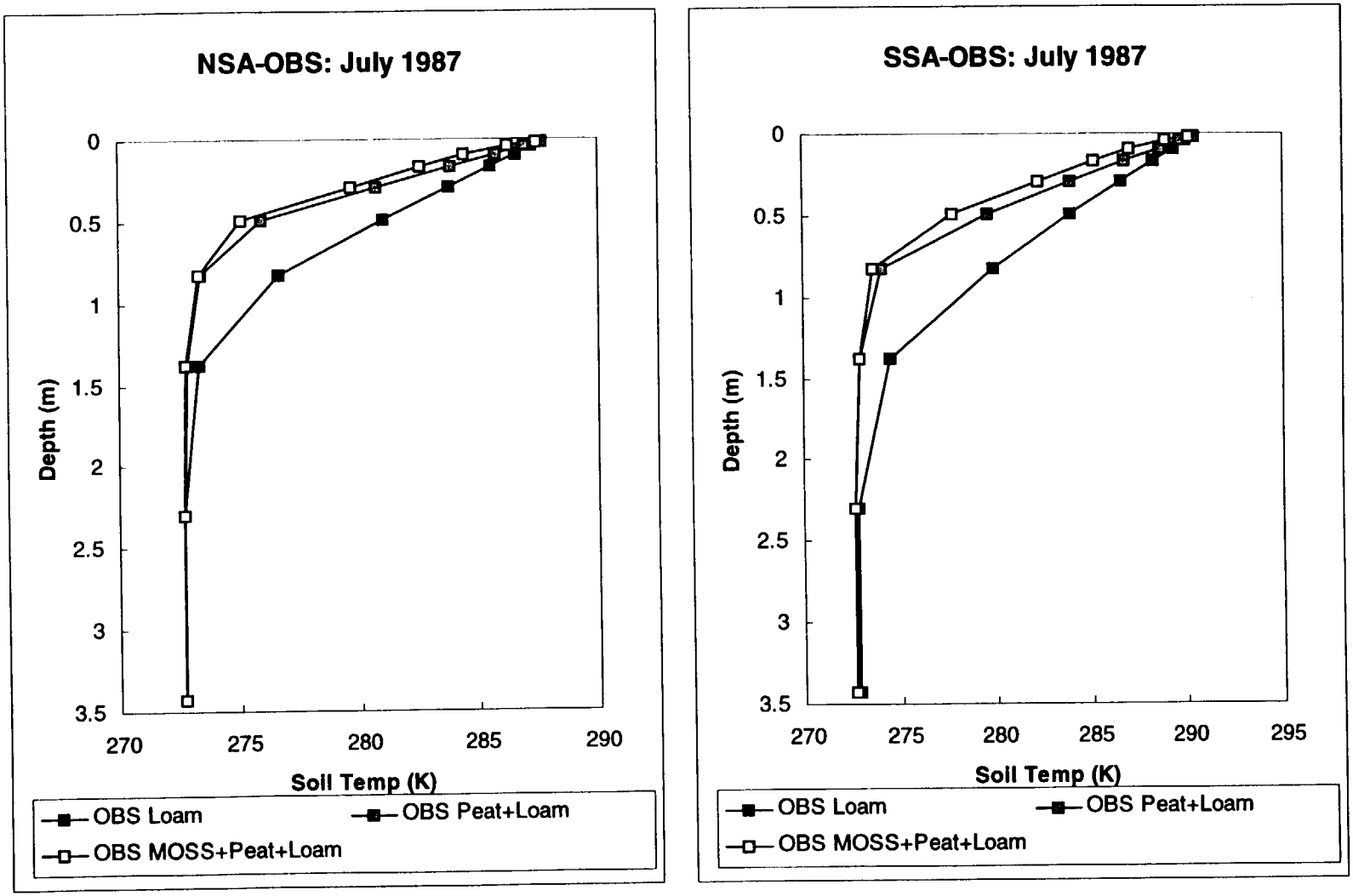

Figure 2.17 **July soil temperature profile for the Old Black Spruce sites in the Northern and Southern Study Areas, using the 10-layer soil model.**

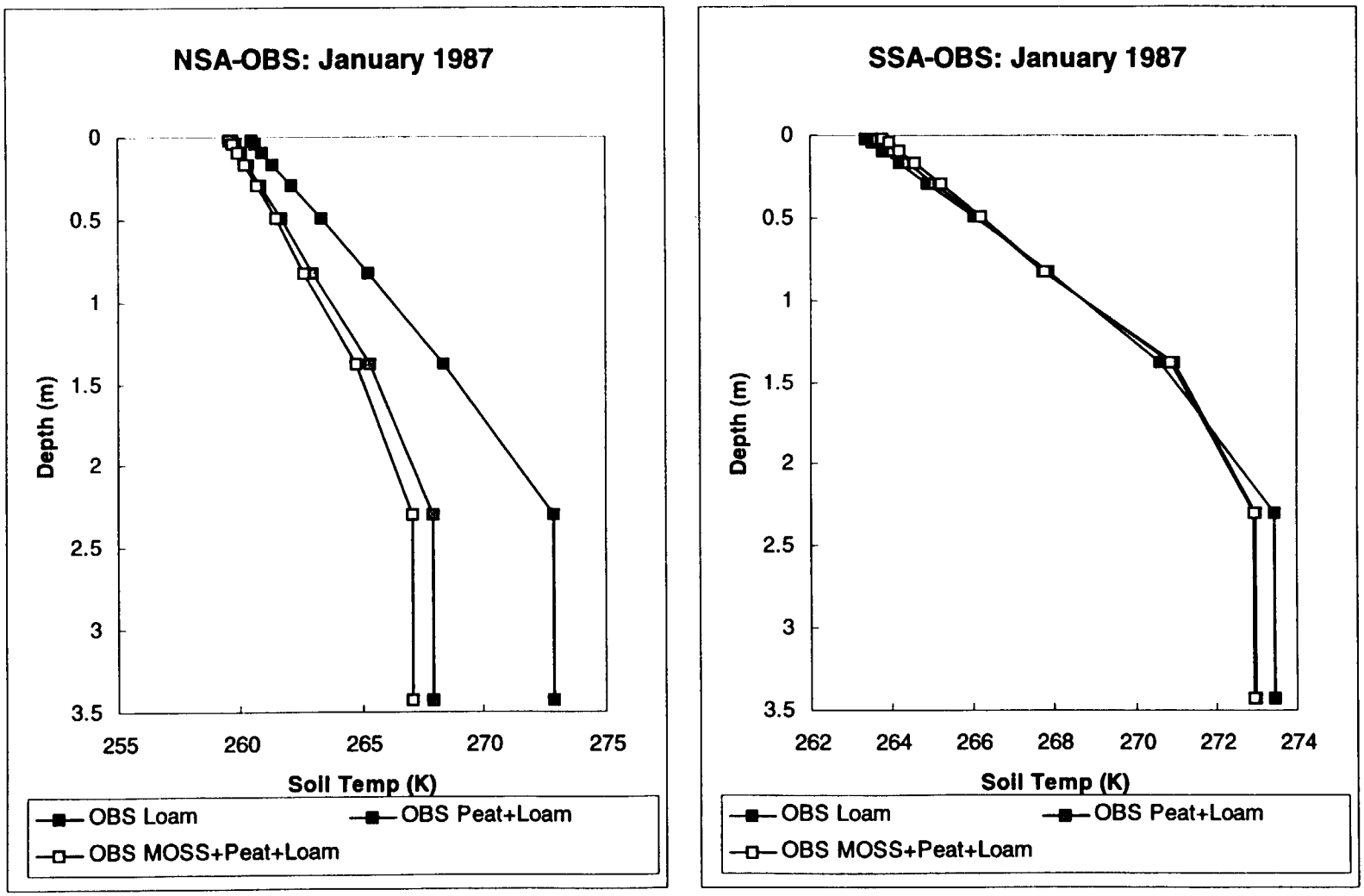

Figure 2.18 **January soil temperature profile for the Old Black Spruce sites in the Northern and Southern Study Areas, using the 10-layer soil model.**

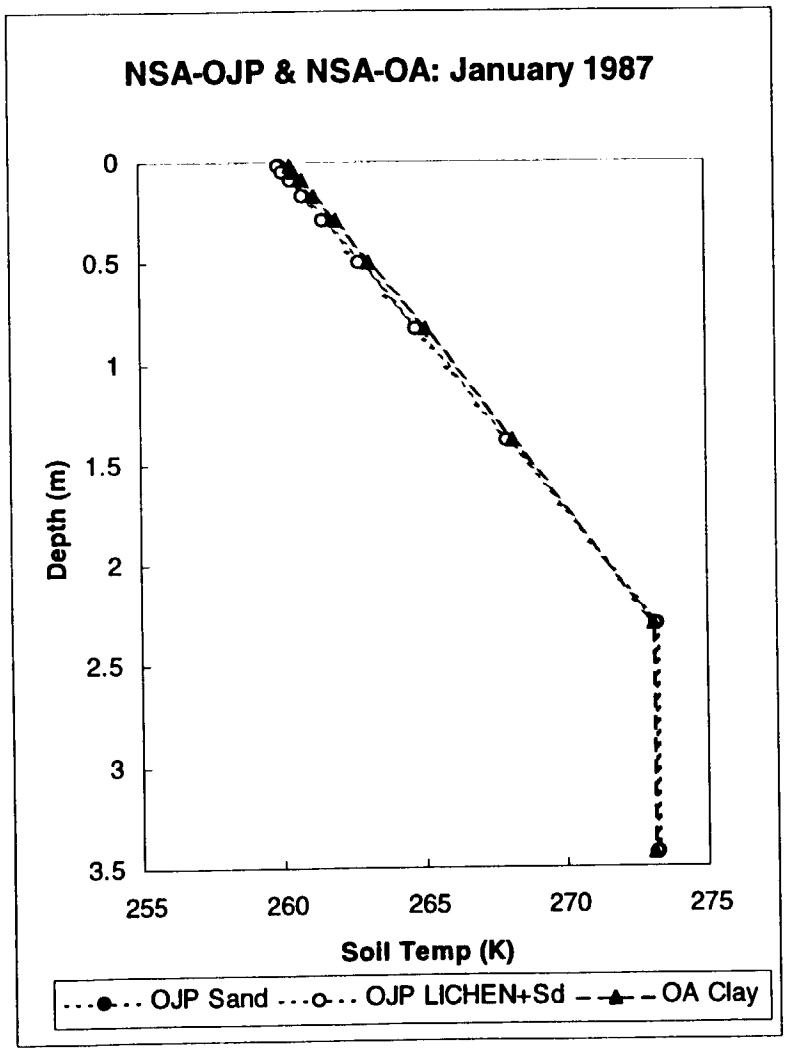

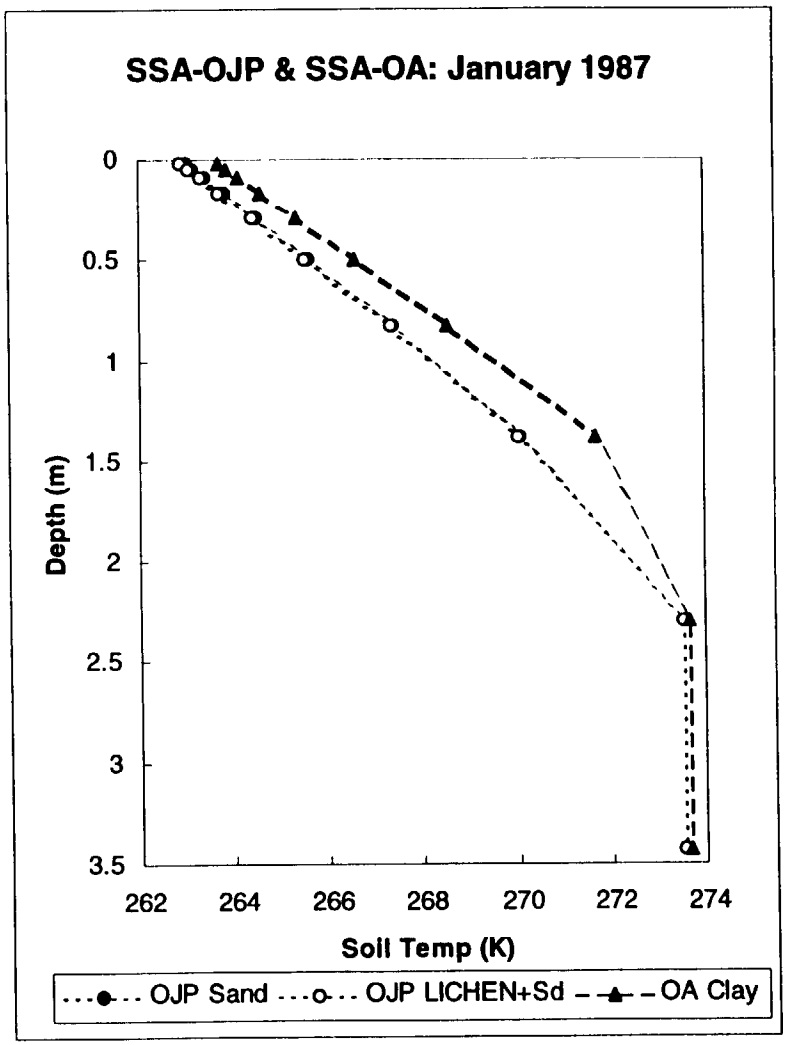

Figure 2.20 **January soil temperature profile for the Old Jack Pine and Old Aspen sites in the Northern and Southern Study Areas, using the 10-layer soil model.**

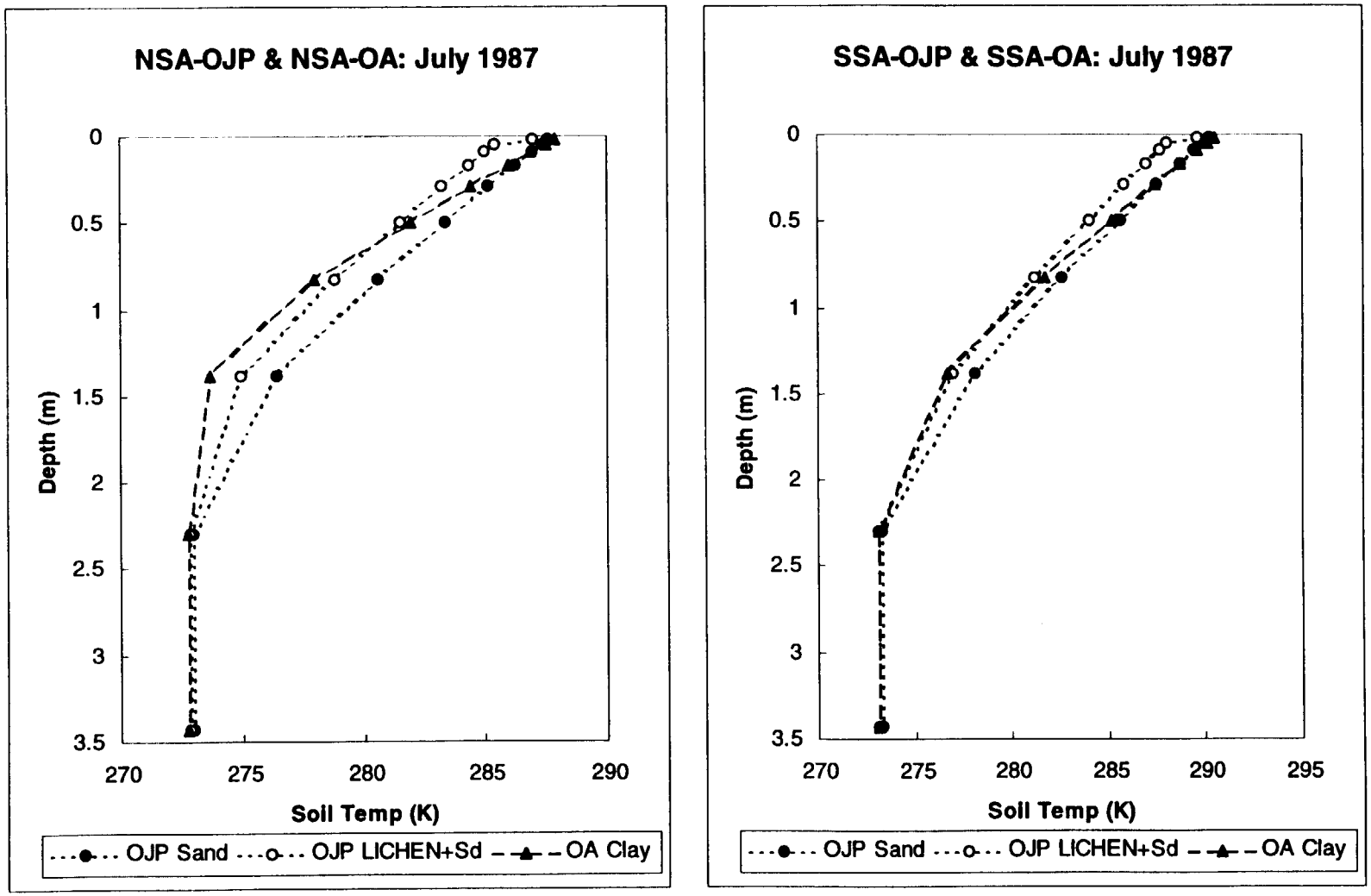

Figure 2.19 **July soil temperature profile for Old Jack Pine and Old Aspen sites in the Northern and Southern Study Areas, using the 10-layer soil model.**

3. A skin temperature diurnal cycle algorithm using satellite data, CCM3/BATS and surface observations (M. Jin)

3.1 Introduction

The diurnal cycle of land surface skin temperature (LSTD) is very important in the study of climate change (Jin et al., 1997; Betts and Ball, 1995). This variable, however, cannot be obtained globally from polar-orbiting satellites because satellites only pass a given area twice per day and because their infrared channels cannot observe the surface when the sky is cloudy.

In order to obtain skin temperature diurnal cycles as part of an EOS investigation, full use is made of satellite measurements and model results to solve this practical problem, by designing an algorithm combining CCM3/BATS with satellite and surface-based observations to interpolate satellite twice-daily skin temperature observations to the diurnal cycle. Solar radiation, clouds, soil wetness and vegetation effects on surface temperature were studied and considered in this algorithm.

We have evaluated this algorithm using FIFE and BOREAS surface field experiments. In addition, regional tests over the Mississippi river basin have been conducted using GOES-8 and AVHRR observations. Preliminary results show an encouraging accuracy of about 1.5-2°K for monthly cloud-free diurnal cycles.

3.2 Data

Surface observations employed from the BOREAS field experiment are from the Southern Study Area (SSA) for 1996. Betts and Ball (1995) provide site-averaged surface observations from the First ISLSCP Field Experiment (FIFE), conducted over a 15 km by 15 km area in central of Kansas from May 1987-1989 (Sellers et al., 1992).

3.3 Methodology

The diurnal cycle of temperature can be viewed as a composition of a diurnal average, daily periodic component, and random aperiodic component (noise). Thus,

$$T_{skin}(t) = \overline{T}_{skin} + \Delta T_{skin}(t) + T'_{skin}(t) \qquad \textbf{Eq. 3.1}$$

where $\overline{T}_{skin}$ is the daily average, $\Delta T_{skin}(t)$ is the relative diurnal cycle (the daily periodic component), and $T'_{skin}(t)$ is the instantaneous disturbance (noise) which is determined by the past or the on-going atmospheric-surface physical processes.

The basic assumption of our method is that the periodic component may vary in amplitude in response to past history and current meteorological conditions, but it has a shape that is invariant or varies at most with a limited number of known factors that do not change rapidly from day to day.

These may include latitude or season because of their control of incident solar radiation, type of vegetation cover because of its effect on albedo and roughness, and soil moisture because of its effect on evapotranspiration. With this assumption of invariance, the daily periodic shape can be estimated from the averaging of a sufficient number of days of hourly data. Given this shape, and assuming that the random noise component can be neglected, skin temperature has only two degrees of freedom so that twice a day measurements as from polar orbiting satellites can be used to estimate both the diurnal average and the daily periodic temperature components.

The first step is to determine skin temperature diurnal cycle typical shapes from CCM3/BATS. One year of hourly model simulations has been analyzed. True observations from BOREAS and FIFE have been employed to validate these typical patterns for different vegetation, soil moisture conditions and seasons.

The vegetation categories used here are defined by the standard BATS classes (see Dickinson et al., 1986). **Figure 3.1** shows the typical July pattern of skin temperature diurnal cycle for crop/mixed farming over 40°-45°N. We sampled and analyzed all model grids within this latitude band for this vegetation cover, normal soil moisture, and clear days. **Figure 3.1(a)** shows a box-and-whiskers diagram representing the range of data. The box in the middle of the diagram is bounded by the upper and lower quartiles, and thus locates the central 50 % of the data. The bar inside the box locates the median. The whiskers extend away from the box to extreme values showing the range from 2.5 % to

97.5 % of the data. **Figure 3.1(b)** gives the diurnal cycle with the daily average subtracted to remove as much of the latitude and altitude influences of different areas. However, it includes influences of vegetation, soil moisture, and solar radiation and thus this pattern varies as a function of latitude/season and surface characteristics. Normalization of such patterns is the "typical pattern" used in this work.

3.4 Results

The model-derived typical patterns have been evaluated by comparing with site-averaged 1987 FIFE observations (**Figure 3.2**), where mixed farming describes the vegetation type.

The monthly skin temperature diurnal cycles from FIFE agree with the modeled typical pattern quite well, with a root mean square less than 0. 5°K for each season. Similarly, the diurnal patterns are validated against data for a forest area at 50-55°N (**Figure 3.3**)

The small differences between the model and observation diurnal patterns may reflect soil moisture effects, differences between assumed and actual vegetation, or defects in the model climate simulations. Another reason for the discrepancy is that the modeled typical pattern is derived from all same-vegetation-grids within the latitude band, but the observation is only over one site or several sites, where the local conditions may be different from the large-scale averages. These differences suggest that measured skin temperature information should further constrain the typical pattern to improve the realism of the Land Skin Temperature (LST) diurnal cycle.

After we designed the LSTD algorithm, we used BOREAS observations to evaluate the results. **Figure 3.4-3.6** shows the cloud-free algorithm-produced diurnal cycle for the clear days in 1987 over FIFE. **Figure 3.4-3.6** are for January, July and September, representing winter, summer, and spring/fall respectively. FIFE 0400 LT (Local time) and 1600 LT measurements are used to fit the typical pattern. The mean values of algorithm-produced and observed diurnal cycle agree closely, with the root-mean-square errors only about 1.5 - 2.5°K. The algorithm is more accurate in summer than it is in winter because of less cloud contamination. Clear days on BOREAS July 1996 have also been used to test our algorithm. **Figure 3.7** is the same as **Figure 3.4**, except for

BOREAS. There were nine clear days in this period. **Figure 3.7(b)** is the average of these nine days. From **Figures 3.4** through **3.7**, we notice the root mean square error of the algorithm is less than 2.5°K. When the sky is covered by clouds for some period of time, the daily temperature variations cannot be precisely estimated without more frequent observations.

3.5 Conclusions

BOREAS observations from 1996 have been used to evaluate the CCM3/BATS modeled skin temperature diurnal cycle (LSTD). Analyses show that CCM3/BATS has produced realistic skin temperature diurnal cycle. The proposed LSTD algorithm has accuracy of 1-2°K for clear days (Jin and Dickinson, 1997).

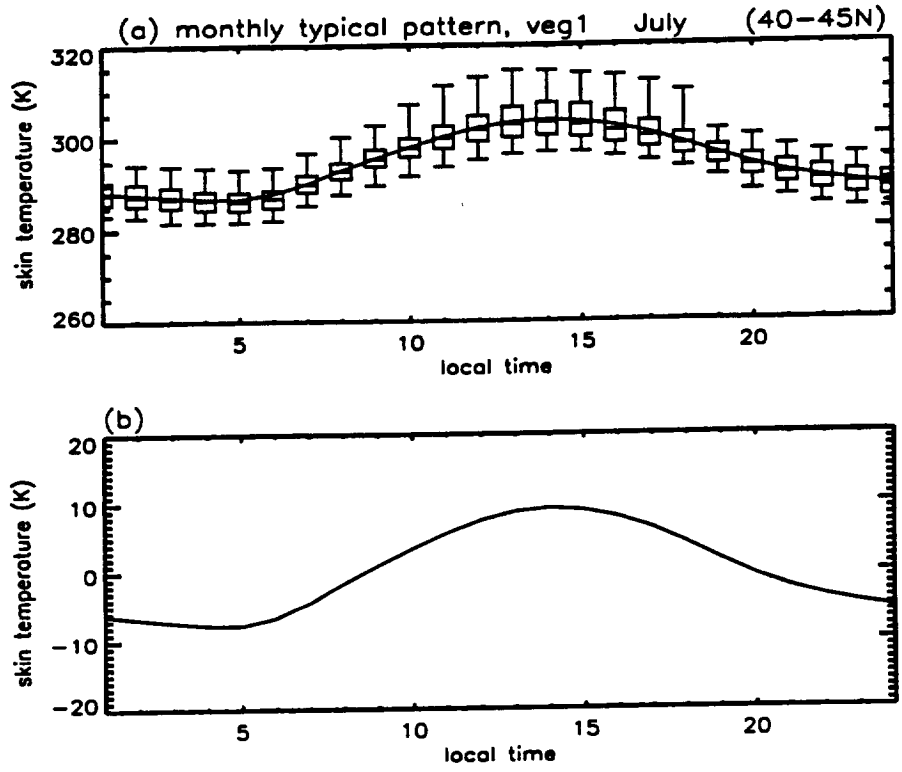

Figure 3.1: July grid-averaged skin temperature diurnal cycle over 40-45°N. Data is from modeled clear-day hourly simulations, for all grids where the vegetation type is crop/mixed farming. (a) Absolute diurnal cycle. (b) Diurnal cycle with the daily average removed from each sample.

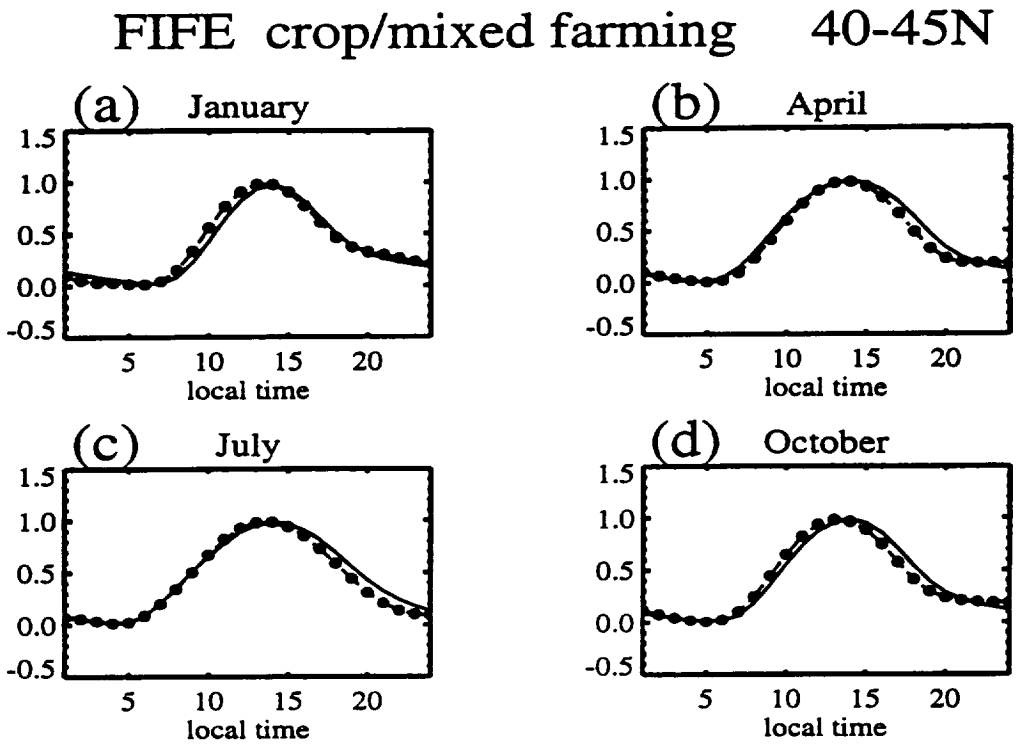

Figure 3.2: Comparison of the typical patterns (solid) and FIFE monthly observations (dot-dashed). FIFE data is site-averaged. Vegetation type over FIFE is crop/mixed farming. Typical patterns are derived from hourly CCM3/BATS simulations. For each month, only model clear days are sampled to get the pattern. (a) January; (b) April; (c) July; (d) October.

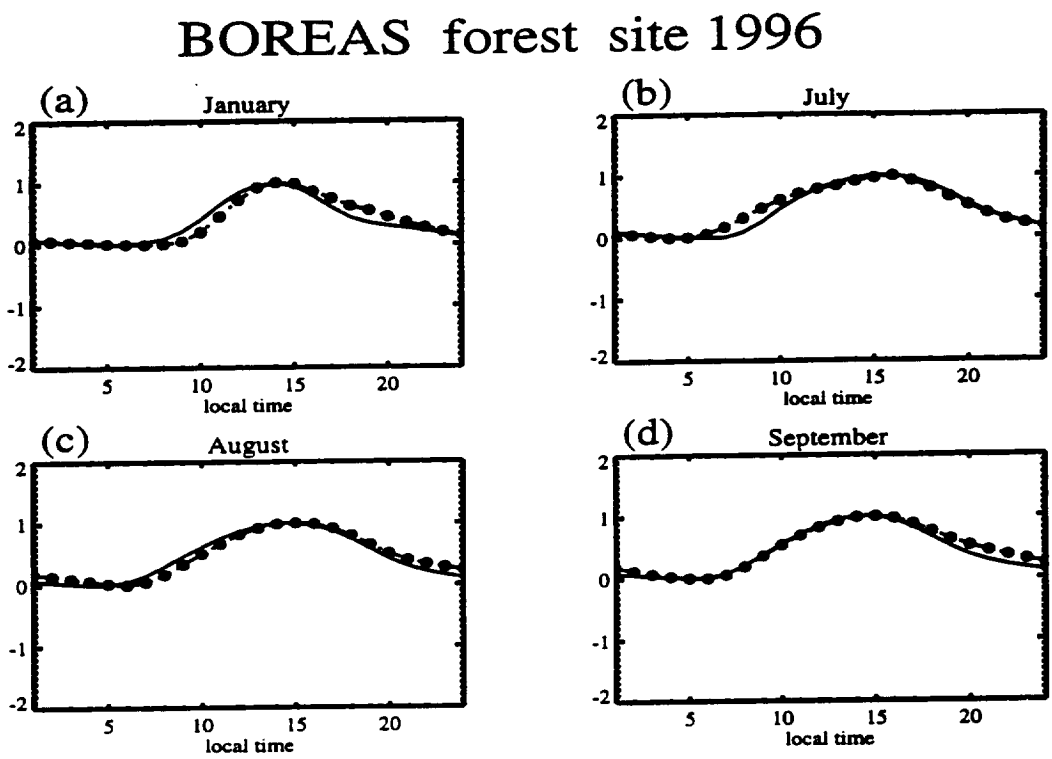

Figure 3.3: Same as Fig.3.2, except for BOREAS. Vegetation type over BOREAS is evergreen needleleaf tree. (a) January; (b) July; (c) August; (d) September. Solid line is for the model typical pattern, and dot-dashed line is from observation.

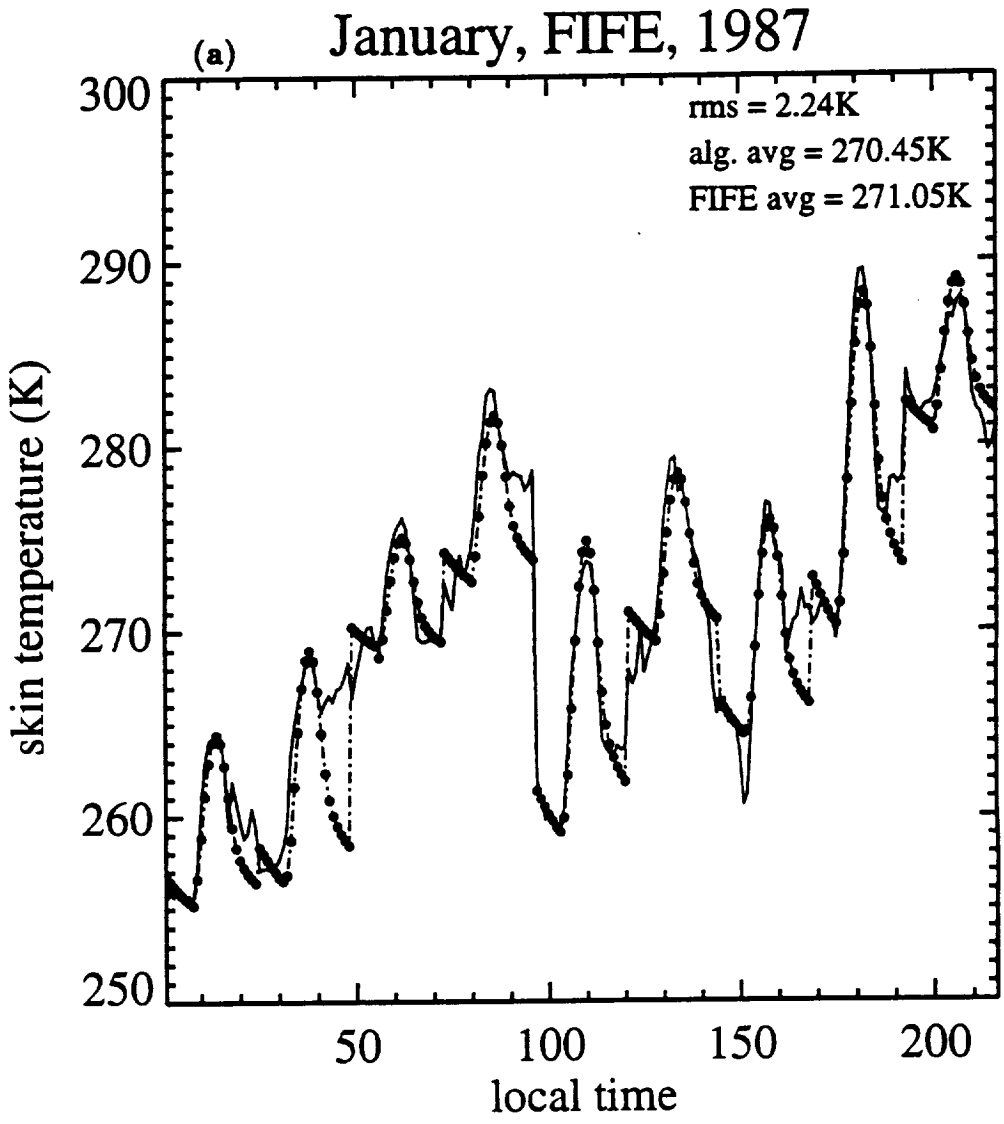

Figure 3.4 Comparison of the algorithm-produced diurnal cycle with FIFE observations for January 1987. Only clear days in each months are analyzed. The dotted line is the calculated diurnal cycle, and the solid line is from observations.

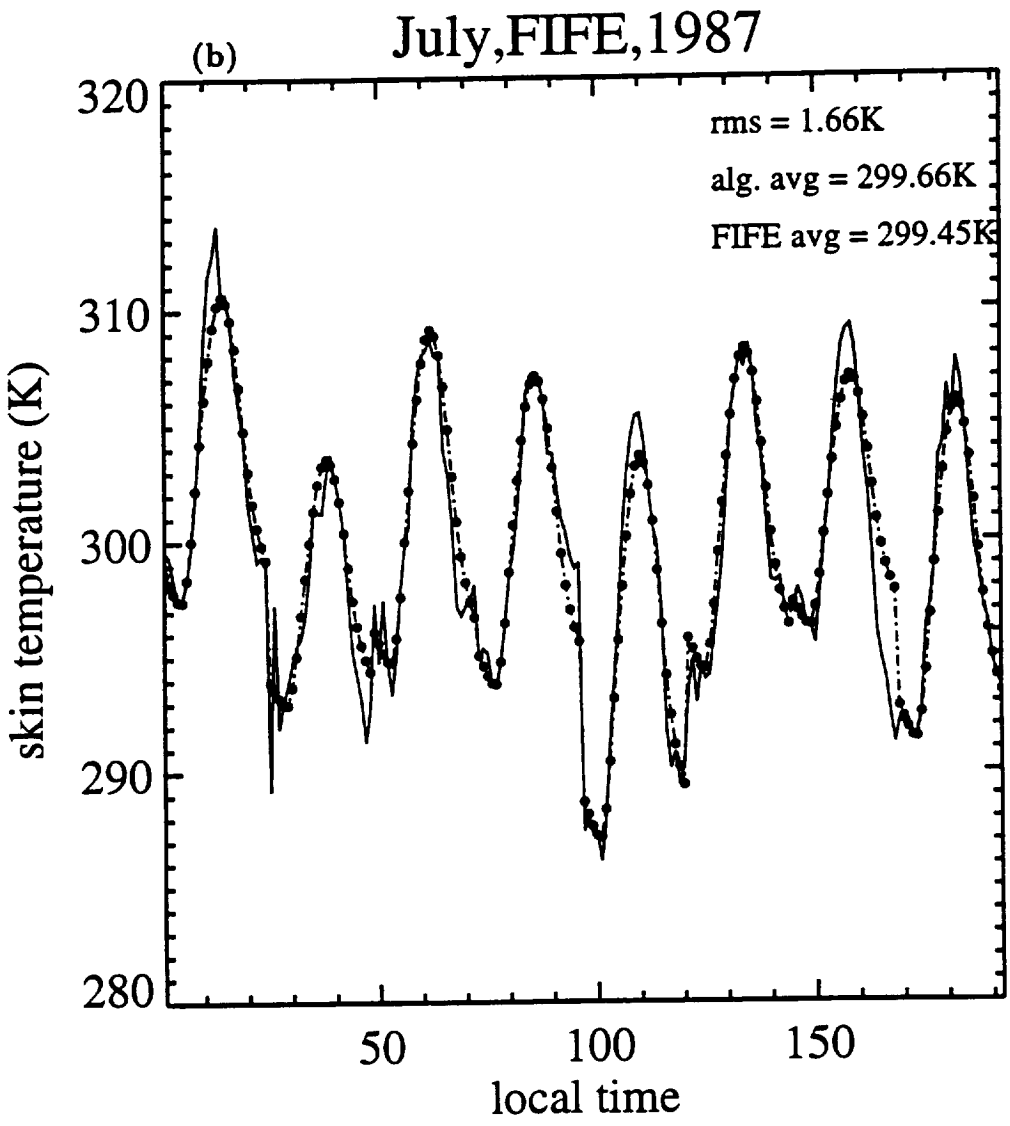

Figure 3.5 Comparison of the algorithm-produced diurnal cycle with FIFE observations for July 1987. Only clear days in each months are analyzed. The dotted line is the calculated diurnal cycle, and the solid line is from observations.

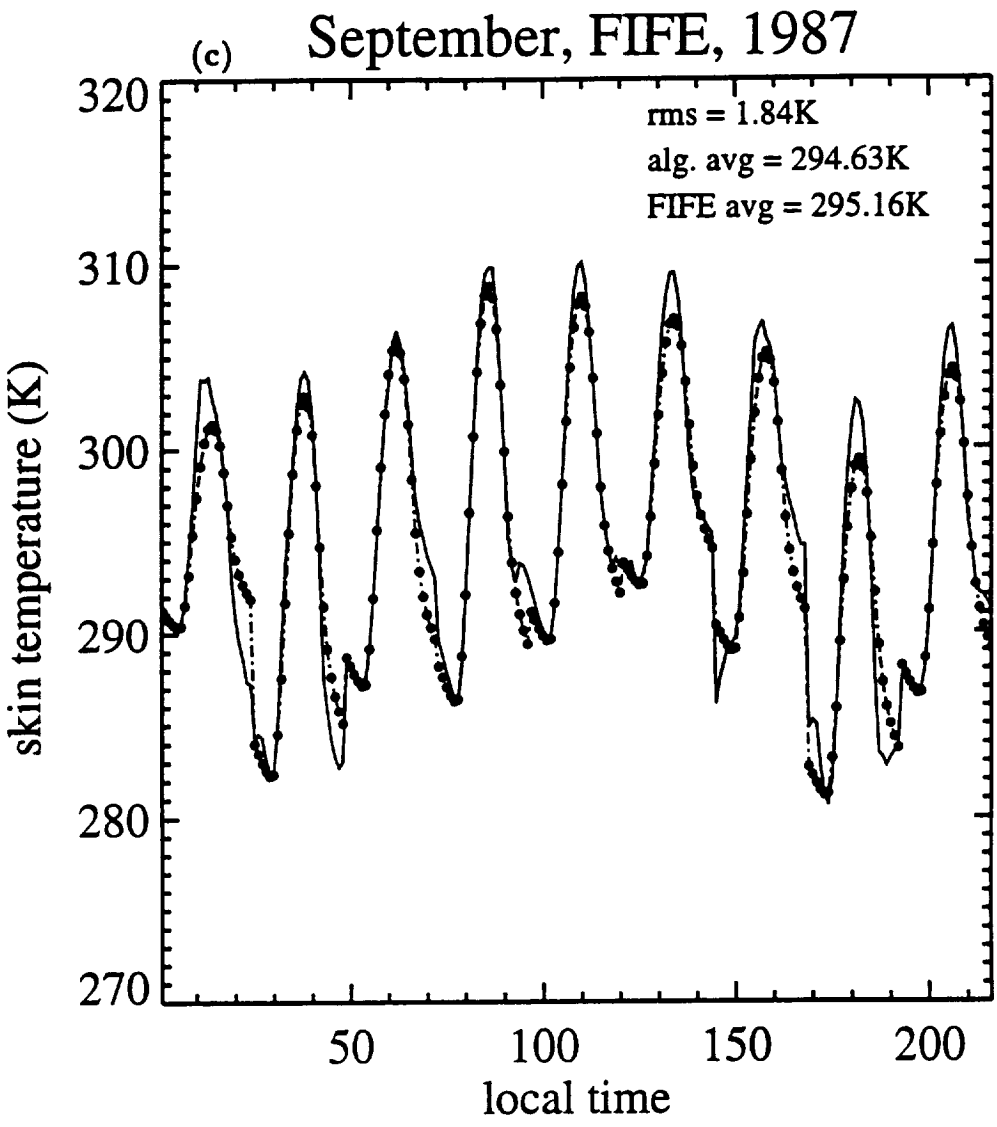

Figure 3.6 Comparison of the algorithm-produced diurnal cycle with FIFE observations for September 1987. Only clear days in each months are analyzed. The dotted line is the calculated diurnal cycle, and the solid line is from observations.

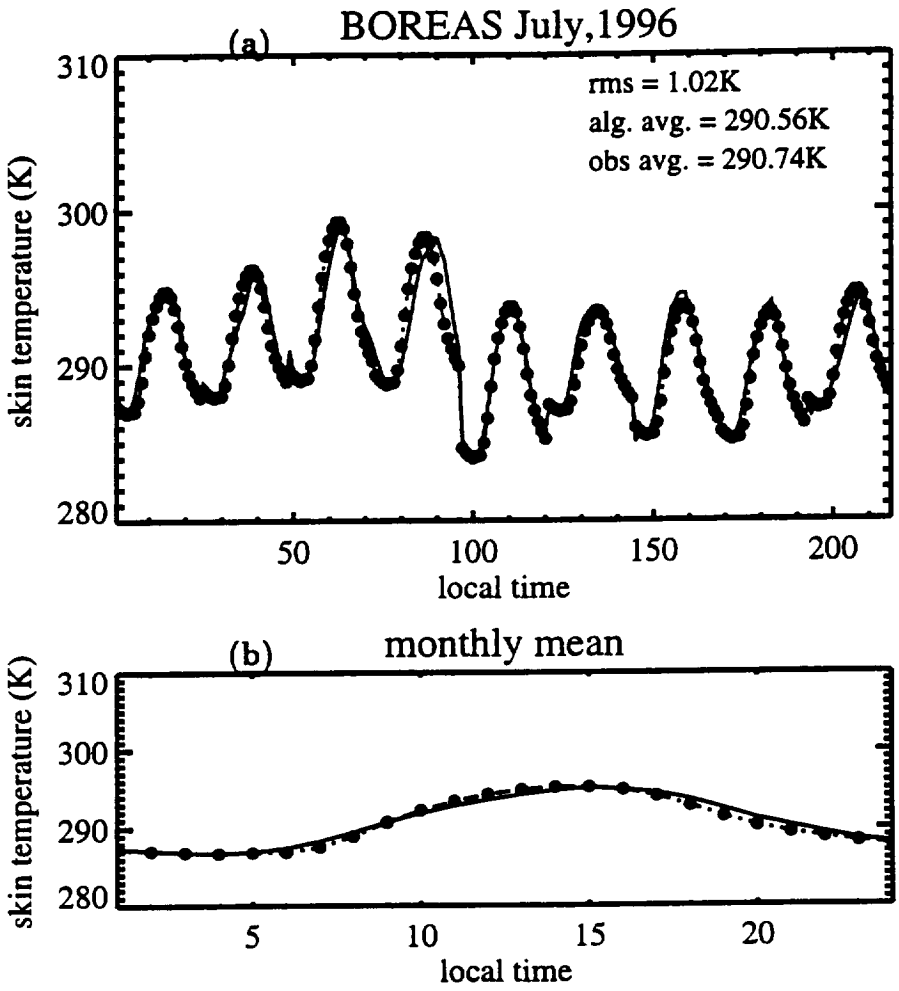

Figure 3.7 Comparison of the algorithm-produced diurnal cycle with BOREAS observations for July 1996. Only clear days in each months are analyzed. The dotted line is the calculated diurnal cycle, and the solid line is from observations.

4. Plant Chemistry Algorithm (K. J. Schaudt)

The general structure of the plant chemistry algorithm, which is designed to remotely sense (from satellites) the ratio of carbon to nitrogen in the plants or trees, was developed prior to BOREAS with laboratory data which was not truly suitable for the job. As observations of leaf reflectance and transmittance of fresh (not dried) leaves along with chemical analysis of the carbon and nitrogen content of the leaves have been extremely hard to find, little progress was made in this research. BOREAS was the first opportunity to obtain both reflectance and transmittance of freshly collected leaves along with the chemical analysis of these leaves. However, the chemical analysis was not given high priority and was not begun until the spring of 1996 and not available until late fall 1996. The focus on the development of the moss and lichen modeling as reported here has made it difficult to make much progress in exploiting this information.

5. Other BOREAS Studies with Off-line BATS (J. C. Morrill)

5.1 Introduction

Several studies separate from the moss/lichen incorporation have also been done at the University of Arizona. These include:

1) Running BATS with the 1989 data as part of the BOREAS Modeling Exercise #1. Results are described in Coughlan and Running (1994).

2) Doing some initial simulations over the NSA and SSA sites with the ISLSCP Initiative 1 Data when it was first released. These were presented at the IUGG Summer Meeting in Boulder, CO. in 1995.

3) While running BATS for GSWP, looking closely at the BOREAS sites as two of the sixteen global sites chosen for diurnal cycle studies. Part of our GSWP work has included a study on the sensitivity of BATS to changes in the diurnal cycle of the downward longwave radiation forcing data.

Most of these studies have served primarily to test BATS sensitivity to boreal forest soil and vegetation parameters. The data from the standard BATS runs are presented as the non-moss/lichen runs in section 2.

5.2 The sensitivity of BATS to changes in the diurnal distribution of downward longwave radiation.

(Some of the material in sections 5.2 through 5.4 previously appeared in Morrill and Dickinson, 1997a, reprinted in its entirety in ***Appendix A****.)*

As part of our NOAA GEWEX work, we are running BATS for the GEWEX/ISLSCP Global Soil Wetness Project. GSWP has been using the 6-hourly atmospheric forcing data from the ISLSCP Initiative 1 data set to drive a dozen land surface models. The accuracy of the 6-hour downward longwave forcing data on the ISLSCP Initiative 1 data was questioned by GSWP participants. In many areas, the data seem to be offset by several hours from what is expected, with maximum downward longwave radiation consistently occurring late at night. Morrill and Dickinson (1997a) examined the

sensitivity of the Biosphere-Atmosphere Transfer Scheme (BATS) to modifying the distribution of the given downwards longwave radiation over the daily cycle in two ways: first by shifting the timing of the input values, second by using a constant average value for each day. That paper focused on continental-scale monthly averages. Of the large-scale average energy terms, only sensible heat showed any significant change. Most of the water balance terms remained virtually unchanged, including root-zone soil moisture values of primary interest to GSWP. For this report, we will present some supplemental material, discussing the effects the input changes have on the monthly average diurnal cycles of energy and water fluxes at the points nearest the two BOREAS study areas. A forthcoming paper (Morrill and Dickinson, 1997b) will present a more detailed analysis of the problem, with a greater focus on changes at smaller temporal and spatial scales.

5.3 The downward longwave radiation data

Downward longwave radiation is more difficult to measure than shortwave radiation, so it is frequently estimated based on easier-to-measure quantities, such as screen temperature and water vapor pressure (Swinbank, 1968; Brutsaert, 1975; Hatfield et al., 1983; Culf and Gash, 1993). Both measured and estimated values of incoming longwave fluxes show similar predictable diurnal trends. In a study by Culf and Gash (1993), which compares clear-sky observations with equation predictions for an area in Niger, the observed and calculated downwards longwave flux both clearly peak from about 1300 to 1900 hours (GMT and local time), with a minimum at 0600. Measured incoming longwave values at a site in South Carolina (Dennehy and McMahon, 1987) and calculated values at several sites in Florida (Walsh, 1971) also show values peaking in the late afternoon/early evening hours .

The ISLSCP Initiative 1 6-hourly forcing data (Sellers et al., 1995b, Meeson et al. 1995) consists of total precipitation, convective precipitation, surface air temperature, dew point temperature, mean wind speed, atmospheric pressure, downward shortwave radiation and downward longwave radiation. The shortwave and longwave radiation values are hybrid products. The 6-hourly downwards longwave radiation was calculated by:

$$LD_6 = LN_L/\Sigma(LN_E)*L_E+\varepsilon*B*[(T1_E+T_E/2]^4 \qquad \textbf{Eq. 5.1}$$

where LD_6 is the hybrid 6-hourly downward longwave radiation, LN_L is the Langley Research Center monthly mean surface longwave net radiation, LN_E is the ECMWF 6-hourly surface net longwave radiation, $T1_E$ is the ECMWF surface temperature at time t, T_E is the ECMWF surface temperature at time (t-1), ε is the emissivity (0.996 for all land surfaces in ECMWF) and B is the Stefan-Boltzman constant.

The data are in 6-hour blocks (average values for the 6-hour time periods beginning 0000, 0600, 1200 and 1800 GMT), so it was necessary to arbitrarily distribute these values among the hourly timesteps. The GSWP project guidelines state that for downwards longwave radiation, air temperature, dew-point temperature, wind speed and surface pressure the average value is to occur three hours into the time period (0300, 0900, 1500, and 1800 GMT) and all other hourly values are to be interpolated linearly between those values. Therefore the diurnal "cycles" of these five variables will consist of only four straight lines.

The result of these interpolations is that downward longwave radiation consistently peaks after sunset (usually between 2000 and 0200 local time, depending upon the location) and minimum downwards longwave radiation occurs in the late morning to early afternoon (0800 to 1600 local time). The diurnal range of values for longwave radiation varies depending upon location and season. At some points the difference between maximum and minimum radiation is less than 2 W/m^2, in other areas it is almost 200 W/m^2. Air temperature follows the expected pattern of peaking in the mid-late afternoons (1400 to 1900 local time). Shortwave radiation was distributed as a function of the cosine of the local zenith angle, with maximum radiation always occurring near local noon. The unaltered shortwave radiation input shows no sign of temporal offsetting.

5.4 BATS sensitivity simulations

BATS was initialized according to project guidelines (soil moisture was initialized at 75% of capacity, surface and sub-surface ground temperatures at the December 1987

mean air temperature) and allowed to spin up for twenty years. Then two years were run for the control case and each of the sensitivity simulations.

The first simulation was the control run (CON) using the unmodified forcing data. For the second run, the entire longwave data set was shifted forward 6 hours in time, so that the maximum and minimum longwave radiation occurred closer to the maximum and minimum surface temperatures. For the third run, the values for the four longwave files for each date were averaged, so that at any given point the hourly longwave radiation was constant throughout each 24-hour period. These second and third simulations will be referred to as the shifted longwave (SLW) case and the average longwave (ALW) case. **Figure 5.1** (and **Appendix A Figure 1**) show examples of the three different longwave diurnal cycles and their relationship to the air temperature cycle. The total downward longwave radiation for each day will be the same for all three simulations. The SLW downward longwave radiation diurnal cycle is clearly similar to that of the surface air temperature, while the CON SLW downward longwave radiation peaks from 1900-0100 local time, as the air temperature is decreasing.

The model was run globally at a 1° by 1° resolution over all land points. The two points determined to be closest to the BOREAS study areas were at 55.5°N, 98.5°W (NSA) and 53.5°N, 105.5°W (SSA).

5.5 Results

In the winter at both BOREAS sites, there is only a small diurnal variation of a few W/m^2 in the downward longwave radiation. Therefore, altering the diurnal distribution has a very little effect to the downward longwave radiation at any particular time (no more than a 2 % increase or decrease at any time). The results to the net longwave radiation at individual timesteps is shown in **Table 5.1**. Note that the range of percent change is greater for the SLW simulation than the ALW simulation. The daily average change to net longwave radiation is not very great, always less than 1%. Daily average sensible heat increases slightly while latent heat decreases.

Table 5.1: Maximum and average changes of net longwave radiation during January diurnal cycles.

	SLW vs CON			ALW vs CON		
	Maximum negative % change	Maximum positive % change	Average % change	Maximum negative % change	Maximum positive % change	Average % change
NSA 1987	-8.4	5.2	-0.07	-5.2	4.7	0.30
NSA 1988	-7.8	15.0	0.37	-7.7	6.6	-0.14
SSA 1987	-9.6	12.2	-0.46	-4.2	7.9	0.08
SSA 1988	-6.7	8.0	0.65	-4.9	6.9	-0.07

In July, the effects of the altered downward longwave radiation on the energy budget are much more noticeable. In the SLW simulation, downward longwave radiation at some timesteps can vary by as much as 12% for the control simulation, with the ALW downward longwave radiation can vary by 6%. Daily average net longwave radiation increases by at least 10% with SLW radiation and 4-9% in the ALW radiation (**Table 5.2** and **Figure 5.1**).

Table 5.2: Maximum and average changes of net longwave radiation during July diurnal cycles.

	SLW vs CON			ALW vs CON		
	Maximum negative % change	Maximum positive % change	Average % change	Maximum negative % change	Maximum positive % change	Average % change
NSA 1987	-33	99	10	-28	47	4
NSA 1988	-38	138	15	-40	51	5
SSA 1987	-36	121	13	-27	70	7
SSA 1988	-43	217	25	-48	98	9

In July, upwards longwave radiation, latent heat flux, sensible heat flux and soil heat flux follow similar patterns to the downward longwave radiation, with SLW > ALW > CON during the late morning through the early evening, while CON > ALW > SLW at night (**Figures 5.2** and **5.3**). Upwards longwave radiation decreased by an average of less than 1%, latent heat decreased 4-10 %, sensible heat flux increased significantly, and the soil heat flux change slightly with no noticeable pattern. July daily average sensible heat at these two sites showed the greatest percent increase, around 25% for the SLW simulation and 13% for the ALW simulation. **Figure 5.3** shows that in July 1987 at Southern Study Area, the SLW sensible heat was often more than 20 W/m^2 greater than the CON sensible heat. (This is much higher than the 4-5 % average increased over all of North America). Runoff increased as evaporation and transpiration decreased, but not with any consistent diurnal pattern. Despite the energy fluctuations, the water balance was not noticeably affected. Surface soil water decreased by less than 0.5% in the SSA, and increased by less than 1% in the NSA.

The only time that the SLW and ALW water terms show any significant diurnal differences from the CON simulation is during the transitional months. Changes in net radiation can significantly affect the timing of snowmelt and any resultant runoff. Figures 5.4-5.5 show snowmelt and total runoff for April 1987 for the Northern and Southern Study Areas. More snowmelt occurs from 0900-1000 in the ALW simulation, when its downward longwave radiation is the greatest, and both the SLW and ALW have more snowmelt from 1200-1500. These snowmelt peaks correspond to similarly-timed peaks in total runoff. Snowmelt can be increased by 25% at some timesteps, while runoff can increase by 60%.

5.6 Conclusions

The distribution of downward longwave radiation over the diurnal cycle can have a noticeable effect on the energy and water budget terms, especially during the months for which the diurnal variation is the greatest. These effects are likely to be greater at some location than others, and will probably be more important on smaller spatial scales. Many of these changes that seem large for one timestep are just noise that will be

averaged out over the course of a day or a month. Soil water content, for example, seems fairly immune to the changes in energy, which is good for GSWP and anyone else concerned only with soil moisture. On the other hand, sensible heat seems to be affected regardless of the temporal and spatial scale of the study. However, those who wish to use the ISLSCP Initiative 1 data for small-scale studies, or who are trying to use site-specific diurnal observational data to validate the model output, may need to consider testing the sensitivity of each model/site to the longwave radiation.

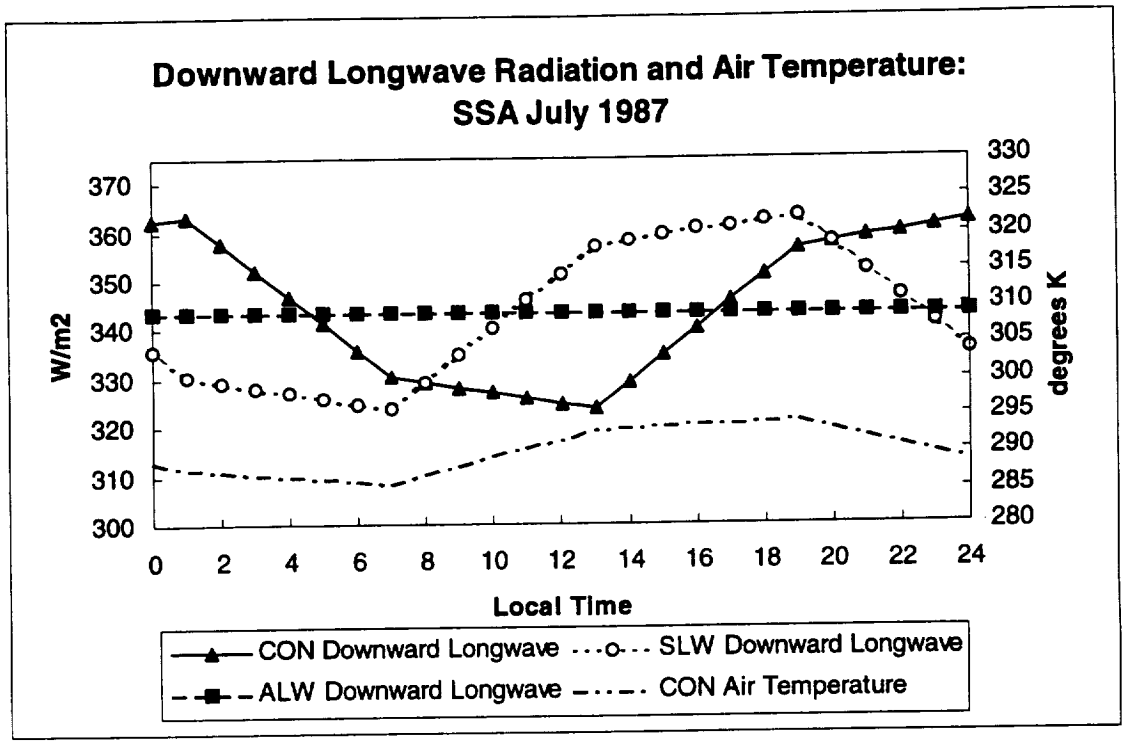

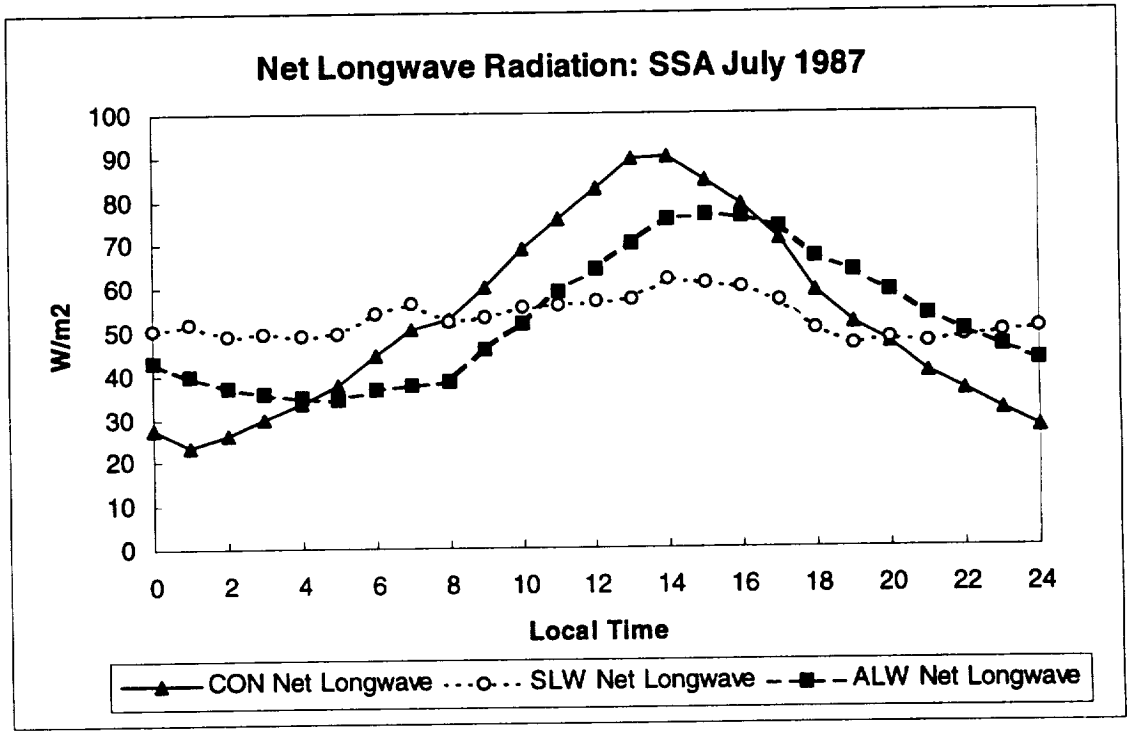

Figure 5.1: **July 1987 diurnal cycles of surface air temperature, downwards longwave radiation and net longwave radiation, at 53.5°N, 105.5°W.**

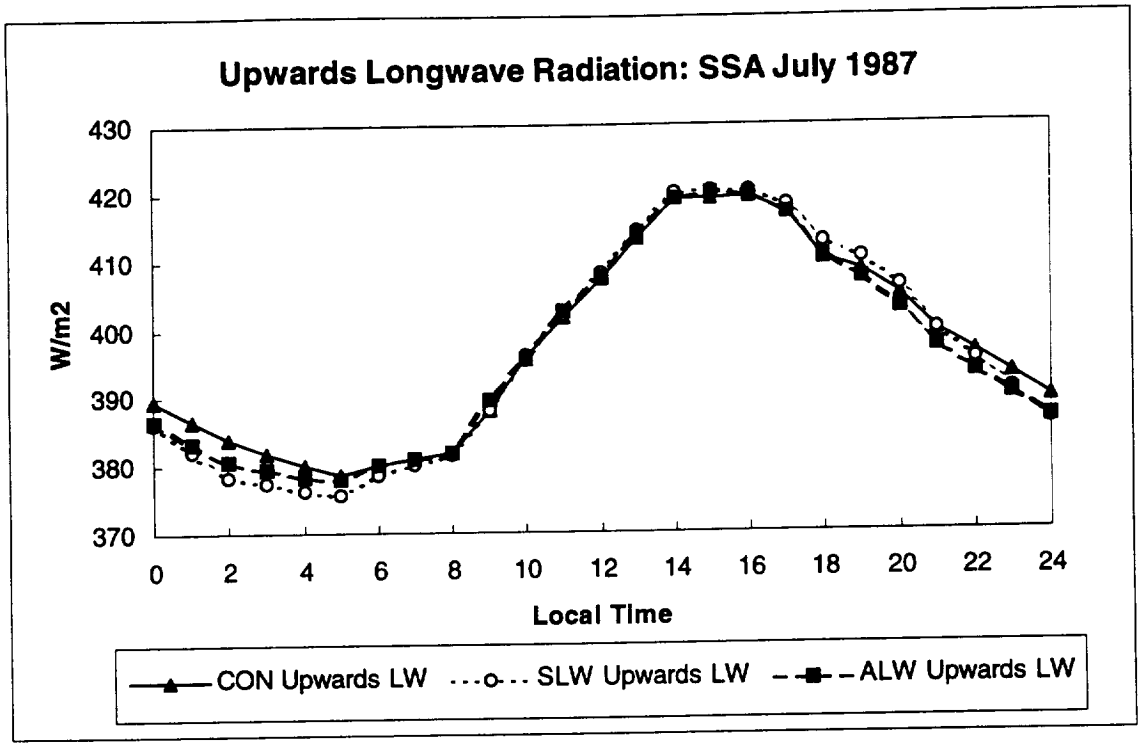

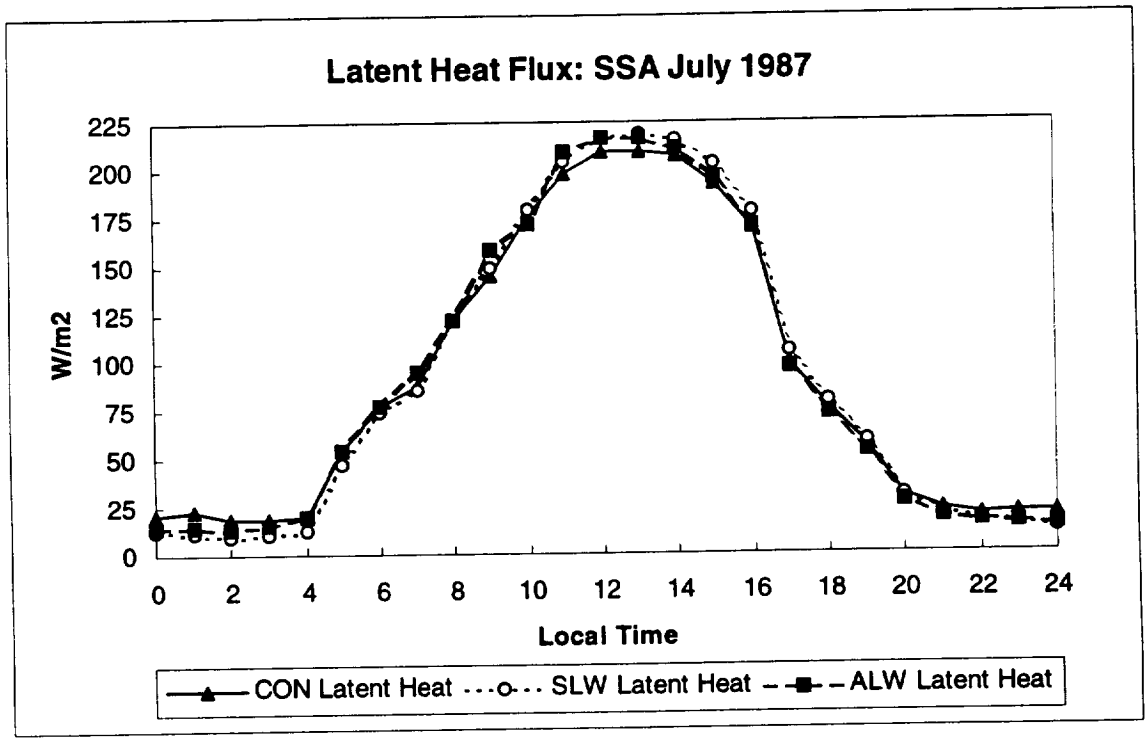

Figure 5.2: **July 1987 diurnal cycles of upwards longwave radiation and latent heat flux, at 53.5°N, 105.5°W.**

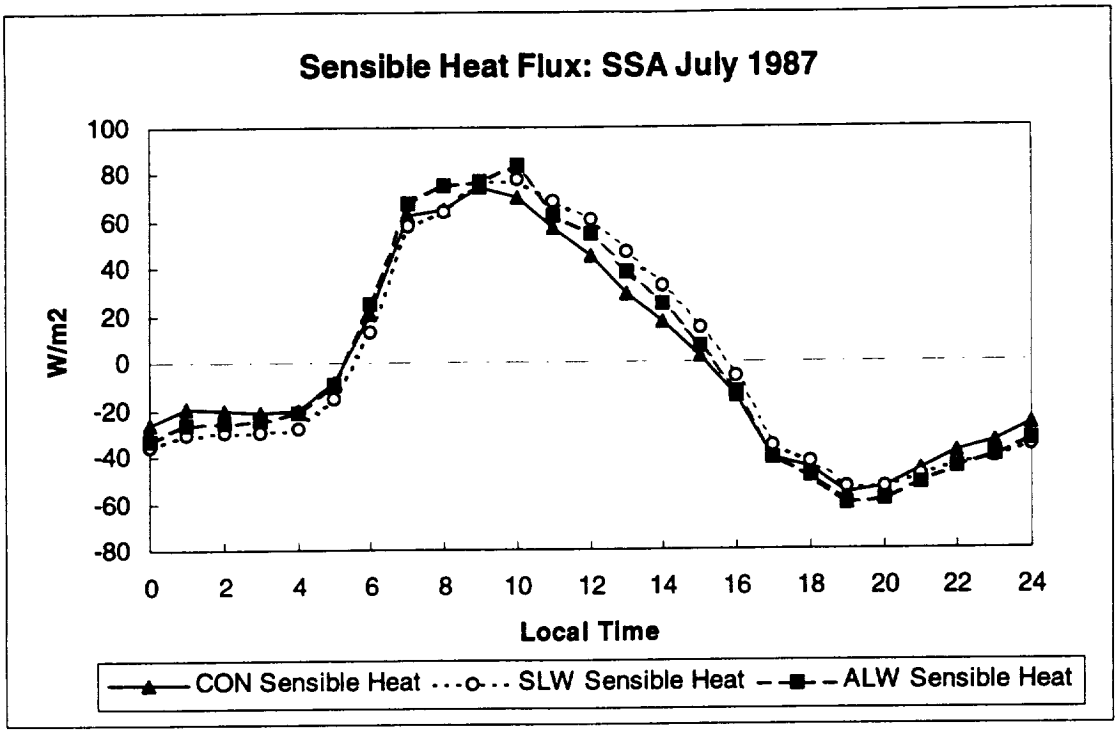

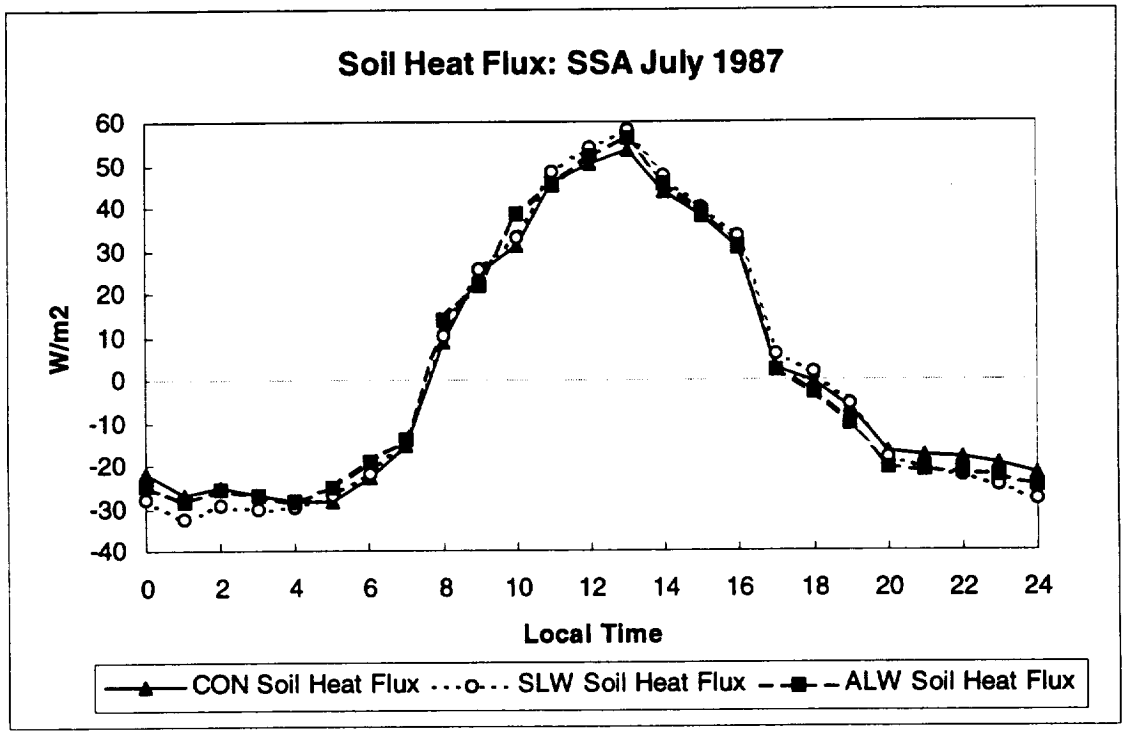

Figure 5.3: **July 1987 diurnal cycles of sensible heat and soil heat fluxes, at 53.5°N, 105.5°W.**

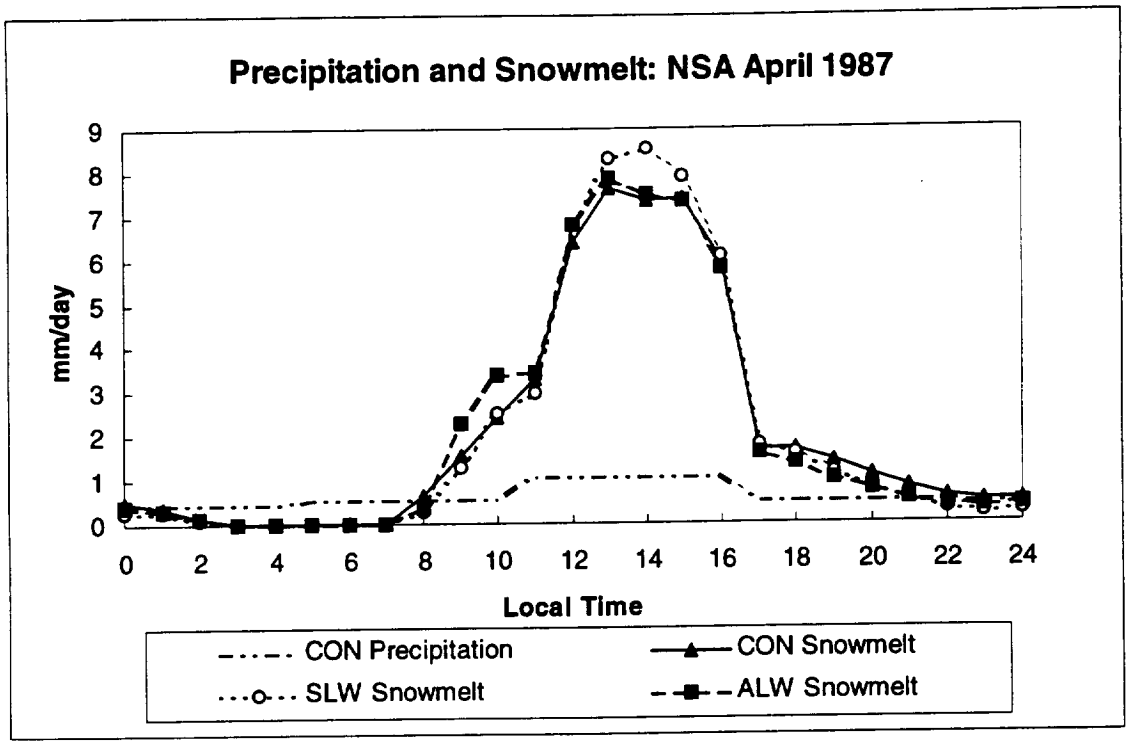

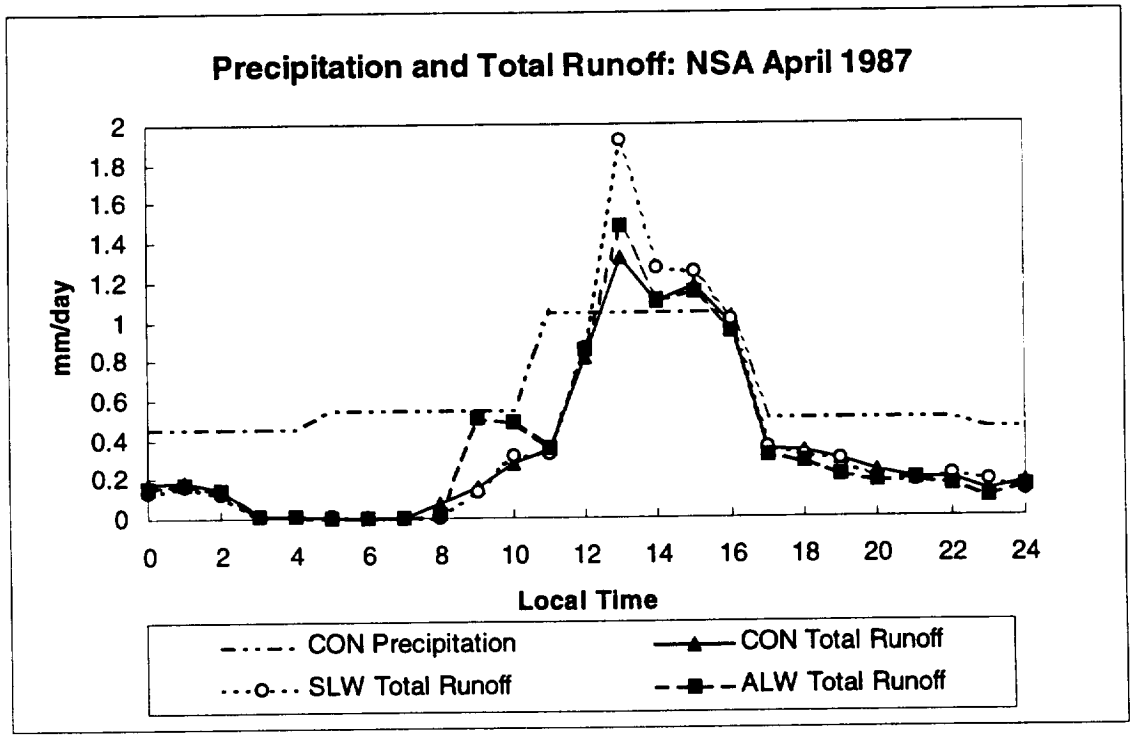

Figure 5.4: **April 1987 diurnal cycles of precipitation, snowmelt and total runoff, at 53.5°N, 105.5°W.**

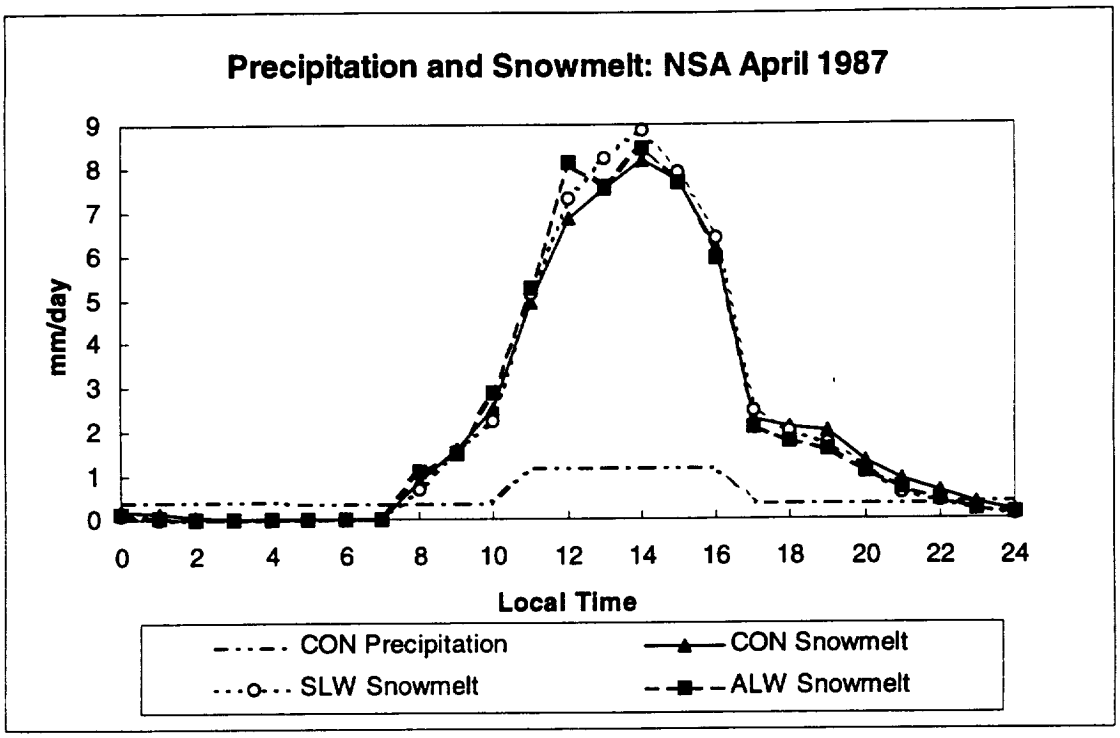

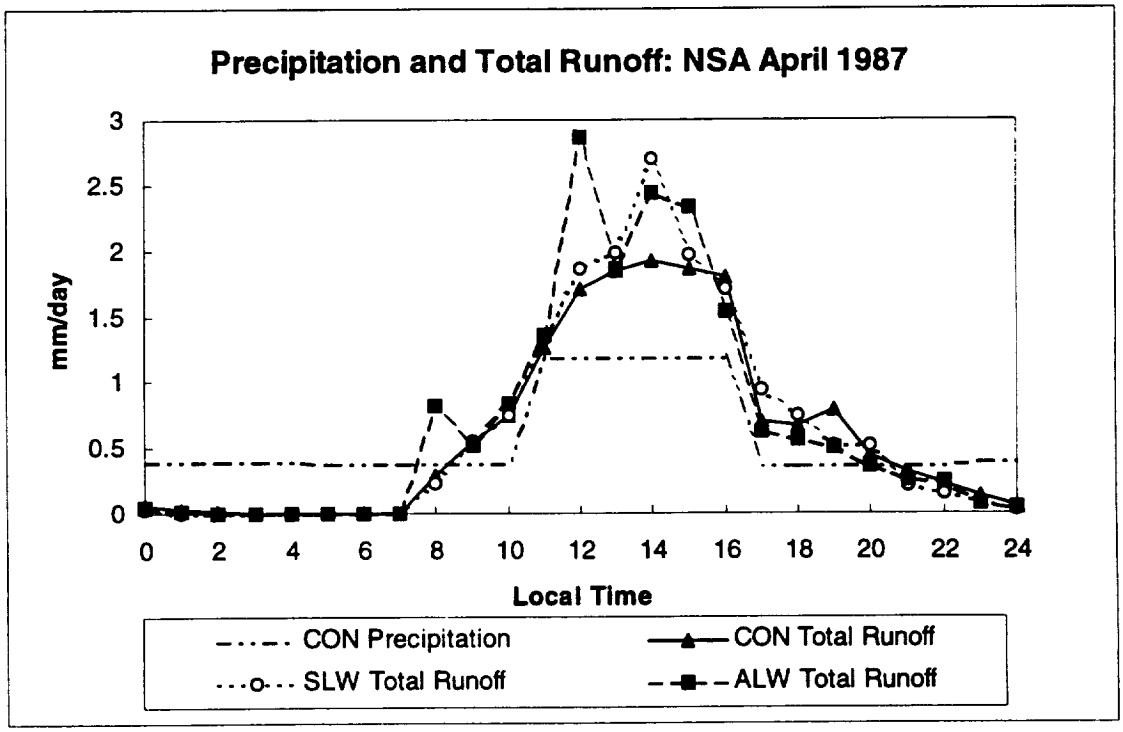

Figure 5.5: **April 1987 diurnal cycles of precipitation, snowmelt and total runoff, at 55.5°N, 98.5°W.**

6. Current Research

Finding and eliminating the source(s) of the irregularities in the 10-layer model is currently a high priority. Sensitivity studies of latent heat and soil moisture and temperature profiles to changes in K_s, b, ϕ, ψ_s, and thermal conductivity are then to be performed. In addition, with the 10-layer model corrected, direct comparisons can be made between the results of the 3-layer and 10-layer models. Efforts continue to locate better forcing and comparison observations.

The BATS/LAMA is to be coupled to the single column CCM3 (SCCM3) model (Hack et. al, 1996), hence allowing the surface to fully interact with the atmosphere and influence the humidity. In order to accurately simulate near-surface processes, it is necessary to have humidity be a feedback from the model, rather than an input. This will allow us to test the capability of the model to produce the observed reductions in transpiration during sunny mid-summer days. If suitable data can be found for use as boundary conditions during 1994 and 1996, results from BATS/LAMA coupled to SCCM3 can be compared directly to the BOREAS observations.

A new and improved carbon model is in the process of being integrated into BATS. This model, along with the observations of the BOREAS team Terrestrial Ecology -4 (TE-4), will be used to incorporate the moss and lichen into the carbon balance in BATS. Additional observations for this work include Dilks and Proctor (1979), Busby and Whitfield (1978), Busby et al. (1978), Longton and Green (1979) and Proctor (1980).

The results of LAMA contained in this report as well as any results with a correct 10-layer model will be presented at the fall 1997 AGU meeting in San Francisco.

A feasibility study for the development of a Lichen And Moss Detection Algorithm (LAMDA) is planned. LAMDA would use remotely sensed (satellite) data to detect the presence of moss or lichen beneath the tree canopies. This will enable climate modelers to determine at which locations the LAMA model should be applied. The algorithm used will be of similar form to the plant chemistry algorithm.

The plant chemistry algorithm is being further developed as time permits.

7. References

Ahti, T., 1977. Lichens of the boreal coniferous zone. In *Lichen Ecology*, (ed. M. R. D. Seaward), pp. 145-81. Academic Press, London.

Antonovski, M. Ya., M. T. Ter-Mikalian and V.V. Furyaev, 1992. A spatial model of long-term forest fire dynamics and its applications to forests in western Siberia. In *A Systems Analysis of the Global Boreal Forests* (eds. H. H. Shugart, R. Leemans and G. B. Bonan), pp. 373-403.

Bates, J. W. and A. M. Farmer, 1992. *Bryophytes and Lichen in a Changing Environment*, Clarendon Press, Oxford.

Betts, A. K. and J. H. Ball, 1995. The FIFE surface diurnal cycle climate. *Journal of Geophysical Research* **100**, 25,769-25,693.

Bonan, G. B., 1989a. A computer model of solar radiation, soil moisture and soil thermal regimes in boreal forests. *Ecological Modeling* **45**, 275-306.

Bonan, G. B., 1989b. Environmental factors and ecological processes controlling vegetation patterns in boreal forests. *Landscape Ecology* **3**, 111-30.

Bonan, G. B., 1992a. Soil temperature as an ecological factor in boreal forests. In *A Systems Analysis of the Global Boreal Forests* (eds. H. H. Shugart, R. Leemans and G. B. Bonan), pp. 126-143.

Bonan, G. B., 1992b. A simulation of environmental factors and ecological processes in North American boreal forests. In *A Systems Analysis of the Global Boreal Forests* (eds. H. H. Shugart, R. Leemans and G. B. Bonan), pp. 404-427.

Bonan, G. B., 1996. *A Land Surface Model (LSM version 1.0) for Ecological, Hydrological, and Atmospheric Studies: Technical Description and User's Guide*, NCAR Technical Note, NCAR/TN-417 +STR, Boulder, Colorado, 150 pp.

Bonan, G. B. and K. J. Davis, 1996. Comparison of the NCAR LSM1 land surface model with BOREAS aspen and jack pine tower fluxes. Submitted to *the Journal of Geophysical Research* BOREAS special issue.

Bonan, G. B. and M. D. Krozukhin., 1989. Simulation of moss and tree dynamics in boreal forests of interior Alaska. *Vegetatio* **84**, 31-44.

Bonan, G. B. and H. H. Shugart., 1989. Environmental factors and ecological processes in boreal forests. *Annual Review of Ecology and Systematics* **20**, 1-28.

Brutsaert, W., 1975. On a derivable formula for long-wave radiation from clear skies, *Water Resources Research* **11**, 742-744.

Busby, J. R., L. C. Bliss, and C. D. Hamilton, 1978. Microclimate control of growth rates and habits of the boreal forest mosses, *Tomenthypnum nitens and Hylocomium splendens*. *Ecological Monographs* **48**, 95-110.

Busby, J. R. and D. W. A. Whitfield, 1978. Water potential, water content and net assimilation of some boreal forest mosses. *Canadian Journal of Botany* **56**, 1551-1558.

Clapp, R. E. and G. M. Hornberger, 1978. Empirical equations for some soil hydraulic properties, *Water Resources Research* **14 (4)** 601-604.

Coughlan, J. and S. W. Running, 1994. "First Results of BOREAS Modeling Exercise #1 for Workshop at Prince Albert, Saskatchewan 23-25 July 1994" Appendix A, 13-18.

Culf, A. D. and J. H. C. Gash, 1993. Longwave radiation from clear skies in Niger: a comparison of observations with simple formulas, *Journal of Applied Meteorology* **32**, 539-547.

Dennehy, K. F. and P. B. McMahon, 1987. Microclimate and actual evapotranspiration in a humid coastal-plain environment, *Journal of Hydrology* **93**, 295-312.

Dickinson, R. E., P. J. Kennedy, and A. Henderson-Sellers, 1993. Biosphere-Atmosphere Transfer Scheme (BATS) Version 1e as coupled to the NCAR Community Climate Model. NCAR Tech. Note, NCAR/TN-387+STR, pp. 72. National Center for Atmosphere Research, Boulder, CO.

Dilks, T. J. K. and M. C. F. Proctor, 1979. Photosynthesis, respiration and water content in bryophytes, *New Phytologist* **82**, 97-114.

Duniker, P., O. Sallnäs and S. Nilsson, 1992. Role of stand simulation in modeling forest response to environmental change and management interventions. In *A Systems Analysis of the Global Boreal Forests* (eds. H. H. Shugart, R. Leemans and G. B. Bonan), pp. 446-465.

During, H. J., 1992. Ecological classification of bryophytes and lichens. In *Bryophytes and Lichen in a Changing Environment* (eds. J. W. Bates. and A. M. Farmer), pp. 1-31. Clarendon Press, Oxford.

Dyrness, C. T. and R. A. Norum, 1983. The effects of experimental fires on black spruce forests in interior Alaska. *Canadian Journal of Forest Research* **13**, 879-93.

ECMWF, The Description of the ECMWF/WCRP Level III-A Global Atmospheric Data Archive. ECMWF Operations Department Shinfield Park, Reading, Berkshire RGE 9AX, England.

Hack, J. T, J. J. Hack, G. B. Bonan, B. A. Boville, B. P. Briegleb, D. L. Williamson, and P. J. Rasch, 1996. Description of the NCAR Community Climate Model. NCAR Tech. Note, NCAR/TN-420+STR, pp. 152. National Center for Atmosphere Research, Boulder, CO.

Hatfield, J. L., R. J. Reginato and S. B. Idso, 1983. Comparison of long-wave radiation calculation methods over the United States, *Water Resources Research* **19**, 285-288.

International GEXEX Project Office, 1995. Global Soil Wetness Project: Version 1.0., 46 pp.

Jin, M. and R. E. Dickinson, 1997. Interpolation of surface radiation temperature measured from polar orbiting satellites to a diurnal cycle. Part 1: Without Clouds. In preparation for submission to the *Journal of Geophysical Research.*

Jin, M., R. E. Dickinson and A. M. Vogelmann, 1997. A comparison of CCM2/BATS skin temperature and surface-air temperature with satellite and surface observations. *Journal of Climate* **10**, 1505-1524.

Korzhukhin, M. D. and M. Ya. Antonovski , 1992. Population-level model of forest dynamics. In *A Systems Analysis of the Global Boreal Forests* (eds. H. H. Shugart, R. Leemans and G. B. Bonan), pp. 334-372.

Larsen, J. A., 1980. *The Boreal Ecosystem.* Academic Press, New York.

Larsen, J. A., 1989. The northern forest border in Canada and Alaska: biotic communities and ecological relationships. *Ecological Studies 70.* Springer-Verlag, New York.

Leemans, R., 1992. The biological component of the simulation model for boreal forest dynamics. In *A Systems Analysis of the Global Boreal Forests* (eds. H. H. Shugart, R. Leemans and G. B. Bonan), pp. 428-445.

Longton, R. E., 1992. The role of bryophytes and lichen in terrestrial ecosystems. In *Bryophytes and Lichen in a Changing Environment* (eds. J. W. Bates. and A. M. Farmer), pp. 32-76. Clarendon Press, Oxford.

Longton, R. E. and S. W. Greene, 1979. Experimental studies on growth and reproduction in the moss *Pleurozium schreberi* (Brid.) Mitt. *Journal of Bryology* **10**, 321-38.

Meeson, B.W., F. E. Corprew, D. M. Myers, J. W. Closs, K.-J. Sun, D. J. Sunday, P.J. Sellers, 1995. ISLSCP Initiative I -- Global Data Sets for Land-Atmosphere Models, 1987-1988. Volumes 1-5. Published on CD by NASA (USA_NASA_GDAAC_ ISLSCP_001-USA_NASA_GDAAC_ISLSCP_005).

Morrill, J. C. and R. E. Dickinson, 1997a The sensitivity of BATS model output to changes in the ISLSCP Initiative 1 downward longwave radiation forcing data. *13th Conference on Hydrology, 77th AMS Annual Meeting, February 2-7, 1997, Long Beach, CA.*, 327-330.

Morrill, J. C. and R. E. Dickinson, 1997b. The sensitivity of BATS to the diurnal distribution of downward longwave radiation. In preparation for submission to the GSWP Special Issue of the *Journal of the Japanese Meteorological Society.*

Payette, S., 1992. Fire as a controlling process in the North American boreal forest. In *A Systems Analysis of the Global Boreal Forests* (eds. H. H. Shugart, R. Leemans and G. B. Bonan), pp. 144-169.

Proctor, M. C. F., 1980. Diffusion resistance in bryophytes. In *Plants and Their Atmospheric Environments* (eds. J. Grace, E. D. Ford, and P. G. Jarvis) The 21st Symposium of the British Ecological Society, pp 219-229.

Pruitt, W. O. Jr., 1978. Boreal Ecology. Edward Arnold (Publishers) Limited, Great Britain.

Richardson, D. H. S., 1981. The Biology of Mosses. Blackwell Scientific Publications, Oxford.

Sellers, P. J., F. G. Hall, G. Asrar, D. E. Strebel, and R. E. Murphy, 1992. An overview of the First International Satellite Land Surface Climatology Project (ISLSCP) Field Experiment (FIFE). *Journal of Geophysical Research* **97**, 18,345-18,371.

Sellers, P. J., F. G. Hall, H. Margolis, B. Kelly, D. Baldocchi, J. den Hartog, J. Cihlar, M. Ryan, B. Goodison, P. Crill, J. Ranson, D. Lettenmaier, and D. E. Wickland, 1995a. The boreal ecosystem-atmosphere study (BOREAS): an overview and early results from the 1994 field year, *Bulletin of the American Meteorological Society* 76, 1549-1577.

Sellers, P.J., B.W. Meeson, J. Closs, J. Collatz, F. E. Corprew, D. Dazlich, F.G. Hall, Y. Kerr, R. Koster, S. Los, K. Mitchell, J. McManus, D. Myers, K.-J. Sun, P. Try, 1995b. An Overview of the ISLSCP Initiative I -- Global Data Sets. On: ISLSCP Initiative I Global Data Sets for Land-Atmosphere Models, 1987-1988. Volumes 1-5. Published on CD-ROM by NASA. Volume 1: USA_NASA_GDAAC_ISLSCP_001. OVERVIEW.DOC.

Shugart , H. H. and I. C. Prentice, 1992. Individual tree-based models of forest dynamics and their application in global research. In *A Systems Analysis of the Global Boreal Forests* (eds. H. H. Shugart, R. Leemans and G. B. Bonan), pp. 313-333.

Skre, O. and W. C. Oechel, 1979. Moss production ina black spruce Picea mariana forest with permafrost near Fairbanks, Alaska, as compared with two permafrost-free stands. *Holarctic Ecology* **2**, 1979.

Sveinbjörnsson, B. and W. C. Oechel, 1992. Controls on growth and productivity of bryophytes: environmental limitation under current and anticipated conditions, In *Bryophytes and Lichen in a Changing Environment* (eds. J. W. Bates. and A. M. Farmer), pp. 77-102, Clarendon Press, Oxford.

Swinbank, W. C., 1963. Long-wave radiation from clear skies, *Quarterly Journal of the Royal Meteorological Society* **89**, 339-348.

Walsh, G. E., 1971. Energy budgets of four ponds in northwestern Florida, *Ecology* **52,** 298-304.

8. Appendix A

P7.3 THE SENSITIVITY OF BATS MODEL OUTPUT TO CHANGES IN THE ISLSCP INITIATIVE 1 DOWNWARD LONGWAVE RADIATION FORCING DATA

Jean C. Morrill * and Robert E. Dickinson
University of Arizona, Tucson, Arizona

1. INTRODUCTION

The GEWEX/ISLSCP Global Soil Wetness Project (GSWP) is using the 6-hourly atmospheric forcing data from the ISLSCP Initiative 1 data set to drive a dozen land surface models. The accuracy of the 6-hour downward longwave forcing data on the ISLSCP Initiative 1 data has been questioned by GSWP participants. In many areas, the data seem to be offset by several hours from what is expected, with maximum downward longwave radiation consistently occurring late at night. This study examines the sensitivity of the Biosphere-Atmosphere Transfer Scheme (BATS) to modifying the distribution of the given downwards longwave radiation over the daily cycle in two ways: first by shifting the timing of the input values, second by using a constant average value for each day. The longwave input changes fortunately did not result in significant changes to the output quantities. Of the large-scale average energy terms, only sensible heat showed any significant change. Most of the water balance terms remained virtually the same as well, including root-zone soil moisture values .

2. THE LONGWAVE DIURNAL CYCLE

Downward longwave radiation is more difficult to measure than shortwave radiation, so it is frequently estimated based on easier-to-measure quantities, such as screen temperature and water vapor pressure (Swinbank, 1968; Brutsaert, 1975; Hatfield et al., 1983; Culf and Gash, 1993). Both measured and estimated values of incoming longwave fluxes show similar predictable diurnal trends. In a study by Culf and Gash (1993), which compares clear-sky observations with equation predictions for an area in Niger, the observed and calculated downwards longwave flux both clearly peak from about 1300 to 1900 hours (GMT and local time), with a minimum at 0600. Measured incoming longwave values at a site in South Carolina (Dennehy and McMahon, 1987) and calculated values at several sites in Florida (Walsh, 1971) also show values peaking in the late afternoon/early evening hours .

These same trends in longwave radiation are found in a simulation of RCCM2/BATS (a revised version of the National Center for Atmospheric Research's second Community Climate Model coupled with the land-surface model BATS) described in Hahmann et al. (1995). The diurnal trends and 6-hour averages correspond to the idea of afternoon/evening maximum in radiation, not late night/early morning maximums.

3. THE ISLSCP INITIATIVE 1 DATA

The ISLSCP Initiative 1 6-hourly forcing data (Sellers et al., 1995, Meeson et al. 1995) consist of total precipitation, convective precipitation, surface air temperature, dew point temperature, mean wind speed, atmospheric pressure, downward shortwave radiation and downward longwave radiation. The shortwave and longwave radiation values are hybrid products. The 6-hourly downwards longwave radiation was calculated by:

$$LD_6 = LN_L/\Sigma(LN_E)*L_E+\varepsilon*b*[(T1_E+T_E/2]^4 \qquad (1)$$

where LD_6 is the hybrid 6-hourly downward longwave radiation, LN_L is the Langley Research Center monthly mean surface longwave net radiation, LN_E is the ECMWF 6-hourly surface net longwave radiation, $T1_E$ is the ECMWF surface temperature at time t , T_E is the ECMWF surface temperature at time (t-1), ε is the emissivity (0.996 for all land surfaces in ECMWF) and b is the Stefan-Boltzman constant.

The data are in 6-hour blocks (average values for the 6-hour time periods beginning 0000, 0600, 1200 and 1800 GMT), so it was necessary to arbitrarily distribute these values among the hourly timesteps. For the GSWP project, guidelines state that for downwards longwave radiation, air temperature, dew-point temperature, wind speed and surface pressure the average value is to occur three

* *Corresponding author address*: Jean C. Morrill, Department of Hydrology and Water Resources, P. O. Box 210011, University of Arizona, Tucson AZ 85721-0011; email: *jean@hwr.arizona.edu*

TABLE 1

Sensible Heat Flux

	Jan 87 CN W/m²	*Jan 87* Δ^S %	*Jan 87* Δ^A %	*Jul 87* CN W/m²	*Jul 87* Δ^S %	*Jul 87* Δ^A %
N. Amer.	-17.52	-1.10	-1.05	13.23	5.48	4.27
S. Amer.	28.97	3.84	2.76	26.09	3.54	2.98
Africa	36.84	4.97	4.30	46.61	4.92	4.01
Europe	-11.69	-2.90	-3.45	18.05	6.02	5.25
N. Asia	-24.50	-0.92	-0.01	7.10	9.05	7.07
S. Asia	9.72	6.99	8.52	23.45	5.38	4.48
Austrl.	52.48	4.49	4.26	35.53	6.10	5.91

Equations for Table 1 and Table 2:

$\Delta^S = [(SL-CN)/CN]*100$ (2)

$\Delta^A = [(AL-CN)/CN]*100$ (3)

Soil heat flux values underwent the largest percent change, even though the real value of the differences were quite small, because the control run values of soil heat flux were themselves small (-3 to +2 W/m², with values usually between -1 and +1 W/m²) In both Januaries there were significant decreases in soil heat flux in South America, Africa, and Australia (**Table 2**) and a significant increases in soil heat flux in southern Asia. These changes were all larger for the SL case than then AL case. In the two Julys, soil heat flux decreased in Africa and Australia and increased in southern Asia. In South America, soil heat flux decreased in July 1987 (-17% SL, -11% AL) and increased in July 1988 (60% SL, 38 %AL). However, these changes had little effect on the total energy budget, as they represented only a few W/m²

TABLE 2

Soil Heat Flux (January 1987)

	Mean CN W/m²	*Mean* SL-CN W/m²	*Mean* AL-CN W/m²	Δ^S %	Δ^A %
N. Amer.	-0.74	-0.01	-0.02	1.36	2.20
S. Amer.	0.63	-0.10	-0.08	-16.52	-12.44
Africa	0.58	-0.21	-0.20	-36.27	-33.71
Europe	-2.89	-0.07	-0.07	2.38	2.36
N. Asia	0.03	0.001	-0.003	2.60	-10.40
S. Asia	-1.48	-0.23	-0.18	15.26	12.05
Austrl.	0.32	-0.21	-0.16	-66.37	-49.06

Average skin temperature decreased in all areas by less than 0.12% (less than 0.5°K). The maximum decrease at a single point was -2.11°K (South America, SL July 1988), the maximum increase 1.05°K (North America, SL July 1987). These small differences tended to be greater in magnitude for the SL simulation. Soil surface and sub surface temperatures also showed a similar very small average decreases, with the maximum decrease (0.1%) occurring in Africa.

5.2 *Water Balance and Soil Water Variables*

Soil moisture in the three layers (surface, root-zone, and total) experienced very little average change on a large scale, but individual points experienced some fairly large fluctuations of values in the surface layer (**Table 3**). The amount of water in the root-zone and total layers remained fairly constant. The various non-dimensional soil wetness values being calculated by the GSWP had no significant changes.

TABLE 3

Surface Soil Moisture (mm water) July 1987

	mean CN	*mean* SL-CN	*mean* AL-CN	*min* SL-CN	*max* SL-CN	*min* AL-CN	*max* AL-CN
N. Amer.	8.14	0.02	0.02	-2.35	0.52	-1.52	0.81
S. Amer.	12.23	0.00	0.02	-3.67	1.21	-3.91	3.17
Africa	6.08	-0.01	0.02	-2.69	3.26	-1.85	3.70
Europe	8.20	0.00	0.02	-1.52	0.65	-0.61	0.72
N. Asia	6.90	0.01	0.02	-0.88	1.37	-2.32	1.49
S. Asia	9.09	0.00	0.01	-5.78	1.82	-5.85	1.88
Austrl.	6.22	0.01	0.02	-0.32	0.29	-0.80	0.36

None of the average water balances quantities had any deviation of more than 0.02 mm/day. There was a smaller than 2% increase in average bare soil evaporation in almost all regions, with the SL increases larger than the AL increases. Mean total evapotranspiration in both simulations decreased an even smaller amount, possibly due to the combination of minute changes in snow evaporation, canopy evaporation and transpiration.

6. CONCLUSIONS

Neither shifting the phase of the incoming longwave radiation cycle, nor abolishing the diurnal cycle in favor of a single daily longwave value, had a significant effect on either the large-scale energy or water budgets in BATS . Even sensible heat, which showed the greatest sensitivity to the alterations in longwave radiation, changed by only a few percent.

hours into the time period (0300, 0900, 1500, and 1800 GMT) and all other hourly values are to be interpolated linearly between those values. Therefore the diurnal "cycles" of these five variables will consist of only four straight lines.

The result of these interpolations is that downward longwave radiation consistently peaks after sunset (usually between 2000 and 0200 local time, depending upon the location) and minimum downwards longwave radiation occurs in the late morning to early afternoon (0800 to 1600 local time). The diurnal range of values for longwave radiation varies depending upon location and season. At some points the difference between maximum and minimum radiation is less than 2 W/m^2, in other areas it is almost 200 W/m^2. Air temperature follows the expected pattern of peaking in the mid-late afternoons (1400 to 1900 local time). Shortwave radiation was distributed as a function of the cosine of the local zenith angle, with maximum radiation always occurring near local noon. The unaltered shortwave radiation input shows no sign of temporal offsetting.

4. SENSITIVITY SIMULATIONS

The model used in this study was the Biosphere-Atmosphere Transfer Scheme (BATS). The model was initialized according to project guidelines (soil moisture was initialized at 75% of capacity, surface and sub-surface ground temperatures at the December 1987 mean air temperature) and allowed to spin up for twenty years. Then two years were run for the control case and each of the sensitivity simulations.

The first simulation was the control run (CN) using the unmodified forcing data. For the second run, the entire longwave data set was shifted forward 6 hours in time, so that the maximum and minimum longwave radiation occurred closer to the maximum and minimum surface temperatures. For the third run, the values for the four longwave files for each date were averaged, so that at any given point the hourly longwave radiation was constant throughout each 24-hour period. These second and third simulations will be referred to as the shifted longwave (SL) case and the average longwave (AL) case. **Figure 1** shows an example of the three different longwave diurnal cycles and their relationship to the air temperature cycle.

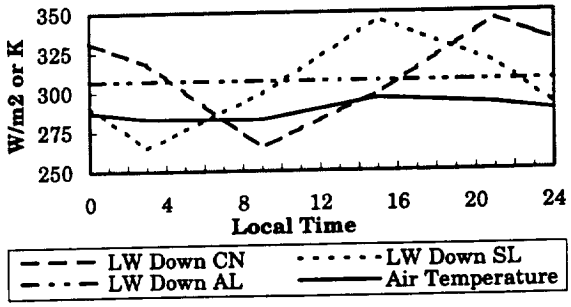

Figure 1. July 1987 mean monthly diurnal cycle of air temperature and downward longwave radiation for the three simulations at 39.5°N, 99.5°E.

5. RESULTS

This paper will deal mainly with comparisons/ changes in January and July monthly averages over seven major continental areas (North America, South America, Africa, Europe, northern Asia, southern Asia and Australia). Specific details about changes to the diurnal cycles of output variables at select individual points will be available at the AMS conference in February.

5.1 *Radiation, Energy and Temperature*

Although the timing of longwave radiation input was changed in the two sensitivity runs, total radiation input remained constant. As a result, changes to the radiation budget were small. Averaged upwards longwave radiation in both the SL and AL cases decreased over the CN mean upwards longwave by less than one percent, as averaged net long-wave radiation decreased 1-2%. Averaged net shortwave radiation altered less 0.1%. The SL and AL latent heat decreased slightly but not significantly in both January and July. The largest changes were to sensible heat flux and upward soil heat flux. In July, mean sensible heat increased over all continental areas by 3-9% (1-3 W/m^2). The increase was larger in the SL case than the AL case (**Table 1**). In January, sensible heat decreased in North America, Europe and northern Asia, and increased in the four southern regions. Although the changes of both the SL and the AL simulations from the control run are usually similar in magnitude, in January, sensible heat over southern Asia increased much more in the SL run than the AL run.

Changes to the soil moisture terms of the most interest to the GSWP were negligible. Therefore, members of the GSWP and others should be able to use the ISLSCP Initiative 1 data for large-scale monthly averages without worrying about possible errors in the longwave radiation data set.

The same conclusion can not be made for short term (daily or hourly) averages and small-scale studies. It is probable that a more detailed analysis will reveal significant changes at individual points, even over a long period of time, which are obscured by large-scale averaging. The results of this second more in-depth study will also be presented at the AMS meeting.

7. LIST OF ACRONYMS

AL	Average Longwave Simulation (3rd of the 3 BATS simulations)
BATS	Biosphere Atmosphere Transfer Scheme
CN	Control Simulation (1st of the 3 BATS simulations)
ECMWF	European Center for Medium-Range Weather Forecasts
GEWEX	Global Energy and Water Cycle Experiments
GMT	Greenwich Mean Time
GSWP	Global Soil Wetness Project
ISLSCP	International Satellite Land Surface Climatology Project
NCAR	National Center for Atmospheric Research
RCCM2	Revised Community Climate Model 2
SL	Shifted Longwave Simulation (2nd of the 3 BATS simulations)

8. ACKNOWLEDGEMENTS

This research was funded by NOAA Grant NA56GP0184.

9. REFERENCES

Brutsaert, W., 1975: On a derivable formula for long-wave radiation from clear skies, *Water Resources Research* **11**, 742-744.

Culf, A. D. and J. H. C. Gash, 1993: Longwave radiation from clear skies in Niger: a comparison of observations with simple formulas, *Journal of Applied Meteorology* **32**, 539-547.

Dennehy, K. F. and P. B. McMahon, 1987: Microclimate and actual evapotranspiration in a humid coastal-plain environment, *Journal of Hydrology* **93**, 295-312.

ECMWF, The Description of the ECMWF/WCRP Level III-A Global Atmospheric Data Archive. ECMWF Operations Department Shinfield Park, Reading, Berkshire RGE 9AX, England.

Hahmann, A. N., D. M. Ward and R. E. Dickinson, 1995: Surface land temperature and radiative response of the NCAR CCM2/BATS land scheme to modifications in the optical properties of clouds, *Journal of Geophysical Research* **100**, 23239-23252.

Hatfield, J. L., R. J. Reginato and S. B. Idso, 1983: Comparison of long-wave radiation calculation methods over the United States, *Water Resources Research* **19**, 285-288.

Meeson, B.W., F. E. Corprew, J.M.P. McManus, D. M., J. W. Closs, K.-J. Sun, D. J. Sunday and P. J. Sellers. 1995: ISLSCP Initiative I -- Global Data Sets for Land-Atmosphere Models, 1987-1988. Volumes 1-5. Published on CD by NASA (USA_NASA_GDAAC_ISLSCP_001-USA_ NASA_GDAAC_ISLSCP_005).

Sellers, P.J., B.W. Meeson, J. Closs, J. Collatz, F. E. Corprew, D. Dazlich, F.G. Hall, Y. Kerr, R. Koster, S. Los, K. Mitchell, J. McManus, D. Myers, K.-J. Sun and P. Try. 1995: An Overview of the ISLSCP Initiative I -- Global Data Sets. On: ISLSCP Initiative I Global Data Sets for Land-Atmosphere Models, 1987-1988. Volumes 1-5. Published on CD-ROM by NASA. Volume 1: USA_NASA_GDAAC_ISLSCP_001. OVERVIEW.DOC.

Swinbank, W. C., 1963: Long-wave radiation from clear skies, *Quarterly Journal of the Royal Meteorological Society* **89**, 339-348.

Walsh, G. E., 1971: Energy budgets of four ponds in northwestern Florida, *Ecology* **52**, 298-304.